ACTIVE CONTROL OF FLOOR VIBRATIONS

by

Linda M. Hanagan

Dissertation submitted to the faculty of the

Virginia Polytechnic Institute and State University

in partial fulfillment of the requirements for the degree of

DOCTOR OF PHILOSOPHY

in

Civil Engineering

APPROVED:

Thomas M. Murray, Chairman

Robert A. Heller

Ricardo A. Burdisso

Raymond H. Plaut

W. Samuel Easterling

Harry H. Robertshaw

December, 1994

Blacksburg, Virginia

ACTIVE CONTROL OF FLOOR VIBRATION

by

Linda M. Hanagan

Thomas M. Murray, Chairman

(ABSTRACT)

The active control of structures is a diverse field of study, with new applications being developed continually. One structural system, which is often not considered a dynamic system, is the floor of a building. In many cases the dynamics of a floor system are neglected in the design phase of a building structure. Occasionally, this omission results in a floor which has dynamic characteristics found to be unacceptable for the intended use of the building. Floor motion of very small amplitudes, often caused by pedestrian movement, is sometimes found objectionable by occupants of the building space. Improving an unacceptable floor system's dynamic characteristics after construction can be disruptive, difficult and costly.

In search of alternative repair measures, analytical and experimental research implementing active control techniques was conducted to improve the vibration characteristics of problem floors. Specifically, a control scheme was developed utilizing the measured movement of the floor to compute the input signal to an electromagnetic actuator which, by the movement of the actuator reaction mass, supplies a force that reduces the transient and resonant vibration levels. Included in the analytical component

of this research is the development of a mathematical model for a full scale experimental test floor. This model is studied, using a matrix computation software, to evaluate the effectiveness of the control scheme. The experimental component of the research serves two purposes. The first is the verification of the system behavior assumed in the analytical component of the research. The second is the verification of control system effectiveness for various excitations, control gains, and actuator locations on the experimental test floor and six additional floors.

ACKNOWLEDGMENTS

The work described in this dissertation has been supported in part by the National Science Foundation (NSF) Grant No. MSS-9201944 and by a grant from NUCOR Research and Development, Norfolk, Nebraska. Financial support of my doctoral education was provided by the Charles E. Minor Fellowship from the College of Engineering and the Charles. E. Via Fellowship provided by the Department of Civil Engineering. I am indebted to these funding sources for making my education and this research possible.

I would like to thank Dr. Thomas M. Murray for his support, guidance and friendship throughout my doctoral studies. Thanks are also extended to my committee members for their suggestions in their various fields of expertise. The multi-disciplinary approach of this work would not have been possible without their help. A special thanks goes to Jerry Nessler at SDRC for his invaluable assistance in configuring the experimental test setup. My appreciation is also extended to the building owners and engineers who provided access to the problem floor systems studied in this research. Additionally, I am very grateful to all of the students, technicians, and secretaries who provided me with a great deal of assistance during this research effort.

Finally, special thanks go to my husband, parents, family and friends for their unwavering support and encouragement throughout my educational and professional pursuits.

TABLE OF CONTENTS

TABLE OF CONTENTS (Continued)

TABLE OF CONTENTS (Continued)

LIST OF FIGURES

Figures Page

Figures Page

Figures Page

LIST OF TABLES

CHAPTER 1

INTRODUCTION AND LITERATURE REVIEW

1.1 Introduction

Excessive floor vibrations are not uncommon in many types of building structures. Problems of this nature have been reported in office buildings, shopping malls, airport concourses, and restaurants, to name a few. One common construction type which is particularly susceptible to floor vibrations is concrete on metal deck supported by steel framing members. This type of floor system is the subject of this research effort and will be emphasized in any further discussion.

Although floor vibrations can result from many sources (e.g., reciprocating machinery, explosions, heavy truck traffic, the most common and problematic floor vibrations are caused by the occupants themselves. Occupants generate floor vibrations from activities such as walking, dancing, jumping, etc. The assessment of "excessive" is, in general, determined by the occupancy requirements. These requirements range from limitations of sensitive equipment to the "comfort" of the occupants.

There are two basic strategies to provide a floor system which is free from excessive floor vibrations. The first, and certainly preferable, is to design a system which will be acceptable with respect to all serviceability and strength requirements for the intended occupancy. The methodologies involved in achieving this goal for floor vibration serviceability requirements are discussed briefly in the Background section of

the Literature Review. This section also provides an insight into the nature of floor vibrations, thus forming a foundation for discussing research in this area. The second strategy is to improve the vibration characteristics of an unacceptable floor system after it is constructed. Some of the traditional methods for improving floor vibration characteristics, which in many cases have shown only marginal success, are structural stiffening, adding mass, or the installation of full or partial height partitions, damping posts, and tuned mass dampers. These methods are discussed in Section 1.2.2.

The purpose of the research discussed in this dissertation is to study an alternative to traditional methods for improving floor vibration characteristics. This alternative method utilizes the implementation of active control to reduce floor vibration. In short, a control scheme has been developed utilizing the measured movement of the floor to compute the input signal to an electromagnetic actuator which, by the movement of the actuator reaction mass, supplies a force that reduces the transient and resonant vibration levels.

Control theory has been implemented in many areas to achieve a desired response in dynamic systems. These can be electrical, mechanical, or even large structural systems, as in the case of a floor system. Most of the research efforts toward practical implementation of active vibration control of large structures have been performed by two groups. The first group centers its research on controlling movements in large civil structures, while the second group aims their research efforts toward the control of large space structures. Each of these groups provides useful insight into the implementation of

active control for controlling floor vibrations. For this reason, a thorough review of the literature has been performed in both areas. Pertinent aspects of this review are presented in Sections 1.2.3-1.2.7.

1.2 Literature Review

1.2.1 Background: The nature of floor vibrations

To provide a useful discussion of active vibration control implementation with respect to floor systems, it is necessary to understand the nature of floor vibrations. A floor system can be a very complex dynamic system, often possessing several closely spaced natural frequencies which contribute significantly to the vibration response. In a case study of an elementary school (Pernica 1990), the floor was shown to possess six different natural frequencies and corresponding mode shapes which contributed significantly to the response at the location of the measurement. These natural frequencies existed over a range of 5-15 Hz. This floor is considered typical for steel-framed floors where the first natural frequency is commonly found to be in the range of 5-8 Hz. (Murray 1991). This is unfortunate because automobile and aircraft comfort studies have found that humans are most acutely sensitive to vibrations in this range (Hanes 1970), a phenomenon that is explained by the fact that many of the major organs in the human body resonate in this frequency range (Murray 1991).

As noted in the introduction, excessive vibration can be characterized as too large for sensitive equipment or too large for occupant comfort. Determining these permissible

levels is an entire research area in itself; however, some of the more widely accepted levels are discussed below. These levels are expressed by researchers in terms of either acceleration, velocity, or displacement amplitudes and are often frequency dependent. There is no consensus as to the most relevant measure for describing acceptable levels.

Ungar et al. (1990) present peak velocity requirements for several facility types which have either sensitive equipment or uses, such as optical research systems or microsurgery. The requirements proposed in this reference are classified according to use and are shown in Table 1.1. In particular, an office environment requires peak velocities of the floor system, due to any source, to remain below 0.016 in/sec to be considered acceptable. For a framed floor responding at a frequency of 7 Hz., this would translate to a peak dynamic displacement of only 0.00036 in. One might note that many of the requirements for more sensitive uses would be difficult to achieve with a slab on grade. Satisfying these requirements will not be the target of this research effort. They are presented merely as a frame of reference and to illustrate the magnitude of displacements which must be accommodated by the proposed control scheme.

Comfort of the occupants is a function of human perception. This perception is affected by factors including the task or activity of the perceiver, the remoteness of the source, and the movement of other objects in the surroundings. A person is distracted by acceleration levels as small as 0.5%g in an office or residential environment. People involved in an activity such as aerobics may be comfortable with acceleration levels up to 5%g (Allen 1990). Multiple-use occupancies must therefore be carefully considered.

Table 1.1 Vibration Criteria (Ungar, et al. 1990)

Facility Equipment or Use	**Velocity** (μin/sec)
Ordinary workshops	32,000
Offices	16,000
Residences; Computer systems	8,000
Operating rooms; Surgery; Bench microscopes at up to 100x magnification; Laboratory robots	4,000
Bench microscopes at up to 400x magnification; Optical and other precision balances; Coordinate measuring machines; Metrology laboratories; Optical comparators; Microelectronics manufacturing equipment - Class A	2,000
Micro-surgery, eye surgery, neuro-surgery; Bench microscopes at magnification greater than 400x; Optical equipment on isolation tables;Microelectronics manufacturing equipment - Class B	1,000
Electron microscopes at up to 30,000x magnification; Microtomes; Magnetic resonance imagers; Microelectronics manufacturing equipment - Class C	500
Electron microscopes at greater than 30,000x magnification; Mass spectrometers; Cell implant equipment; Microelectronics manufacturing equipment - Class D	250
Microelectronics manufacturing equipment - Class E; Unisolated laser and optical research systems	130

Class A: Inspection, probe test, and other manu-facturing support equipment.

Class B: Aligners, steppers and other critical equipment for photolithography with line widths of 3 microns or more.

Class C: Aligners, steppers and other critical equipment for photolithography with line widths of 1 micron.

Class D: Aligners, steppers and other critical equipment for photolithography with line widths of 1/2 micron; includes electron-beam systems.

Class E: Aligners, steppers and other critical equipment for photolithography with line widths of 1/4 micron; includes electron-beam systems.

Webster and Vaicaitis (1992) describe a facility that has both dining and dancing in a large open area. The floor was noted to have a first natural frequency of 2.4 Hz., which is in resonance with the beat of many popular dance songs. This resonance response produced maximum acceleration and displacement levels of 7%g and 0.13 in., respectively. Such levels actually caused sloshing waves in drinks and noticeable bouncing of the chandeliers. The occupants found these levels to be quite objectionable.

Perception is also affected by the nature of the vibration response. Human response to steady-state excitation was extensively studied by Reiher and Meister (1931). Results of this study are summarized by the right hand scale of Figure 1.1. Steady-state vibration will disturb at much lower levels than vibration which is transient. Lenzen (1966) was perhaps one of the first researchers to quantify the perception of transient vibration. He noted that the main factor influencing the effect of vibration on humans was the amount of damping in the system. If the floor vibrations were damped to a small amplitude prior to 5 cycles of oscillation, the occupant felt only the initial impact, no vibration. Conversely, if the vibration persisted beyond 12 cycles, the occupant responded as if to steady state vibration. He further quantified this phenomenon as follows:

a) definitely perceptible floor: displacement amplitude after 5 cycles was greater than 40% of the initial amplitude

b) perceptible or barely perceptible floors: displacement amplitude after 5 cycles ranged between 20% and 40% of the initial amplitude

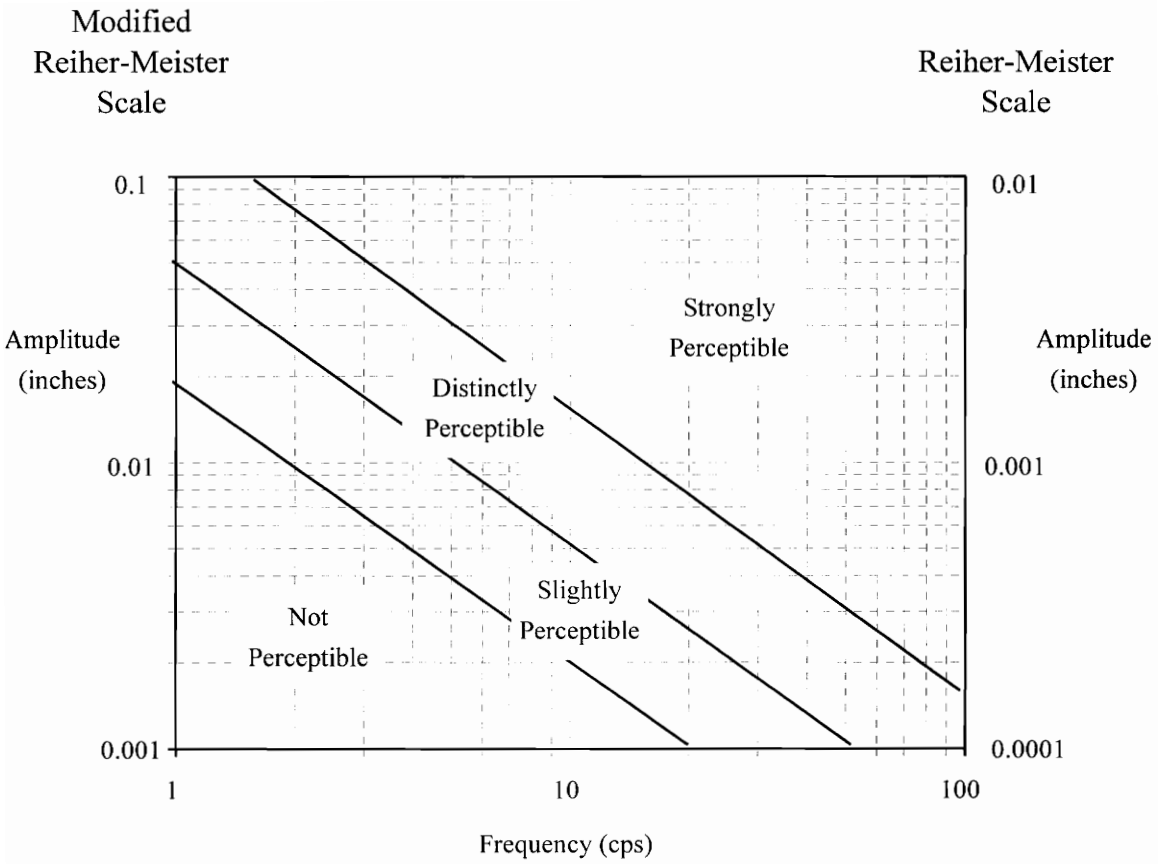

Figure 1.1: Modified Reiher-Meister and Reiher-Meister Scales
[Reiher and Meister 1931; Lenzen 1966]

c) imperceptible floors: displacement amplitude after 5 cycles was less than 20% of the initial amplitude

The net result of this research was the Modified Reiher-Meister scale for transient vibrations. The modification entails a shift in the Reiher-Meister scale by a factor of ten. This scale is represented by the left hand axis of Figure 1.1.

Another commonly referenced scale is that of the International Standards Organization (ISO 1992). The scale is represented by a baseline acceleration vs. frequency curve with multipliers for different occupancy and vibration types. A logarithmic plot of the baseline curve and a satisfactory magnitude curve for office environments subjected to intermittent and continuous vibration is shown in Figure 1.2. As points of comparison, the velocity-based limit for peak magnitude, as specified by Ungar *et al.* (1990), and the limits suggested by Allen and Murray (1993) are also shown.

Research on the evaluation of floor systems provides useful insight into the factors governing the successful implementation of an active control strategy. Many different scales and criteria are available which address the subjective evaluation of floor vibration. Factors included in these subjective evaluations include the natural frequency of the floor system, the maximum dynamic amplitude (acceleration, velocity, or displacement) due to certain excitations, and the amount of damping present in the floor system. At the present time, most of the design criteria utilize either a single impact function to assess vibrations which are transient in nature or a sinusoidal function to assess steady-state vibrations from rhythmic activities. The floor excitation in office and

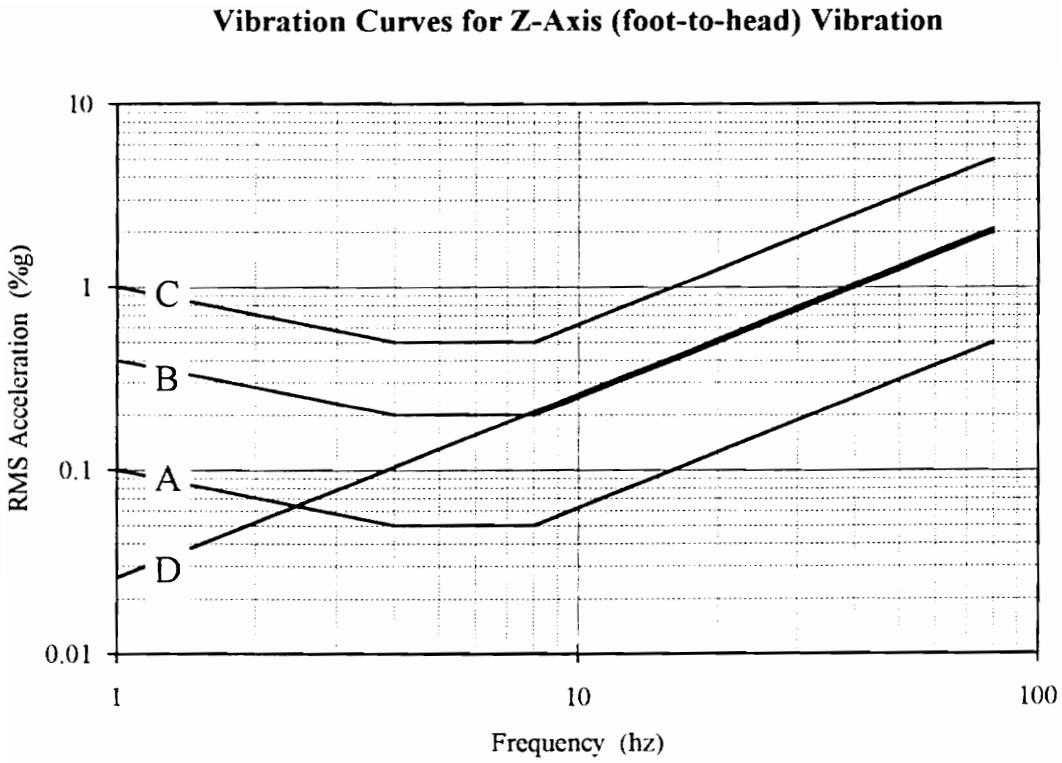

A: ISO baseline curve (ISO 1992)
B: ISO magnitude limit for satisfactory continuous and intermittent vibration in office environments (ISO 1992)
C: Allen and Murray limit for office environments (Allen and Murray 1993)
D: Ungar and Sturtz limit for peak magnitudes in office environments (Ungar et al. 1990)

Figure 1.2 Limits of Satisfactory Magnitudes of Floor Vibration with Respect to Human Response in Office Environments

residential environments is generally due to the intermittent movement of occupants. The vibration response is, therefore, considered transient and floor response is commonly evaluated on the basis of a single impact function (Murray 1991).

Many floor vibration researchers over the years have utilized, both experimentally and analytically, the forcing function known as the "heel-drop impact" to assess the transient response of a floor system. Experimentally, the standard heel-drop is the time dependent force of a 190 lb. person raising up onto his or her toes and dropping his heels through a distance of 2 in. to impact the floor. An approximation to the standard heel-drop has been quantified as a ramp function with a 600 lb. peak and a 50 millisecond duration (Murray 1979). This simplified excitation function can be implemented using hand calculations for simple systems (Murray 1991). The heel-drop impact is used in this active control research as one appropriate excitation for studying the behavior of the control system.

A final point of discussion, important to understanding the nature of floor vibrations and subsequently designing a control strategy, is that a floor, as a dynamic system, is constantly changing throughout the life of the structure. As the occupants move furnishings, one obvious change in the system is the mass and its distribution. Pernica (1990) studied the effect of architectural components on the floor vibration characteristics. With the addition of partitions, ductwork, furniture, and carpeting, changes in the natural frequencies, mode shapes and the amount of damping in the system were noted.

Numerous points were made in the above discussion which are crucial in the selection and evaluation of a control strategy. Many of these points will be reiterated in the Overview of Research in Section 1.3.

1.2.2 Traditional methods for improving floor vibration characteristics

With all of the scales and criteria available to design engineers to evaluate a floor design before construction, floors with excessive levels of vibration are still built. These floors often require repair measures to improve the dynamic characteristics. Traditional methods for improving floor vibration characteristics vary widely in both cost of implementation and obtrusiveness. The relative advantages and disadvantages of these methods are discussed to illustrate the need for alternative solutions for repairing problem floors.

Perhaps the largest improvement can be achieved by installing full height partitions. In addition to providing support, full height partitions have been noted to increase the damping in a floor system to 14% of critical (Allen 1975). Care must be taken in adding full height partitions because they can also increase the possibility of transmitting annoying vibrations to other locations in the building. Full height partitions are often ruled out because of their intrusion into the building space when an open plan is desired. Adding damping is also proposed by Allen (1975). Damping can be added to a system by a device termed a damping post. This post, which possesses a viscoelastic

material at mid-height, is connected between floors. No successful installation of this type of post has been found in the literature.

Structural stiffening of the framing members has only limited effect on the perception of vibration. Because perception is a function of both frequency and amplitude (refer to Figure 1.1), the net effect of structural stiffening is to increase frequency while reducing amplitude, thus providing no useful change in the system. Adding concrete thickness to the floor system has been reported to improve floor characteristics by increasing structural damping, while reducing system amplitude and frequency (Allen 1975). Two major factors can preclude the use of this repair measure. First, the existing structural system may not have adequate strength to support the additional load. Second, adding additional concrete to a floor system is very disruptive if the structure is already occupied.

Tuned mass dampers (TMD's) have been utilized to add damping to floor systems, thus reducing transient and resonant vibration responses. Tuned mass dampers are the least obtrusive of the remedial measures discussed so far because they can often be installed in the ceiling or in a closet. They are also the most closely related repair measure to the active control scheme being studied in this research. The successful implementation of tuned mass dampers for the control of large steady-state floor vibrations has been reported by several researchers.

A case study of a problem floor was described in Section 1.1 (Webster and Vaicaitis 1992). From floor measurements the damping was estimated to be on the order

of 3% of critical in the first mode of vibration. To improve the vibration characteristics of this floor, four TMD's were installed at various locations. The dampers were experimentally shown to reduce the amplitude of the steady-state vibration by approximately 60% at an estimated construction cost of $220,000.

Another case study (Thornton *et al.* 1990) describes the improvement of a gymnasium floor due to the installation of TMD's. During aerobic workouts in the gymnasium, annoying floor vibrations were reported by the office personnel on the floor below. Although no specific results were reported, the physical education teachers were noted as saying that the floor felt "much stiffer" and the office personnel noted a "dramatic improvement".

A very thorough treatment of the design and implementation of TMD's is presented in a series of papers by Setareh and Hanson (1992a; 1992b; 1992c). Excessive steady-state vibrations were produced in the balcony sections of a concert hall during rock concerts. Again, a problem of resonance existed with the first natural frequency of the floor system at 2.5 Hz. TMD's were installed to control the first and second modes of vibration, resulting in a 70% decrease in steady state amplitudes. The damping increased from 1.6% to 8%.

Another comprehensive case study of a TMD installation is discussed by Bell (1994). Excessive footfall vibration on a bridge-like floor span was reported in a newly constructed museum space. The damping in the fundamental mode of vibration was measured to be approximately 1% of critical. A TMD, weighing approximately 4% of

the equivalent mass in the fundamental mode, was installed and reported to increase damping from 1% to 5.8% of critical. The tuned mass damper was constructed of commercially available springs and concrete blocks. The damping devices were fluid dashpots in which the viscosity of the fluid was adjusted to provide optimum damping to the TMD.

Finally, research reported by Shope and Murray (1994) describes results from the installation of multiple TMD's on an experimental test floor. The uniqueness of this installation is twofold. First, the configuration is different from that described in other installations. The mass/spring portion is constructed as a simple beam device. The damping is supplied by multi-celled liquid filled bladders confined in rigid containers. The second unique quality of this installation is that control is sought, using many devices, in several modes of the vibration response.

The merits and effectiveness of TMD's are strongly illustrated by the research presented above. It is the relative shortcomings of TMD's, not so explicitly described in the discussion above, that make active control an attractive alternative. The mechanisms that provide the damping to the TMD are often ineffective for very small amplitudes, thus rendering the TMD ineffective. The "success" for many of the TMD installations described above was because the amplitudes were large. Control of smaller amplitudes (possible with the active control scheme) is necessary for many problem floors. An active system can also furnish a greater degree of control using the same amount of reactive mass. This is important because the weight of the control device is usually

limited by the strength of the structure. The advantages of the active control scheme over the passive TMD will be discussed more thoroughly in Chapter 3.

1.2.3 Overview of active control in buildings and large space structures

The goal of this overview and the subsequent sections is to lay a foundation for the discussion of active structural control and to review the literature pertinent to this research effort of controlling floor vibrations. As noted in the Introduction, rigorous study of active structural control has been pursued by different groups of researchers with the intent of controlling two different kinds of structures, namely large civil engineering structures (LCES) and large space structures (LSS). The line between these two groups has become blurred. With the declining budget of the space program, many of the researchers originally concerned with LSS control are now focusing their efforts toward LCES.

Research in the area of structural control for LCES has literally exploded in recent years. The proceedings from the US/China/Japan Trilateral Workshop on Structural Control (1992) is a 322-page volume with 34 papers. The 1993 International Workshop on Structural Control produced a 600-page volume with 55 papers. Most recently, in August 1994, researchers at the First World Conference on Structural Control presented 232 papers on this heavily explored subject. Along with conference papers, there are numerous journals and books which have published information on structural control. Control of LCES has generally focused on one of two areas, controlling bridges and

controlling lateral motion of buildings, with more emphasis being on the latter. Along with LSS literature, much of this literature has been reviewed with the intent of developing a rational approach for controlling floor motion.

Whether controlling bridges, buildings, space structures, or floors, the active control of structures can be broadly classified by three characteristics: 1) the control mechanism utilized in imparting control forces to the structure, 2) the sensing techniques used in measuring the excitation and response of the structure, and 3) the control law utilized in determining the control forces to act on the structure.

Control Mechanisms. There are many control mechanisms which have been studied analytically and/or experimentally. They have been reviewed for LCES in many papers (Reinhorn and Manolis 1985; Reinhorn and Manolis 1989; Soong 1988). Two of these mechanisms are of particular interest in controlling floor vibrations. The first mechanism is active tendon control. This application has been described in two configurations. To control lateral movement in buildings, active tendons can replace or supplement passive diagonal members in lateral force resisting frames. Active tendons can also be employed in beam-like structures. Active tendons were employed in a king post truss to control deformations (Roorda 1980).

The second mechanism is a moving mass. The moving mass has many names including active mass damper, active mass driver, shaker, reaction mass actuator, and proof-mass actuator. Whatever the name, it relies basically on the inertial forces

generated by a moving mass. As expected, this mechanism has been employed on many types of structures for the purpose of vibration suppression.

Control Laws. Classification of control laws for generating control forces depends on the type of information processed in addition to how it is processed. In the broadest terms, control laws can be classified according to the information processed, which can fall into three categories (Soong 1988):

1) A system which utilizes only measured response variables in computing the control forces is termed closed-loop control or feedback control.
2) A system which utilizes only measured excitation forces in computing the control forces is termed open-loop control or feedforward control.
3) A system which utilizes both the measured response and the measured excitation is termed open-closed loop control.

With respect to occupant induced floor vibrations, the only practical category is closed-loop control because of the nature of the excitation forces.

Within the realm of closed-loop control, there are many different control laws which have been developed. The most commonly used methods were first developed for general lumped parameter systems and were later adapted to the control of structures (Meirovitch 1985). Because they are discrete methods, they require a discrete model of the distributed system. This implies an approximation to the actual system which often results in what is called spillover. Spillover can reduce the effectiveness of the control

system and can often cause unforeseen instabilities. The specifics of spillover will be discussed in the next section.

Most of the lumped parameter control laws mentioned above fall into one of two categories: direct output feedback (DOFB) and modern modal control (MMC). The distinction between the two methods is best noted by Balas (1979a). In DOFB, the sensor outputs are multiplied by a gain matrix to produce control actuator commands. The MMC approach utilizes a state estimator to approximate the controlled mode states from the sensor outputs and applies control gains to these estimated states to produce the control actuator commands.

The selection between these two methods depends on the control objectives. Because MMC requires the on-line calculation of the estimated states, the effectiveness of this method is limited by computer capacity and model fidelity. On the other hand, the on-line calculations of DOFB require less computer capacity to provide "real time" control. The basic trade-off between these two methods is that MMC requires fewer sensors and actuators to produce the same degree of control (Balas 1978; 1979a).

With increasing computer capabilities and the relatively high cost of actuators and sensors, DOFB, on first inspection, may not seem very attractive when compared with MMC. Given an accurate, unchanging system model, this may be true; however, floor systems are difficult to accurately model and they are certainly not unchanging.

A particular form of DOFB is presented by Balas (1979b). This form is called direct velocity feedback (DVFB). In this method velocity sensor output is directly

multiplied by gains and fed back to collocated force actuators (i.e., the actuator force and velocity sensor are at the same location on the structure). The merit of this method lies in the nature of the spillover. Unlike DOFB and MMC, the narrow restrictions of DVFB result in a stabilizing spillover effect. In fact, in the absence of actuator and sensor dynamics, DVFB is unconditionally stable (Balas 1979b).

Control laws are further classified by the method in which the control gains (whether for DOFB or MMC) are selected. The two most commonly used are optimal control and pole allocation (Brogan 1974). The method of optimal control provides a solution for the control design based on the minimization of a cost or performance index. Pole allocation seeks to determine control gains which will place the closed loop poles of the controlled system in certain specified locations. Both of these methods are discrete methods which can suffer from detrimental spillover if some precaution is not taken. Numerous investigators have sought techniques to compensate for control and/or observation spillover (Balas 1978; Ibidapo-Obe 1985; Skelton and Likens 1978) while others have abandoned these techniques in search of more "rational" approaches dealing with the continuum (Meirovitch 1985; Oz 1985).

Oz (1985) notes that many control approaches, including those noted above, can never be fully realized because of approximations such as modal truncation and spatial discretization. While this criticism is duly noted, these methods have been successfully implemented in real structures (that is, if success is measured by whether the dynamics of the structural system have been improved, rather than exactly calculated). Some

examples of experimental implementation using discrete methods are presented in Section 1.2.7.

1.2.4 Modeling and spillover effects in active control

The problems associated with discretizing a continuous system give rise to one of the great debates in controlling continuous systems. As summarized by Goh (1982), this debate entails whether to discretize and reduce the continuum to a system of ordinary differential equations or to stay with the continuum and work with partial differential equations to design the controller. There are some very strong arguments for finite discretization even with its inherent problems. The strongest argument is that complex systems, such as a floor, described by ordinary differential equations can be solved, while those described by partial differential equations often cannot.

The most popular method for discretizing a continuous structural system is by the finite element method (Balas 1982). The finite element method generates a reduced order model (ROM) by spatial discretization. The infinite dimensional distributed-parameter system is reduced to an n-dimensional subspace, disregarding the residuals. As n goes to infinity, the reduced order model approaches the exact solution. In practice, complex flexible systems can be described by large finite-dimensional systems.

The most acute problems in discretizing the system arise when the system is further reduced to a practical size for control implementation. As noted earlier, on-board

computer limitations constrain the controller dimension, thus increasing the effects of spillover already minimally present in the larger dimensional system.

Spillover effects can be easily described in the context of modal control for a large- dimensional lumped-parameter system. The equations of motion of a lumped-parameter structure under the general excitation can be written in matrix form as follows (Soong 1988):

$$M\ddot{\mathbf{x}} + C\dot{\mathbf{x}} + K\mathbf{x}(t) = D\mathbf{u}(t) + E\mathbf{f}(t)$$

where

M, C, K are the n x n mass, damping, and stiffness matrices, respectively,

$\mathbf{x}(t)$ is the n-dimensional displacement vector,

$\mathbf{u}(t)$ is the r x 1 control force matrix,

D is the n x r control force position matrix,

$\mathbf{f}(t)$ is the m x 1 applied load matrix, and

E is then x m applied load position matrix.

This equation can be rewritten in modal coordinates as follows (Chung 1987):

$$M^*\ddot{\eta} + C^*\dot{\eta} + K^*\eta = D\,u(t) + E\,f(t)$$

where the physical and modal coordinates are related by $x(t) = \Phi\eta(t)$. This can be partitioned into controlled (modeled) and residual modes as follows:

$$\begin{Bmatrix} x_c(t) \\ x_r(t) \end{Bmatrix} = \begin{bmatrix} \Phi_c & \Phi_r \end{bmatrix} \begin{Bmatrix} \eta_c(t) \\ \eta_r(t) \end{Bmatrix} = \begin{bmatrix} \Phi_{cc} & \Phi_{cr} \\ \Phi_{rc} & \Phi_{rr} \end{bmatrix} \begin{Bmatrix} \eta_c(t) \\ \eta_r(t) \end{Bmatrix}$$

The coordinates $x_c(t)$ are those available for measurement and the coordinates $x_r(t)$ are unavailable for measurement. In closed loop linear feedback control, the control force takes the form $u(t) = -G_1\eta - G_2\dot{\eta}$, where G_1 and G_2 are the corresponding gains of the modal displacements and velocities. It should be noted that in the case of positive control gains, the net effect of the control force is to add stiffness and damping to the system. When considering a reduced number of controlled modes, η becomes η_c and the residual modes are neglected in computing the control gains G_1 and G_2. This gives rise to the phenomenon called control spillover. Assuming normal modes, the modal system above can be partitioned as follows:

$$\begin{bmatrix} M_c^* & 0 \\ 0 & M_r^* \end{bmatrix}\begin{Bmatrix} \ddot{\eta}_c \\ \ddot{\eta}_r \end{Bmatrix} + \begin{bmatrix} C_c^* & 0 \\ 0 & C_r^* \end{bmatrix}\begin{Bmatrix} \dot{\eta}_c \\ \dot{\eta}_r \end{Bmatrix} + \begin{bmatrix} K_c^* & 0 \\ 0 & K_r^* \end{bmatrix}\begin{Bmatrix} \eta_c \\ \eta_r \end{Bmatrix} = \begin{Bmatrix} \Phi_c^T D \\ \Phi_r^T D \end{Bmatrix} u(t) + \begin{Bmatrix} \Phi_c^T F \\ \Phi_r^T F \end{Bmatrix} f(t)$$

where $u(t) = -G_1\eta_c - G_2\dot{\eta}_c$. While the control gains were optimized to improve the characteristics of K_c^* and C_c^*, the control forces have also "spilled over" into the residual terms noted K_r^* and C_r^* which were previously zero.

Additional spillover results from using estimated coordinates as feedback, $u(t) = -G_1\eta_{ce}(t) - G_2\dot{\eta}_{ce}(t)$. Estimated coordinates are computed from the available feedback measurements by $\eta_{ce}(t) = \Phi_{cc}^{-1}x_c(t)$. Remembering that the measurements, $x_c = \Phi_{cc}\eta_c + \Phi_{cr}\eta_r$, possess residual modes as well as controlled modes, the control vector becomes $u(t) = -G_1\eta_c(t) - G_2\dot{\eta}_c(t) - G_1\Phi_{cc}^{-1}\Phi_{cr}\eta_r(t) - G_2\Phi_{cc}^{-1}\Phi_{cr}\dot{\eta}_r(t)$, where the last two terms are considered the observation spillover.

The controlled system C^* and K^* matrices, including spillover, are then computed as:

Uncontrolled system damping matrix	Computed control forces	Control spillover	Observation spillover

$$C^* = \begin{bmatrix} C_c^* & \\ & C_r^* \end{bmatrix} + \begin{bmatrix} \Phi_c^T D G_2 & 0 \\ 0 & 0 \end{bmatrix} + \begin{bmatrix} 0 & 0 \\ \Phi_c^T D G_2 & 0 \end{bmatrix} + \begin{bmatrix} 0 & \Phi_c^T D G_2 \Phi_{cc}^{-1} \Phi_{cr} \\ 0 & \Phi_r^T D G_2 \Phi_{cc}^{-1} \Phi_{cr} \end{bmatrix}$$

Uncontrolled system stiffness matrix	Computed control forces	Control spillover	Observation spillover

$$K^* = \begin{bmatrix} K_c^* & \\ & K_r^* \end{bmatrix} + \begin{bmatrix} \Phi_c^T D G_1 & 0 \\ 0 & 0 \end{bmatrix} + \begin{bmatrix} 0 & 0 \\ \Phi_c^T D G_1 & 0 \end{bmatrix} + \begin{bmatrix} 0 & \Phi_c^T D G_2 \Phi_{cc}^{-1} \Phi_{cr} \\ 0 & \Phi_r^T D G_2 \Phi_{cc}^{-1} \Phi_{cr} \end{bmatrix}$$

As noted earlier, if precautions are not taken to assess the impact of the spillover terms on the control implementation, the result can be reduced control effectiveness or even control-induced system instabilities.

1.2.5 Considerations for proof-mass actuators

An electromagnetic actuator is used in this research to deliver control forces to the experimental test floor. This type of actuator, also referred to as a proof-mass actuator, can be modeled as a single-degree-of-freedom system possessing a discrete mass, a spring, and a dashpot (Zimmerman and Inman 1990). The control force is generated in the electromagnetic coil and reacts against the structure and the inertial mass.

Two basic issues must be considered when using a proof-mass actuator to apply the control force. First, the dynamics of the proof-mass are introduced into the control loop. Second, a proof-mass actuator has limitations on the magnitude of the control force

it can generate. These issues have been addressed by many researchers. The pertinent aspects of this research are described below.

Control/Structure Interaction. In the absence of actuator and sensor dynamics, structural control by means of collocated direct velocity feedback is unconditionally stable (Balas 1979b). Instabilities can, however, be introduced into the controlled system as a result of actuator dynamics. Inman (1990) schematically presents the nature of the interaction for a lumped-parameter system with discrete point mass actuators. The actuator dynamics are assumed to be of second order in time and some stability theorems for such a system are derived.

Goh and Caughey (1985) also note the controller-induced instabilities in collocated velocity feedback resulting from second-order actuator dynamics. The unstable controlled system frequencies were found near the resonant frequency of the actuator. Results from computer simulations are presented to illustrate this phenomenon The role of actuator dynamics in the control scheme is illustrated by Dyke *et al.* (1993) for a hydraulic actuator. Modeling and compensation for the dynamics are presented and experimentally verified. The control/structure interaction is another factor which must be considered in the implementation of an active control algorithm.

Force/Stroke Limitations. Proof-mass actuators possess limitations in their ability to generate control forces. The nature of these limitations, their effect on the control scheme, and techniques for incorporating these limitations into the controller have been studied by several researchers. The force output limitation of a proof-mass actuator

has two sources (Linder *et al.* 1991; Linder *et al.* 1992; Linder *et al.* 1993). The first limitation is a result of the stroke length, which is the physical length of travel of the inertial mass. This limitation, defined as stroke saturation, cannot be violated because damage can result in the actuator and shocks will be imparted on the structure. The second limitation is the electromechanical force that can be supplied by the electromechanical subsystem (Linder *et al.* 1993). These limitations create a nonlinearity in the controller which imposes a constraint on the operating region of the actuator (Linder *et al.* 1992).

Several non-linear control schemes are presented by Linder *et al.* (1992) to account for actuator limitations. The most straightforward solution is a command limiter, where the input force to the actuator is limited so as not to exceed either the stroke or force constraints. Parameters of the actuator (stiffness and damping) also play an important role in defining the operating region of an actuator. Methods of analysis for optimizing these parameters are also presented by Linder *et al.* (1993).

1.2.6 Miscellaneous issues in the experimental implementation of active control

Several miscellaneous topics remain which must be discussed to provide a thorough understanding of the factors involved in implementing active control of floor systems. Application of control through the use of a digital system has the advantage of increased flexibility of the control programs as well as a decision-making capability (Franklin *et al.* 1990). However, these advantages do not come without some drawbacks.

As a signal is both discretized and quantized by analog-to-digital conversion, certain errors can result due to the information lost. Quantization errors, due to finite word length in the computer, can be described as truncation and roundoff errors. These errors can be amplified by complex controller calculations.

The sampling process results in an effective time delay due to the zero order hold present in the digital to analog converter. The effect of the zero order hold can be reasonably assessed by introducing a time delay of T/2, where T is the sample rate, into the analysis of the continuous system (Franklin *et al.* 1990). One should also note that this time delay causes large phase shifts at higher frequencies, thus reducing the effectiveness of the controller at those high frequencies. Such phase shifts can also produce instabilities in the system.

The sample rate selected, limited by hardware capabilities, has a large effect on system performance. In addition to the time delay effect noted above, an effect called frequency aliasing can also degrade system performance. If the sampling rate is not high enough to digitally represent a high frequency component, this component will alias itself as a lower frequency component. Compensation for this phenomenon is generally achieved by the use of an analog signal prefilter which attenuates the higher frequencies. These prefilters can also cause low frequency phase shifts, resulting again in system degradation (Franklin *et al.* 1990).

Although not limited to digital systems, system noise and other disturbances not related to the system response must be considered. Additional factors are noted by Lewis

(1992, Chapter 6); but are not expanded on here. To summarize, the tradeoff between many factors must be carefully considered when implementing a control scheme digitally.

Sensors have practical limitations which must be addressed in implementing active control. Sensors possess a limited bandwidth over which accurate measurements can be taken. Measurements outside of this range are often not reliable for use in computing control forces. Reducing the effect of measurements outside the bandwidth of the sensor is sometimes necessary. Sensors also have limitations regarding the amplitude of the measurement. Low amplitudes may possess large errors due to sensitivity limitations, while large amplitudes can produce sensor damage or excessive voltages. Accounting for these limitations is necessary for successful experimental implementation of active control.

1.2.7 Experimental implementation of active control in building type structures

Experimental implementation often serves as a proving ground for many theoretical advances. To implement theories in active control, the experimentalist must cross the disciplinary boundaries of structural dynamics and control theory into signal processing, modal analysis, electromagnetics, and piezoelectrics, just to name a few. Assumptions of ideal force actuators, ideal sensors, noiseless signals, or perfect unvarying models of the structure cannot be made, no matter how controlled the experimental environment. In the above active control overview, the explosion of literature pertaining to structural control of LCES was noted. Much of this literature

pertains to experimental implementation in building-type structures. The following discussion of research is not intended as an exhaustive overview of every experimental implementation reported. It is intended, rather, to provide insight into the current state of experimental research.

Because the focus of this dissertation research is controlling floors, experiments involving active deformation control in beam-like structures are quite pertinent. Roorda (1980) presents results from several experiments which are of significant importance to note. In one experiment, vibrations in a king post truss are controlled by the use of active tendons. The tendon force is delivered by an electro-hydraulic servo-valve and actuator. A time delay and subsequent phase shift are found in this type of system. Using acceleration feedback, the author notes that the time delay coupled with the low pass filter characteristics provide a damping effect. Although not explicitly stated, one may also note that this phase shift is not uniform throughout the frequency spectrum and can produce instabilities at the higher modes.

Another simple experiment reported by Roorda (1980) utilizes an electromagnetic device to impart control forces on a low frequency cantilevered structure. In this experiment, the effect of varying the phase and magnitude of the control force is studied in an analog control configuration. One may also extrapolate from the findings in this experiment that time delay is of little consequence for an analog control system utilizing an electromagnetic device at this type of frequency range.

Automatic deformation control (ADC) for a precast girder is presented by Bouten and Meyr (1985). In this experiment, reinforcing strands are made active by use of pneumatic cushions. This application is termed ADC because the main goal is to control the static deformations created by a moving load rather than vibration suppression; however, vibration suppression is addressed. The author notes the impracticality of a passive TMD, due to the varying parameters of the system (i.e. moving loads and changing material properties), for vibration suppression. Instead, he proposes an adaptive algorithm which, in effect, creates a passive tuned mass damper with active parameters. This, however, was scheduled for future implementation.

The implementation of active lateral response control for seismically excited buildings is perhaps the most vigorously pursued application of active control in civil engineering. Among the most extensive of these experimental research programs in the U.S. is that of the State University of New York (SUNY) at Buffalo. Under the direction of T. T. Soong and A. M. Reinhorn, several researchers have applied active structural control to a quarter-scale shear frame type structure through the use of active tendons (Soong *et al.* 1985; Lin *et al.* 1987; Chung *et al.* 1988; Chung *et al.* 1989). A three-story shear frame model can be configured to respond as a single-degree-of-freedom system or as a three-degree-of-freedom system. The seismic excitation is delivered at the base of the structure by a shake table, which can be programmed for various base excitations.

Initially, the single-degree-of-freedom configuration was utilized in linear state feedback experiments (Soong *et al.* 1985; Chung *et al.* 1988). An optimal control

algorithm was used to determine the control gains for the various states used in calculating the control force. The investigators report displacement reductions of 95% of the initial response. The damping ratio was increased from 1.24% to as much as 50% of critical. Experimental results were also compared to analytical results and minor discrepancies in effectiveness were reported. The effects of time delay and their method of compensation were noted. Several instantaneous optimal control algorithms were also implemented on the s.d.o.f. structure (Lin *et al.* 1987).

The initial experiments were then extended to the structure configured for three degrees of freedom (Chung *et al.* 1989). The effects of control and observation spillover are explained and illustrated in the experimental results. Good agreement between experimental and analytical results is reported. Because adverse effects and structural instabilities can result due to the presence of imperfect conditions, a note of caution is also extended by the authors.

More recently, the researchers from SUNY Buffalo report results from a full-scale implementation of an active bracing system (Soong *et al.* 1991; Reinhorn and Soong 1992; Reinhorn *et al.* 1993). The test structure, located in Tokyo, Japan, is a four-bay six-story building. Four active braces were installed, two in each direction, at the ground level of the test structure. The top story houses an experimental active mass damper which was used to excite the structure in the experimental tests of the active bracing system. The control law used velocity feedback in the computation of the control force.

The control system was shown to reduce the response of the structure due to experimental excitation and actual ground motion.

Japanese researchers report many installations of active control systems in actual buildings in addition to several full-scale experimental implementations. The Kyobashi Seiwa Building, built in 1989, is reported to be the first building in the world that has an active control system (Inoue *et al.* 1993). An in-depth review of this installation is reported by Kobori *et. al.* (1991a; 1991b). This ten-story office structure utilizes an active mass driver (AMD) control system to reduce lateral movement. In the design of the system (Kobori, *et al.* 1991a), several control algorithms were investigated. The complicated control algorithms, requiring full state feedback, were rejected due to their lack of robustness in the presence of modeling and computational errors.

Because of the 1:4 floor aspect ratio in the Kobori building, large torsional modes existed in addition to the lateral modes. The control scheme implemented in the actual building consisted of two active mass dampers, with control forces computed by a simple linear feedback law. Specifically, the control forces are computed from the lateral and torsional velocity response at the roof level. In addition to the linear feedback circuit, a nonlinear element was introduced to limit the magnitude of the output signal so as not to exceed the limitations imposed by the AMD's. The success of this installation has led to similar installations in other buildings. Active control systems, similar to that described by Kobori, are reported to exist in 13 buildings in Japan (Izumi *et al.* 1993).

A review of the current experimental implementation studies points out the interaction between control law complexity and controlled structure complexity. Simple structures, such as those examined by Chung *et al.* (1989) can exploit the control efficiency of full state feedback, while more complex structures, such as the ten-story building (Kobori *et al.* 1991a; 1991b), require algorithms which are more robust to parameter, measurement, and computation errors. Such errors can render a system ineffective or even unstable.

1.2.8 Summary and Conclusions

Problem floors are built and viable repair solutions must be found. Correcting a floor system with disturbing levels of floor vibration is not a trivial task. Successful implementations of tuned mass dampers are almost exclusively limited to situations where the displacement amplitudes are very large.

The need for alternative repair measures for floor vibration problems has been thoroughly justified. Active control has been proven effective for many different applications. Many of the concepts in these applications can be extended and modified to suit the particular needs involved in improving the dynamic behavior of an unacceptable floor system.

1.3 Overview of Research

The purpose of this research is to study active control as a method to improve the dynamic characteristics of an unacceptable floor system. This approach uses an electromagnetic reaction-mass actuator to reduce occupant induced floor vibration.

Chapter 2 reviews four preliminary investigations and activities necessary for the analytical and experimental studies in later chapters. These are: 1) design and construction of an experimental test floor, 2) determination of test floor member and material properties, 3) construction and calibration of a force plate, and 4) determination of actuator and sensor properties. An analytical study of the control scheme is presented in Chapter 3. In this study, an analytical model, including the control scheme, is developed for the experimental test floor. Using this model, the effectiveness of the linear control scheme is evaluated, comparisons with tuned mass dampers are made, and the development and evaluation of a non-linear circuit is discussed. The experimental verification of the active control scheme, described in Chapter 4, serves two purposes. The first is the verification of the system behavior assumed in the analytical studies of Chapter 3. The second is the verification of control system effectiveness for various excitations, control gains, and actuator locations. The active control scheme was experimentally implemented on six additional floors and is discussed in Chapter 5. Finally, a summary, recommendations for future research, and conclusions are presented in Chapter 6.

CHAPTER 2

REVIEW OF PRELIMINARY INVESTIGATIONS AND ACTIVITIES

2.1 Design and Construction of the Experimental Test Floor

A full scale test floor was designed and constructed for use in the experimental implementation of active structural control. In designing the test floor, several characteristics were desired to make the test floor as close to a real floor system as possible. As noted in the Background, complaints of annoying floor vibrations have been commonly reported in office type occupancies with steel joist and concrete floor systems, even when these floors have been properly designed for strength. The test floor is, therefore, of this construction type and was designed for the strength required by an office occupancy.

A joist span of 25 ft. with joist spacing of 30 in. was selected. These are common dimensions for this construction type. The girder span was limited to 15 ft. because of space limitations. The lightweight concrete slab, which is supported by 1.0C metal deck, has a $3\frac{1}{2}$ in. total thickness. The girders are supported by 8 in. diameter pipe columns welded to base plates which are anchored to the concrete lab floor with anchor bolts. Plan and section views detailing the test floor are shown in Figure 2.1. The calculations for this design are presented in Appendix A.1

Calculations, presented in Appendix A.2, were also performed to evaluate the dynamic behavior of the proposed design. An "unacceptable" floor system, with respect

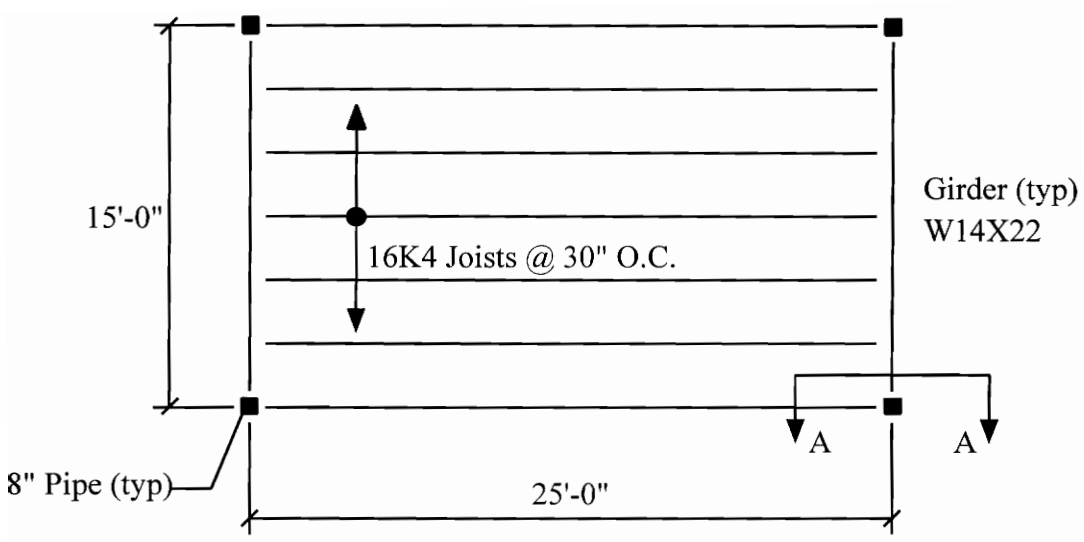

Plan of Test Floor

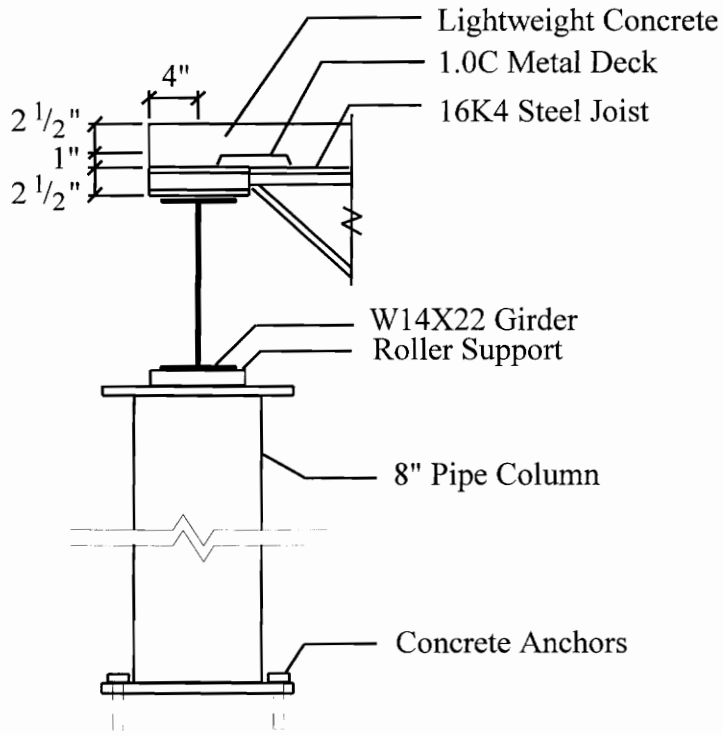

Section A-A

Figure 2.1 Plan and Section of Experimental Test Floor

to occupant induced floor vibrations, is desired for the experimental test floor so that improvements can be made using active control. The criterion developed by Murray (1991), applicable to office and residential environments, was used in this evaluation. In this criterion, an acceptable floor is predicted if the following inequality is satisfied:

$$D > 35\ A_o\ f + 2.5 = D_{req'd}$$

where

D = predicted damping for finished floor structure, % critical

$D_{req'd}$ = damping required for satisfactory finished floor structure

A_o = maximum dynamic amplitude due to a heel drop impact, in., and

f = first natural frequency of floor system, Hz.

The damping predicted for the floor system is approximately 1-2%, much less than the 7.9% computed to be required ($D_{req'd}$) for an acceptable floor system. Therefore a problem floor, with respect to walking vibrations, is predicted for this design configuration.

2.2 Determination of Actual Test Floor Member and Material Properties

A finite element model is used, as described in Chapter 3, to extract the floor parameters for use in the analytical evaluation of the controlled system. To model the floor system as accurately as possible, measured properties were determined and recorded as described in the following subsections.

2.2.1 Joist properties

A static load test was performed on four of the seven joists prior to the erection of the deck. The load was applied by hanging sand bags, in 60 lb. increments, from the bottom chord of each joist at the center of the joist span. The maximum load applied was 300 lb. Dial gages were used to record the incremental displacements at each end of the joist in addition to the center of the joist span. The average joist displacement, corrected for support movement, was found to be 0.081 in. at a load of 300 lb. The moment of inertia for the joist is computed with the above information as follows:

$$I_j = \frac{P\ell^3}{48E\Delta} = \frac{300\text{lb}(25\text{ft} \cdot 12\text{ in / ft})^3}{48(29{,}000{,}000\text{psi})(0.081\text{ in})} = 80.1\text{ in}^4$$

(The moment of inertia, calculated from joist manufacturer's data, was 67.7 in^4.)

2.2.2 Concrete properties

Test cylinders were made from the same batch of concrete used for the test floor slab. Two of the cylinders were tested at 10 days (data for 28 days were unavailable). The average concrete weight, as determined by weighing the cylinders, was 115.7 pcf. The average concrete strength was computed from compressive tests to be 4,100 psi at 10 days. The modulus of elasticity, E_c, and the modular ratio, n, for the concrete is computed from the above information as follows:

$$E_c = 33(w_c)^{1.5}\sqrt{f'c} = 33(115.7\text{psi})^{1.5}\sqrt{4{,}100\text{psi}} = 2{,}630{,}000\text{ psi}$$

$$n = \frac{E_s}{E_c} \frac{29\text{ksi}}{2.63\text{ksi}} = 11.0$$

2.2.3 Girder properties

From experimental research, investigators (Lenzen 1966; Murray 1991) have reported composite behavior of joist and beam sections (regardless of the type of deck connection) subjected to small loads. There is some debate in the literature regarding the composite behavior of a girder supporting joists because the deck does not rest directly on the girder flange. Allen and Murray (1993) suggest an assumption of partially composite behavior pending future research. For the purposes of settling this debate for the experimental test floor, a static load test was performed to assess the load versus displacement relationship for the test floor girders. Several months after the placement of the concrete, both girders were loaded simultaneously with sandbags. The sandbags were distributed over each girder in 60 lb./ft. increments up to 180 lb./ft. Dial gages were used to record the displacement at each support and at the center of each girder span. The graph in Figure 2.2 shows three load versus centerline displacement plots for the girder. Two of the plots are theoretical predictions for composite and non-composite behavior. The theoretical lines are computed as follows:

$$\Delta = \frac{5w\ell^4}{384EI}$$

where

Δ = displacement at the center of the span

w = uniformly distributed load

ℓ = girder span, 15 ft

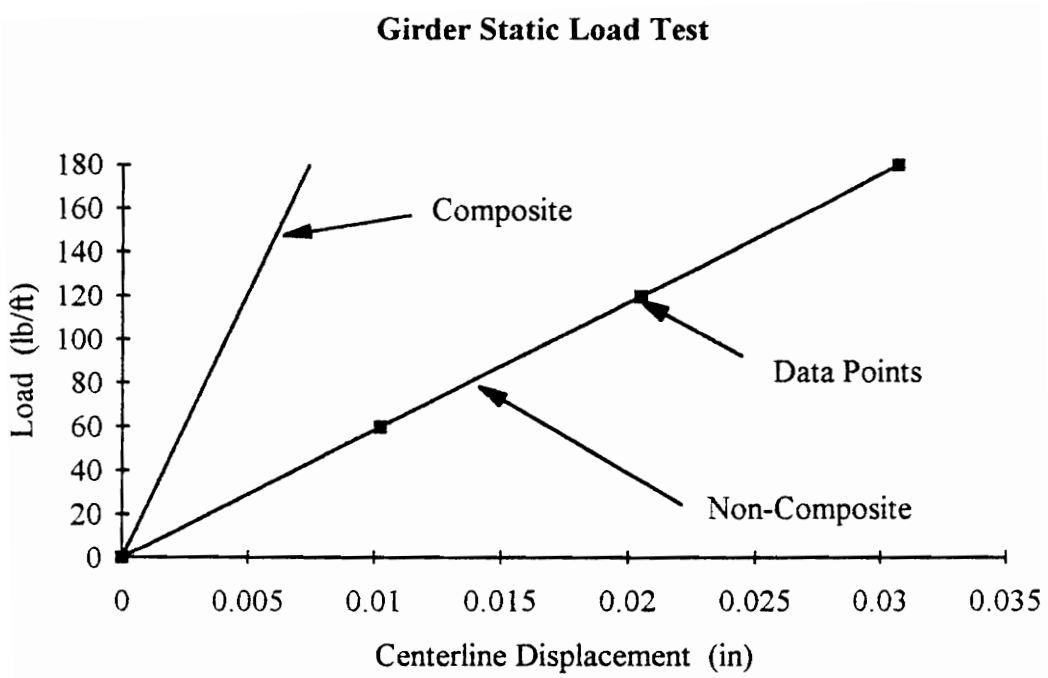

Figure 2.2 Static Load vs. Displacement Plots for Experimental Test of Girders

E = modulus of elasticity for steel, 29,000 ksi

I = composite or non-composite moment of inertia as computed below

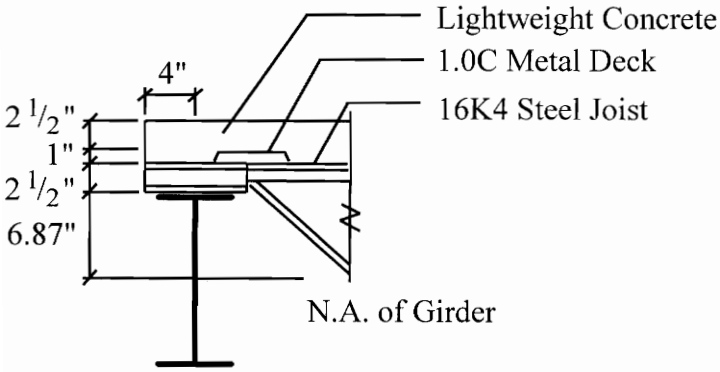

Girder Properties

$I = 199 \text{ in}^4$

$A = 6.49 \text{ in}^2$

$d = 13.740 \text{ in.}$

Concrete Properties:

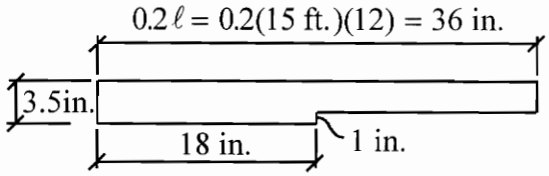

n = modular ratio = 11.0

$$A_c = \frac{(36 \text{ in.})(2.5 \text{ in.}) + (18 \text{ in.})(1.0 \text{ in.})}{11.0} = 9.82 \text{ in}^2$$

$$\bar{y} = \frac{(36 \text{ in.})(2.5 \text{ in.})(1.25 \text{ in.}) + (18 \text{ in.})(1.0 \text{ in.})(3.0 \text{ in.})}{(36 \text{ in.})(2.5 \text{ in.}) + (18 \text{ in.})(1.0 \text{ in.})} = 1.54 \text{ in.}$$

$$I_s = \frac{(36)(2.5)^3}{12(11.0)} + \frac{(18)(1)^3}{12(11.0)} + \frac{(36)(2.5)(0.29)^2}{11.0} + \frac{(18)(1.0)(1.46)^2}{11.0}$$

$$= 8.57 \text{ in}^4$$

Composite Moment of Inertia:

Distance from top of slab to neutral axis of composite section:

$$\bar{y} = \frac{6.49 \text{ in}^2(12.87 \text{ in.}) + 9.82 \text{ in}^2(1.54 \text{ in.})}{6.49 \text{ in}^2 + 9.82 \text{ in}^2} = 6.05 \text{ in.}$$

Transformed moment of inertia of composite section:

$$I_{tr} = 8.57\ in^4 + 9.82\ in^2(4.51\ in.)^2 + 199\ in^4 + 6.49\ in^2(6.82\ in.)^2 = 553.7\ in^4$$

Non-composite moment of inertia:

$$I_{tr} = 8.57\ in^4 + 199\ in^4 = 207.6\ in^4$$

The results plotted in Figure 2.2 lead to the conclusion that the girder behavior, for small loads, is most accurately modeled using non-composite section properties.

2.3 Construction and Calibration of the Force Plate

A measurement device called a force plate was used in the experimental studies to measure the excitation force imparted to the test floor. The force plate was constructed of four cantilever beam type load cells, each with a 500 lb. load capacity. A 12 in. x 12 in. x 3/8 in. bottom plate supports the four load cells. Load is transferred into the load cells by a 16 in. x 16 in. x 3/8 in. top plate supported at each corner by the load cells. The Nikkei load cells, model NSB-500, produce a voltage output which is proportional to the force measured. Each load cell was attached to a junction box which sums the voltages from the four load cells producing a single voltage output.

Calibration of the force plate was done by a static load test. The force plate was placed on a scale and loaded with steel plates to a maximum load of approximately 300 lb. The voltage output was recorded at 20 lb. increments. The change in voltage was linear throughout the load range. The calibration factor for the force plate, as determined from the static load test, is 68,124 lb/volt.

2.4 Determination of Actuator and Sensor Properties

A reaction mass actuator was used to impart control forces to the floor structure. This type of actuator introduces additional dynamics to the controlled system. As noted in the literature review, these dynamics can produce instabilities in a controlled system which would otherwise be stable. Including the actuator dynamics in the analytical studies is critical in assessing both the stability and effectiveness of the control scheme. Similarly, any dynamics introduced by the velocity sensor must also be included. An experimental study was conducted to determine the properties of the actuator and sensor. The limitations of these devices must also be carefully considered in the control scheme.

2.4.1 Sensor properties

The velocity sensor being used in the experimental studies is a PCB model 368A. The manufacturer lists a 2.5 Hz. to 2500 Hz. bandwidth of operation for this sensor. The lower limit on this bandwidth is a result of the inherent sensor dynamics. This sensor is actually a piezoelectric accelerometer with an integrator circuit. To determine the properties of this integrator circuit, both the velocity sensor and an accelerometer were subjected to the same random movement. Using a dynamic signal analyzer, a frequency response function (FRF) was recorded with the accelerometer as input and the velocity sensor as output. The integrator circuit can be expressed as a filter whose dynamics are reflected in the FRF noted above. The relationship is described by the following equations expressed in the frequency domain:

$$FRF = \frac{V}{\ddot{X}} = \frac{\ddot{X} \cdot filter}{\ddot{X}} = filter$$

where

$\ddot{X}$ = acceleration response of the random movement as measured by the accelerometer,

$V = \ddot{X} \cdot filter$ = filtered acceleration response as measured by the velocity sensor.

From the experimental FRF, the properties of the filter are estimated. Magnitude and phase plots of the experimental and estimated FRF's are shown in Figure 2.3. The Laplace transform of the estimated filter is expressed as follows:

$$filter = \frac{s}{s^2 + 2\zeta_f \omega_f s + \omega_f^2}$$

where

$\omega_f = 2\pi(1.75hz)$ = natural frequency of second order filter

$\zeta_f = 0.55$ = filter damping

This filter closely emulates the magnitude of an ideal integrator at frequencies above 2 Hz.

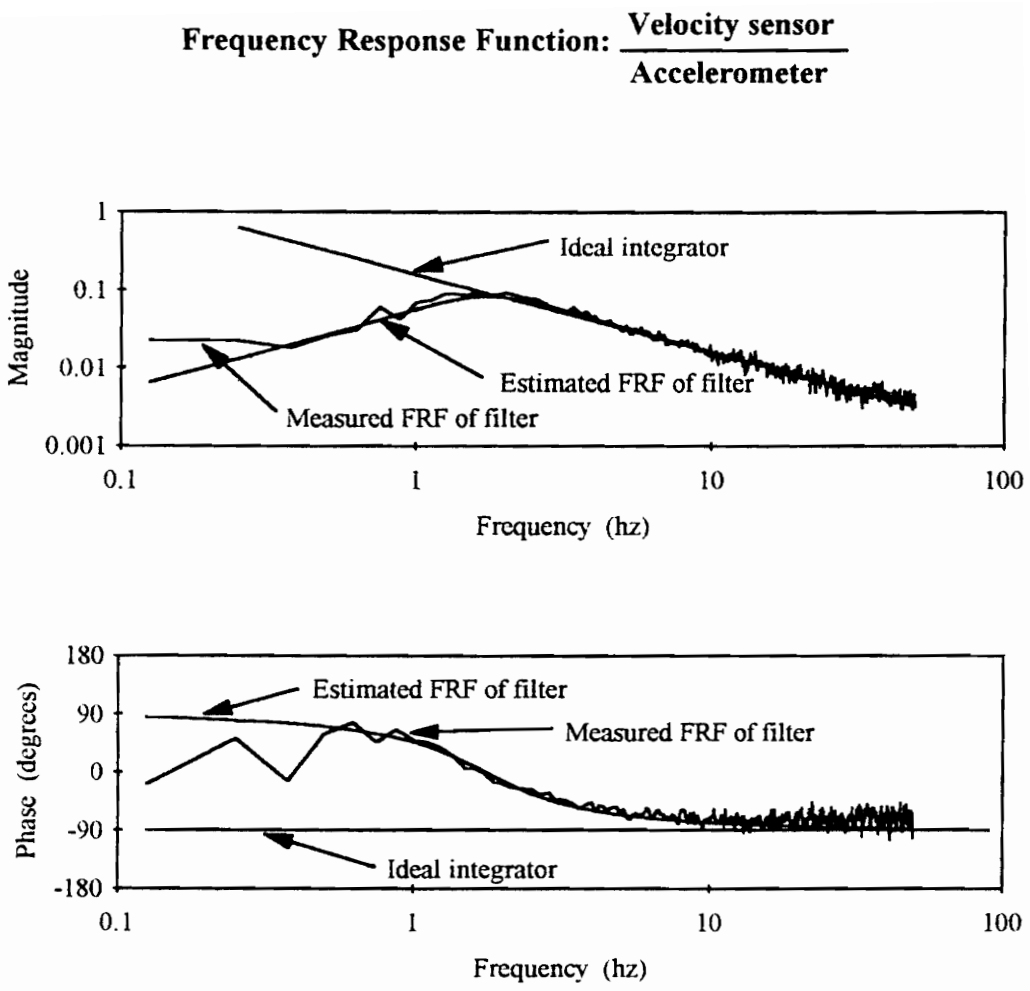

Figure 2.3 Magnitude and Phase Plots of Sensor Dynamics

2.4.2 Actuator properties

The actuator used in the experimental implementation of active control is an "Electro-seis Model 400" shaker manufactured by APS Dynamics. The dynamic behavior of the shaker can be closely described by a linear second order model (Zimmerman and Inman 1990). Illustrations of the shaker and the theoretical model are shown in Figure 2.4. The second-order model of the shaker possesses discrete masses, m_a and m_p, which represent the reaction (active) mass and the parasitic mass (support frame, etc.), respectively. The spring stiffness, k_a, is supplied by the suspension system which consists of elastic bands attached to the support frame and the reaction mass. The internal damping, due to internal motor properties and friction, is represented by c_a and is assumed to be viscous.

An experimental investigation to determine these properties was undertaken. This investigation is described and the results are presented. The first phase of the investigation was to determine the weight of the reaction mass. The manufacturer's data lists a reaction mass weight of 67 lb. To confirm this value, the actuator was placed on top of a force plate and an accelerometer was attached to the reaction mass. The shaker was driven by a random voltage input and two FRF's were measured as follows:

$$\text{FRF}(1) = \frac{\text{Force out}}{\text{Voltage in}}$$

$$\text{FRF}(2) = \frac{\text{acceleration} \cdot m_a}{\text{Voltage in}}$$

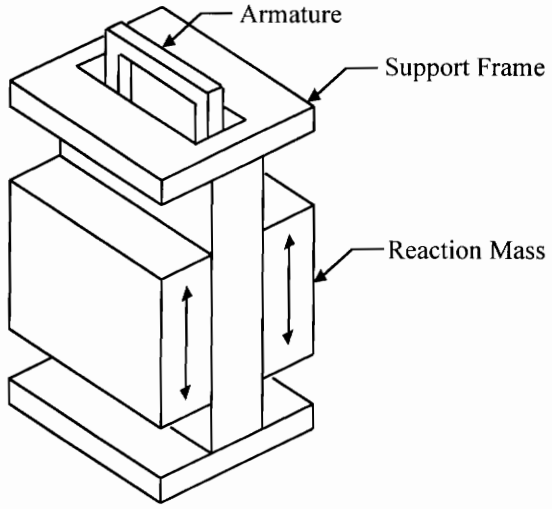

Reaction Mass Actuator: Electro-Magnetic Shaker

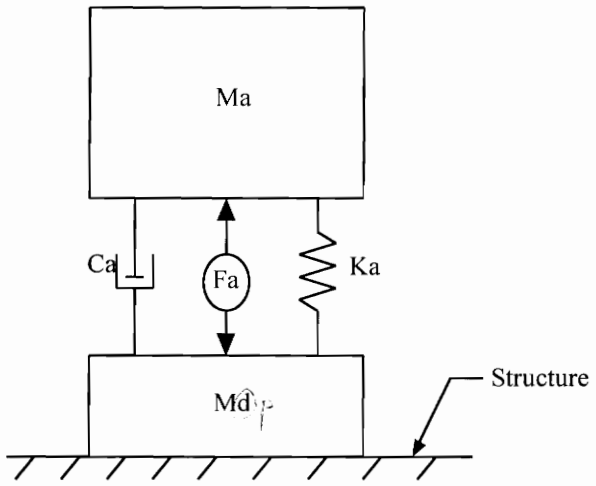

Theoretical Shaker Model

Figure 2.4 Illustration of Electro-Seis Model 400 Shaker and Theoretical Shaker Model

where

Force out: force measured by the force plate

Acceleration: acceleration measured by the accelerometer

m_a: 67 lb/386.4 in/sec^2

Voltage in: creates force in the electromagnetic coil, F_a, which is proportional to the voltage input to the shaker.

These frequency response functions are plotted in Figure 2.5. Because the force out is equivalent to the product of the mass and acceleration, the similarity of the plots confirms the assumed value for the reactive mass.

The next phase of the experimental investigation was to determine the other properties of the actuator. The linear model of the actuator can be expressed as follows:

$$\ddot{y} + 2\zeta_a\omega_a\dot{y} + \omega_a^2 y = F_a/m_a$$

where

$\ddot{y}$, $\dot{y}$, y = acceleration, velocity, displacement of the reaction mass

$\omega_a = \sqrt{k_a/m_a}$ = natural frequency of the actuator, rad./sec.

$\zeta_a = \dfrac{c_a}{2\sqrt{m_a k_a}}$ = damping ratio of the actuator

The natural frequency and the damping ratio can be estimated from the graphs in Figure 2.5. The peak in the magnitude indicates a natural frequency of approximately 1.5 Hz. The slope of the phase at this frequency indicates a damping ratio of approximately 0.29.

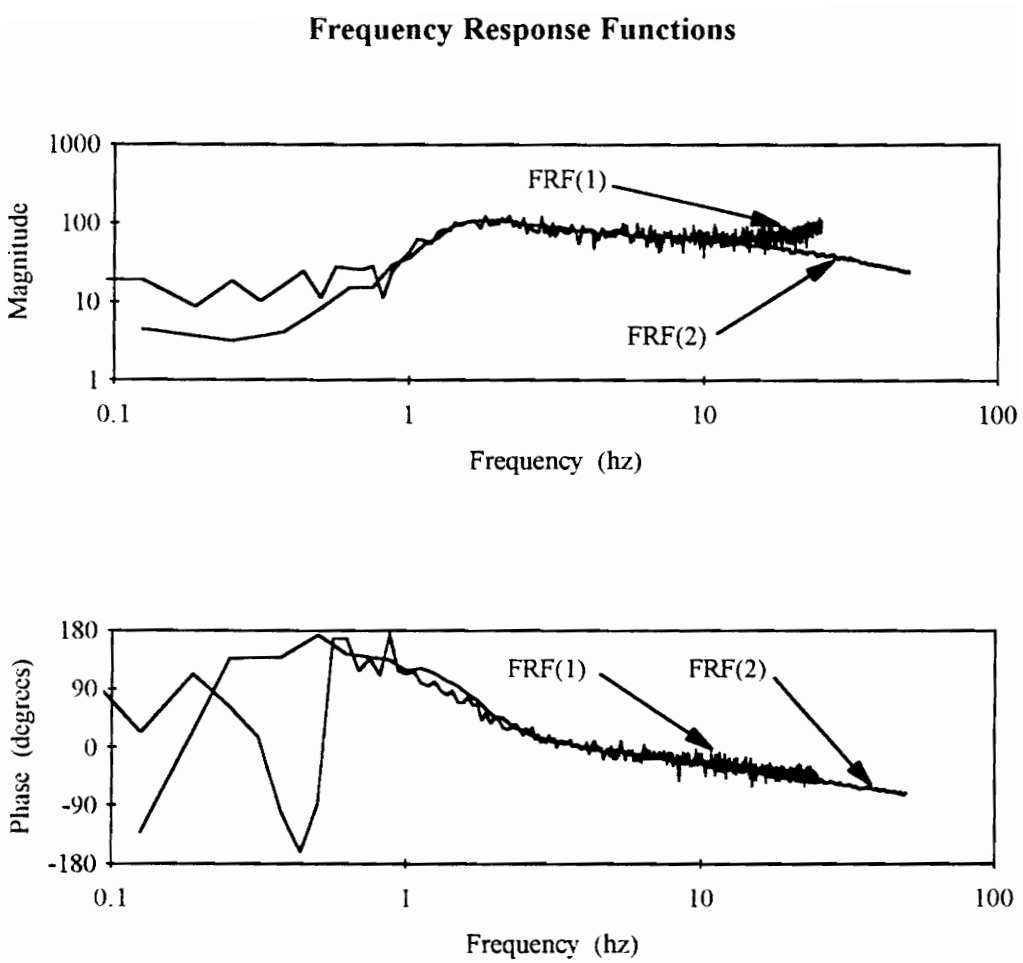

Figure 2.5 Experimental Frequency Reponse Functions for Force and Acceleration times Mass Output

As noted previously, the force in the electro-magnetic coil, F_a, is proportional to the input voltage. This relationship, as determined from experimental results, is $F_a = 60$ times the input voltage.

Stroke and force limitations must be determined and incorporated into the control circuit. The stroke of the actuator is ±3 in. and the maximum output force, as listed in the manufacturer's data, is 100 lb. for frequencies above 2.2 Hz. The actuator is driven by a voltage command input to the amplifier. This voltage command input is limited to 0.5 volts for a random input signal . Voltages above 0.5 volts trip circuit breakers in the amplifier. This limits the force in the electro-magnetic coil to 30 lb.

To confirm the properties of the actuator and velocity sensor, an FRF was measured and compared with the theoretical FRF of the modeled system. A schematic of this model is shown in Figure 2.6. The measured and theoretical FRF's are shown in Figure 2.7. The theoretical model compares well with the experimental results in the frequency range of 1 to 10 Hz. Above 10 Hz., there is some magnitude roll-off. This is not of major concern because the modes of vibration which contribute significantly to the floor response are not generally much over 10 Hz.

Theoretical Model of the Actuator and Velocity Sensor

$$FRF = \frac{V_{out}}{V_{in}}$$

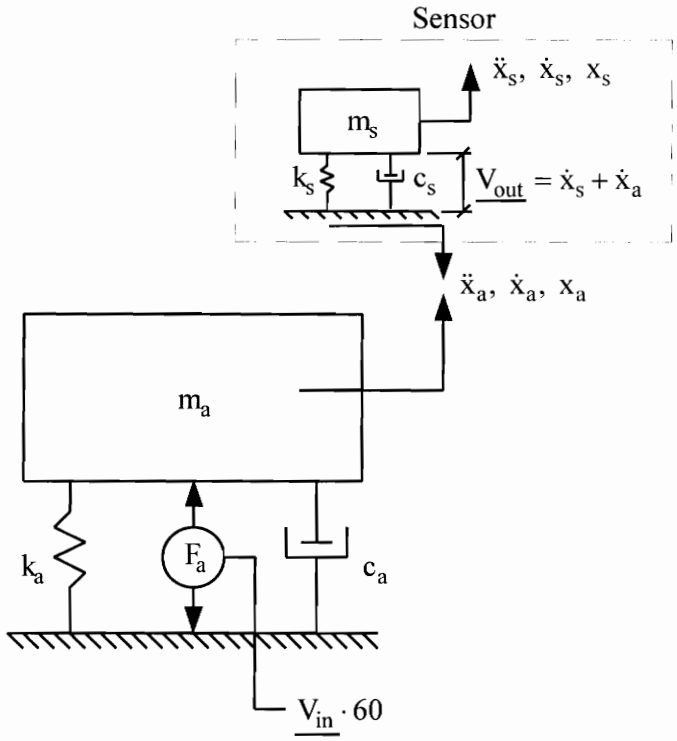

Sensor Properties

$m_s = 1$

$k_s = \omega_s^2 = 120.9$ lb/in

$c_s = 2\zeta_s\omega_s = 12.1$ lb/(in/sec)

V_{out} = Voltage output from sensor

Actuator Properties

$m_a =$ 67 lb / 386.4(in/sec)

$k_a = m_a\omega_a^2 = 15.4$ lb/in

$c_a = 2\zeta_a\sqrt{m_a k_a} = 5.46$ lb/(in/sec)

$F_a = V_{in}(\text{volts}) \cdot 60$

$V_{in} =$ Voltage input to shaker

Figure 2.6 Theoretical Model and Properties of the Actuator and Velocity Sensor

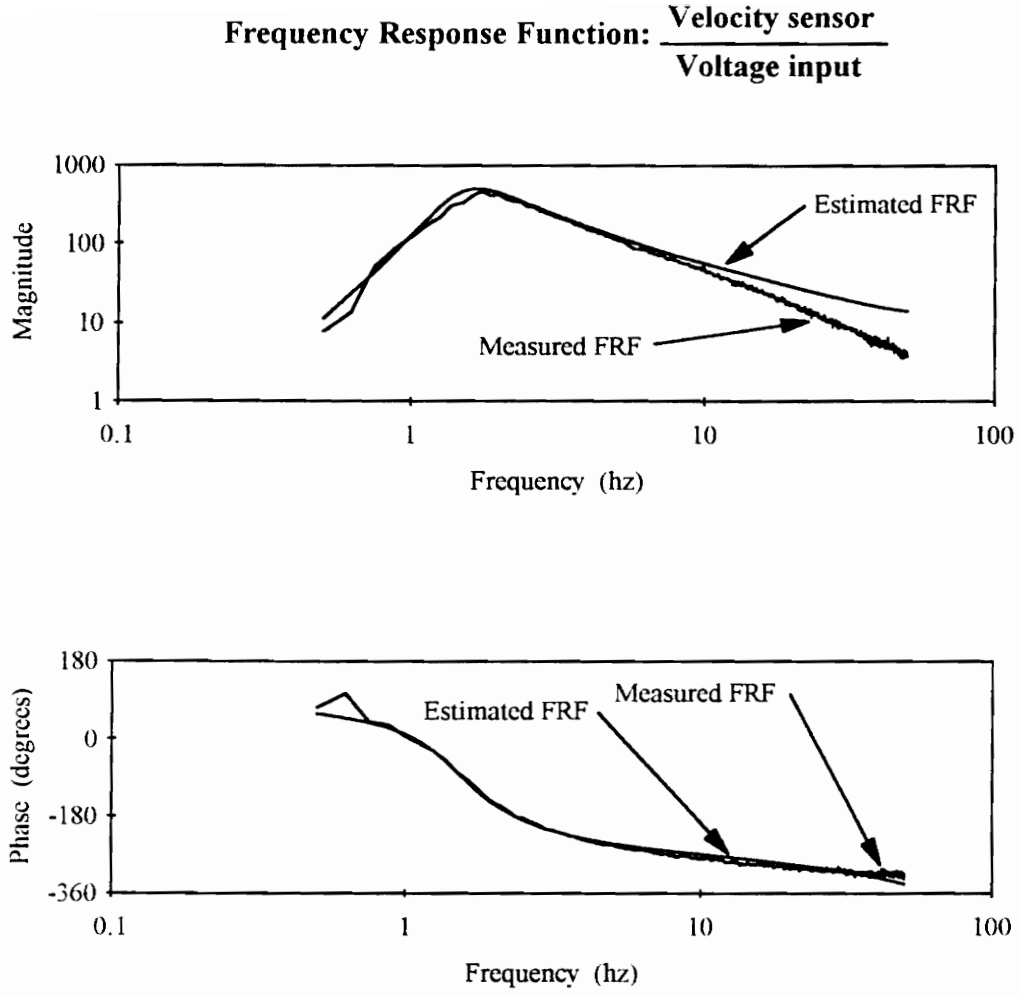

Figure 2.7 Experimental and Estimated Frequency Response Functions for the Actuator and Velocity Sensor System

CHAPTER 3

ANALYTICAL EVALUATION OF TEST FLOOR CONTROL

3.1 Development of Analytical Model

An analytical model of the controlled floor system is developed and studied using matrix computation software called MATLAB (MATLAB 1993). MATLAB has a set of routines in the Control System Toolbox (Grace *et al.* 1992) specifically designed for studying control systems. The routines require a state space representation of the system. In the following subsections the state-space representation of the system model is developed and specific parameters for the experimental test floor are derived.

3.1.1 The state-space representation

The state-space representation of a lumped-parameter system is best illustrated by an example. Consider a two-degree-of-freedom system described as follows by the system of differential equations in matrix form:

$$\begin{bmatrix} m_1 & 0 \\ 0 & m_2 \end{bmatrix} \begin{Bmatrix} \ddot{y}_1 \\ \ddot{y}_2 \end{Bmatrix} + \begin{bmatrix} c_1 + c_2 & -c_2 \\ -c_2 & c_2 \end{bmatrix} \begin{Bmatrix} \dot{y}_1 \\ \dot{y}_2 \end{Bmatrix} + \begin{bmatrix} k_1 + k_2 & -k_2 \\ -k_2 & k_2 \end{bmatrix} \begin{Bmatrix} y_1 \\ y_2 \end{Bmatrix} = \begin{Bmatrix} F_1(t) \\ F_2(t) \end{Bmatrix} \tag{3.1}$$

The general form of the state space realization is

$$\dot{X} = AX + BU \tag{3.2}$$

$$Y = CX + DU \tag{3.3}$$

where

X = state vector

Y = output vector

U = input vector

For the example above, the state vector can be defined as $x_1 = y_1$, $x_2 = y_2$, $x_3 = \dot{y}_1$, and $x_4 = \dot{y}_2$ and the system of equations is written in terms of the state vector and rearranged as follows:

$$\begin{Bmatrix} \dot{x}_1 \\ \dot{x}_2 \\ \dot{x}_3 \\ \dot{x}_4 \end{Bmatrix} = \begin{bmatrix} 0 & 0 & 1 & 0 \\ 0 & 0 & 0 & 1 \\ \frac{-(k_1+k_2)}{m_1} & \frac{k_2}{m_1} & \frac{-(c_1+c_2)}{m_1} & \frac{c_2}{m_1} \\ \frac{k_2}{m_1} & -\frac{k_2}{m_1} & \frac{c_2}{m_1} & -\frac{c_2}{m_1} \end{bmatrix} \begin{Bmatrix} x_1 \\ x_2 \\ x_3 \\ x_4 \end{Bmatrix} + \begin{bmatrix} 0 & 0 \\ 0 & 0 \\ \frac{1}{m_1} & 0 \\ 0 & \frac{1}{m_2} \end{bmatrix} \begin{Bmatrix} F_1(t) \\ F_2(t) \end{Bmatrix} \tag{3.4}$$

$$\begin{Bmatrix} y_1 \\ y_2 \\ \dot{y}_1 \\ \dot{y}_2 \end{Bmatrix} = \begin{bmatrix} 1 & 0 & 0 & 0 \\ 0 & 1 & 0 & 0 \\ 0 & 0 & 1 & 0 \\ 0 & 0 & 0 & 1 \end{bmatrix} \begin{Bmatrix} x_1 \\ x_2 \\ x_3 \\ x_4 \end{Bmatrix} + \begin{bmatrix} 0 & 0 \end{bmatrix} \begin{Bmatrix} F_1(t) \\ F_2(t) \end{Bmatrix} \tag{3.5}$$

In this form, the matrices A, B, C, and D defining the state space are easily identified.

3.1.2 Modal model including actuator and sensor dynamics

The behavior of the distributed-parameter floor system is simulated mathematically using a lumped-parameter model possessing m modal coordinates and n spatial coordinates. This mathematical model is formulated as follows:

$$M^* \cdot \ddot{Z} + C^* \cdot \dot{Z} + K^* \cdot Z = \Phi^T \cdot F(t) \tag{3.6}$$

$$y = \Phi \cdot Z \tag{3.7}$$

$$\dot{y} = \Phi \cdot \dot{Z} \tag{3.8}$$

where

$$\ddot{Z} = \begin{Bmatrix} \ddot{z}_1 \\ \ddot{z}_2 \\ \vdots \\ \ddot{z}_m \end{Bmatrix} = \begin{matrix} \text{modal} \\ \text{acceleration;} \\ \text{vector} \end{matrix} \quad \dot{Z} = \begin{Bmatrix} \dot{z}_1 \\ \dot{z}_2 \\ \vdots \\ \dot{z}_m \end{Bmatrix} = \begin{matrix} \text{modal} \\ \text{velocity;} \\ \text{vector} \end{matrix} \quad Z = \begin{Bmatrix} z_1 \\ z_2 \\ \vdots \\ z_m \end{Bmatrix} = \begin{matrix} \text{modal} \\ \text{displacement} \\ \text{vector} \end{matrix}$$

$$\dot{Y} = \begin{Bmatrix} \dot{y}_1 \\ \dot{y}_2 \\ \vdots \\ \dot{y}_n \end{Bmatrix} = \begin{matrix} \text{spatial} \\ \text{velocity;} \\ \text{vector} \end{matrix} \quad Y = \begin{Bmatrix} y_1 \\ y_2 \\ \vdots \\ y_n \end{Bmatrix} = \begin{matrix} \text{spatial} \\ \text{displacement;} \\ \text{vector} \end{matrix} \quad F(t) = \begin{Bmatrix} F_1(t) \\ F_2(t) \\ \vdots \\ F_n(t) \end{Bmatrix} = \begin{matrix} \text{input} \\ \text{force} \\ \text{vector} \end{matrix}$$

$$\Phi = \begin{bmatrix} \Phi_{11} & \Phi_{12} & \cdots & \Phi_{1m} \\ \Phi_{21} & \Phi_{22} & \cdots & \Phi_{2m} \\ \vdots & \vdots & \ddots & \vdots \\ \Phi_{n1} & \Phi_{n2} & \cdots & \Phi_{nm} \end{bmatrix} = \begin{bmatrix} \Phi_1 \\ \Phi_2 \\ \vdots \\ \Phi_n \end{bmatrix} = \begin{matrix} \text{modal} \\ \text{transformation} \\ \text{matrix} \end{matrix}$$

$$M^* = \begin{bmatrix} 1 & 0 & \cdots & 0 \\ 0 & 1 & & 0 \\ \vdots & & \ddots & \\ 0 & 0 & & 1 \end{bmatrix}_{mxm} = \begin{matrix} \text{modal} \\ \text{mass} \\ \text{matrix} \end{matrix}$$

$$C^* = \begin{bmatrix} 2\zeta_1\omega_1 & 0 & \cdots & 0 \\ 0 & 2\zeta_2\omega_2 & & 0 \\ \vdots & & \ddots & \\ 0 & 0 & & 2\zeta_m\omega_m \end{bmatrix} = \begin{matrix} \text{modal} \\ \text{damping} \\ \text{matrix} \end{matrix}$$

ζ_i = modal damping coefficient for i_{th} mode

ω_i = natural frequency for i_{th} mode

$$K^* = \begin{bmatrix} \omega_1^2 & 0 & \cdots & 0 \\ 0 & \omega_2^2 & & 0 \\ \vdots & & \ddots & \\ 0 & 0 & & \omega_m^2 \end{bmatrix} = \begin{matrix} \text{modal} \\ \text{stiffness} \\ \text{matrix} \end{matrix}$$

This model of the floor system can be expanded to include the actuator dynamics and the signal input to the amplifier. The actuator adds an additional degree of freedom to the system as follows:

$$\left[\begin{array}{c|c} M^* + \Phi_a^T \cdot m_d \cdot \Phi_a & 0 \\ \hline 0 & m_a \end{array}\right] \left\{\begin{array}{c} \ddot{Z} \\ \hline \ddot{z}_{m+1} \end{array}\right\} + \left[\begin{array}{c|c} C^* + \Phi_a^T \cdot c_a \cdot \Phi_a & -c_a \cdot \Phi_a^T \\ \hline -c_a \cdot \Phi_a & c_a \end{array}\right] \left\{\begin{array}{c} \dot{Z} \\ \hline \dot{z}_{m+1} \end{array}\right\}$$
$$+ \left[\begin{array}{c|c} K^* + \Phi_a^T \cdot k_a \cdot \Phi_a & -k_a \cdot \Phi_a^T \\ \hline -k_a \cdot \Phi_a & k_a \end{array}\right] \left\{\begin{array}{c} Z \\ \hline z_{m+1} \end{array}\right\} = \left\{\begin{array}{c} \Phi^T \cdot F(t) \\ \hline 0 \end{array}\right\} + \left[\begin{array}{c} \Phi_a^T \\ \hline -1 \end{array}\right] \cdot F_a(t) \qquad (3.9)$$

where

$\ddot{z}_{m+1}, \dot{z}_{m+1}, z_{m+1}$ = actuator mass acceleration, velocity, and displacement, respectively

m_a, m_d, c_a, k_a = actuator properties as noted in Figure 2.4

Φ_a = actuator coordinate transformation vector at spatial coordinate a

$F_a(t) = 60 \cdot v(t)$ =shaker input force as noted in Figure 2.4

v(t) = voltage input signal to shaker amplifier

The sensor dynamics must also be added to a particular output coordinate. The system of equations above can be expressed in the state space, including the sensor dynamics, by defining the state space variables in the general form:

$$\dot{X} = AX + BU \tag{3.10}$$

$$Y = CX + DU \tag{3.11}$$

where

$$X^T = \{x_1 \quad x_2 \quad \cdots \quad x_{2n+4}\}^T = \{z_1 \quad \cdots \quad z_{m+1} \quad \dot{z}_1 \quad \cdots \quad \dot{z}_{m+1} \quad z_s \quad \dot{z}_s\}^T$$

$$Y^T = \{y_1 \quad y_2 \quad \cdots \quad y_n \quad y_a \quad \dot{y}_1 \quad \dot{y}_2 \quad \cdots \quad \dot{y}_n \quad \dot{y}_a \quad \dot{y}_s$$

$$A = \left[\begin{array}{cccc:cc} 0_{mxm} & 0_{mx1} & I_{mxm} & 0_{mx1} & 0_{mx1} & 0_{mx1} \\ 0_{1xm} & 0 & 0_{1xm} & 1 & 0 & 0 \\ -\dfrac{K^* + K_a^*}{M^* + M_a^*} & \dfrac{k_a \cdot \Phi_a^T}{M^* + M_a^*} & -\dfrac{C^* + C_a^*}{M^* + M_a^*} & \dfrac{c_a \cdot \Phi_a^T}{M^* + M_a^*} & 0_{mx1} & 0_{mx1} \\ \dfrac{k_a \cdot \Phi_a}{m_a} & -\dfrac{k_a}{m_a} & \dfrac{c_a \cdot \Phi_a}{m_a} & -\dfrac{c_a}{m_a} & 0 & 0 \\ \hdashline 0_{1xm} & 0 & 0_{1xm} & 0 & 0 & 1 \\ -\omega_s^2 \cdot \Phi_s & 0 & -2\zeta_s\omega_s \cdot \Phi_s & 0 & -\omega_s^2 & -2\zeta_s\omega_s \end{array}\right]$$

where

$$K_a^* = \Phi_a^T \cdot k_a \cdot \Phi_a$$

$$C_a^* = \Phi_a^T \cdot c_a \cdot \Phi_a$$

$$M_a^* = \Phi_a^T \cdot m_a \cdot \Phi_a$$

Φ_s = sensor coordinate transformation vector at spatial coordinate s

ω_s, ζ_s = sensor properties as noted in Figure 2.6

y_a, $\dot{y}_a$ = actuator displacement and velocity, respectively

$\dot{y}_s$ = velocity sensor output

$$U = \begin{Bmatrix} F(t) \\ F_a(t) \end{Bmatrix}$$

$$B = \begin{bmatrix} 0_{mxn} & 0_{mx1} \\ 0_{1xn} & 0 \\ \dfrac{\Phi^T}{M^* + M_a^*} & \dfrac{\Phi_a^T}{M^* + M_a^*} \\ 0_{1xn} & -\dfrac{1}{M^* + M_a^*} \\ \hline 0_{1xn} & 0 \\ 0_{1xn} & 0 \end{bmatrix}$$

$$C = \begin{bmatrix} \Phi & 0_{nx1} & 0_{nxm} & 0_{nx1} & 0_{nx1} & 0_{nx1} \\ 0_{1xm} & 1 & 0 & 0 & 0 & 0 \\ 0_{nxm} & 0_{nx1} & \Phi & 0_{nx1} & 0_{nx1} & 0_{nx1} \\ 0_{1xm} & 0 & 0_{1xm} & 1 & 0 & 0 \\ 0_{1xm} & 0 & \Phi_s & 0 & 0 & 1 \end{bmatrix}$$

$$D = \begin{bmatrix} 0_{1xn} & 0 \end{bmatrix}$$

The partitions in matrices A, B, and C denote the additional dynamics added by the sensor to the system. This system of equations represents a multi-input/multi-output system which was used in MATLAB to study active control of floor vibrations.

3.1.3 Determination of test floor system matrices

To study the experimental test floor, the floor system matrices K* and C* (Equation 3.6), must be determined. The first decision to be made is the number of modes, m, to be included in the analytical model. Several factors affected this decision. Research by Pernica (1990) quantifies dynamic load factors for walking and other rhythmic activities. These factors were experimentally determined by measuring the forces created by these activities. Walking has been shown to produce an excitation which, when expressed in the frequency domain, has frequency content at harmonic multiples of the step frequency. The frequency magnitude at each harmonic decreases as the multiple of the step frequency increases. The step frequency for walking was observed to be between 1 and 3 Hz. Dynamic load factors were found to be 0.56, 0.28, 0.16, 0.09 for the first four harmonics of the step frequency. Because of this relationship, higher-frequency modes (>30 Hz.) of vibration do not contribute significantly to the response of a floor system excited by walking vibrations. The higher-order modes are, therefore, neglected in the analytical model.

Preliminary testing of the test floor confirmed that only the lower-frequency modes of vibration contributed significantly to the floor response due to walking or heel drop excitation. The first five modes of vibration are therefore included in the analytical model. Because K^* and C^* are global parameters (i.e., not unique to a single floor location), they can be determined from relatively few experimental measurements. A series of experimental heel drop tests was conducted to determine the natural frequency

and damping ratios for the first five modes of vibration. A frequency response function was computed from experimental force and velocity measurements at several locations on the test floor. A sample measurement recorded at the center of the test floor is shown in Figure 3.1. The frequency response shows three sharp peaks, corresponding to the three different modes of vibration excited by the heel drop at the center of the floor. Other modes, producing no amplitude at the center of the test floor, were determined from heel drop measurements at the center of the girder and at the center of an edge joist. The frequency, ω_d, at the first sharp peak, mode 1, is 7.3 Hz. The damping ratio for this frequency can be determined by a method called quadrature peak picking (Inman 1994, p. 379). In a lightly damped system, the modal damping ratio, ζ, is related to the two frequencies, ω_a and ω_b, corresponding to the points on the magnitude plot where the magnitude equals $/\sqrt{2}$ times the magnitude at the peak. The modal damping ratio is defined as follows:

$$\zeta = \frac{\omega_b - \omega_a}{2\omega_d}$$

Table 3.1 lists the first five natural frequencies and damping ratios, as determined by this method.

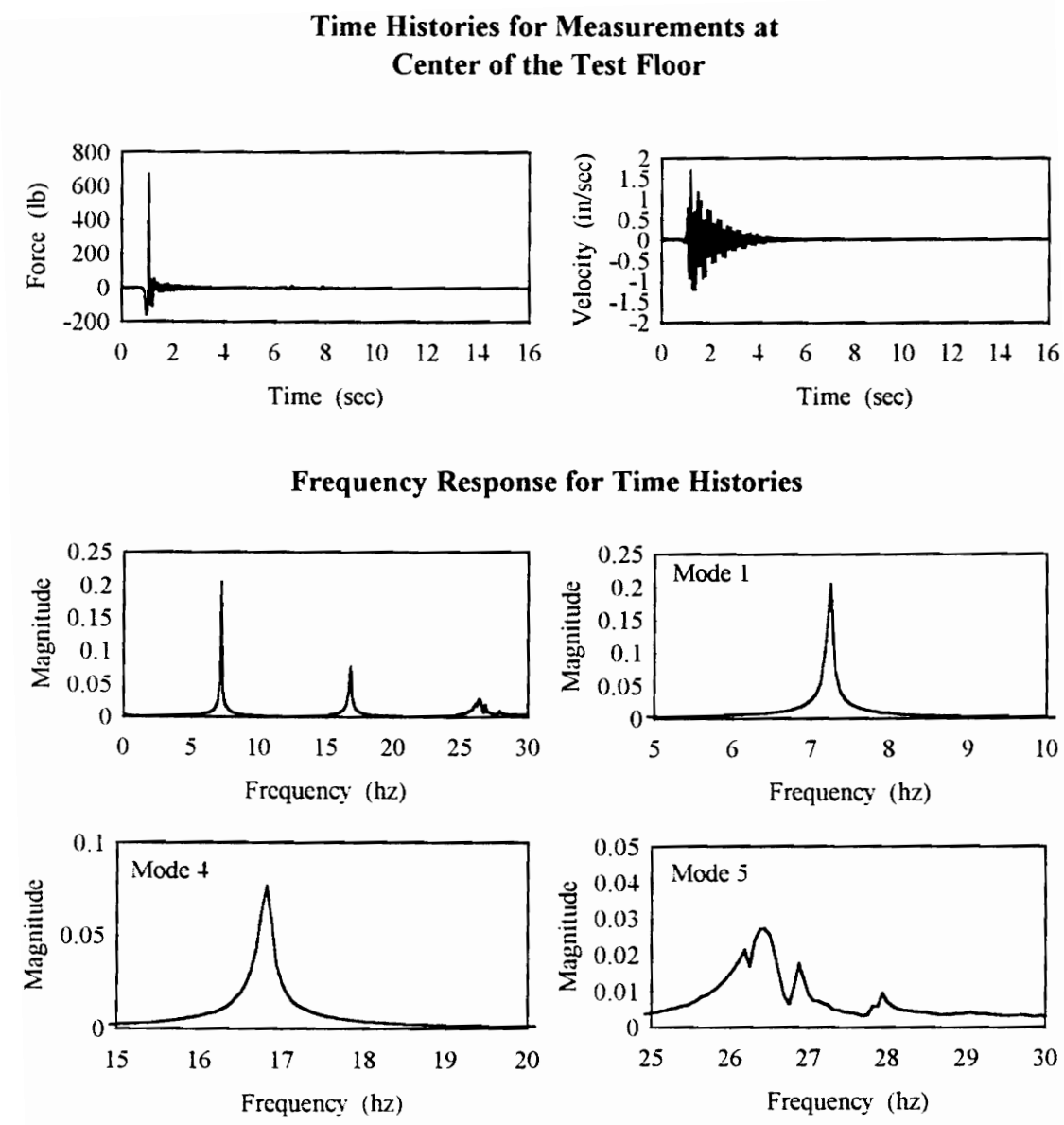

Figure 3.1 Time Histories and Frequency Response
at the Center of the Test Floor

Table 3.1 Experimentally Determined Natural Frequencies and Damping Ratios for Experimental Test Floor

	Frequency (Hz.)	Damping ratio (ζ)
Mode 1	7.3	0.0050
Mode 2	9.4	0.0085
Mode 3	16.5	0.0085
Mode 4	16.9	0.0050
Mode 5	26.5	0.0055

The mode shapes corresponding to these natural frequencies could also be determined through experimental testing using the methods of experimental modal analysis. With the experimental equipment and software available for this research, experimental modal analysis would be a very tedious and time-consuming endeavor. The aim of this research is not to construct a precise modal model of the test floor. The aim is to construct a model whose dynamic behavior resembles that of the test floor. A finite element model will, therefore, be used to construct the Φ matrix. The finite element model is described in the following section.

3.1.4 Finite element model of test floor

The FE model developed utilizes beam elements for modeling the steel framing members, and plate elements for modeling the concrete slab and deck, in a single plane. This model is best described as a grid model and has been shown (Morley and Murray 1993) to be successful in predicting dynamic floor behavior.

The model was developed using a commercially available structural analysis software package called SAP90 (Wilson and Habibullah 1992). A mesh size of 30 in. x 30 in. was used, producing 77 spatial coordinates in the system. Measured properties, as recorded in Chapter 2, were used in the analysis. Details of the model are shown in Figure 3.2. An analysis was also performed using a refined mesh size of 15 in. x 15 in. No significant change was noted in the dynamic response of the system due to this refinement. The 30 in. x 30 in. mesh is therefore considered sufficiently fine for the purposes of this study.

After the construction of the model, SAP90 was used to compute the first 10 eigenvalues and eigenvectors of the system. The first natural frequency, related to the lowest eigenvalue, computed from the model was compared with that measured experimentally on the test floor. The first natural frequency of the test floor is 7.3 Hz. The model predicted 8.5 Hz. A more accurate prediction of floor behavior was desired. Further experimental testing revealed significant movement at the supports. An experiment was conducted to quantify the effect of the support displacement.

The actuator was placed at the center of the test floor. A 7.3 Hz sine wave was used to drive the shaker and excite the floor at the first natural frequency. The peak velocities were measured at the center of the floor and over each support. These displacements are shown in Table 3.2.

Finite Element Model Properties and Geometry

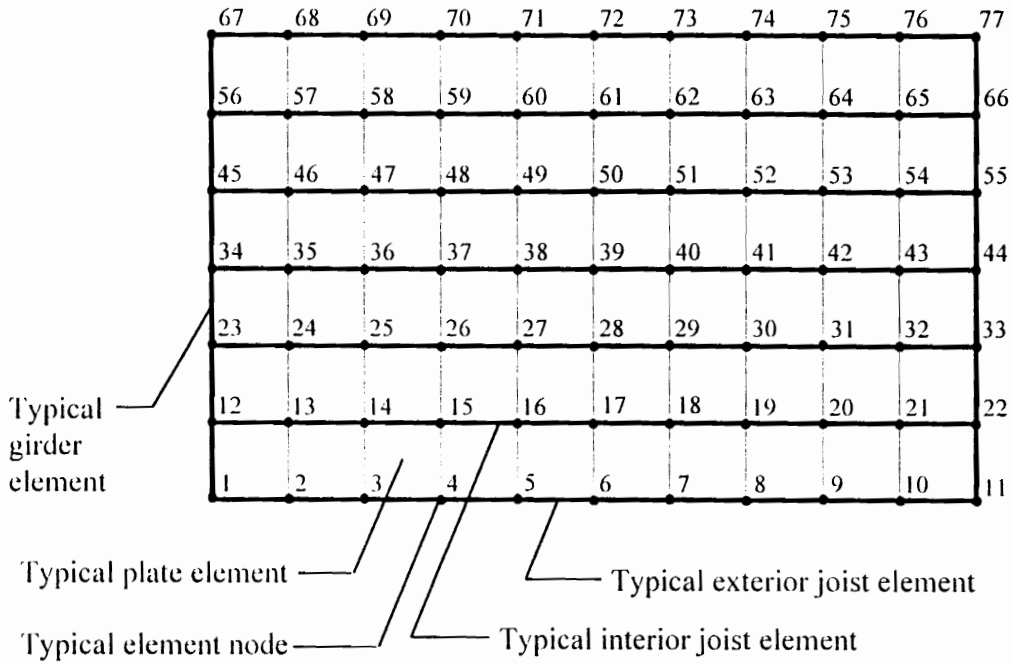

Element Properties

Beam elements:	Girder	Interior joist	Exterior joist	Plate elements:	
Iy (in^4)	199	181.7	175.3	Bending thickness (in)	3
A (in^2)	6.49	1.90	1.90	Membrane thickness (in)	3
E (psi)	29,000,000	29,000,000	29,000,000	E (psi)	2,630,000
w (lb/in)	1.84	0.538	0.538	w (lbs/in^3)	0.0716

Figure 3.2 Finite Element Model Properties and Geometry

Table 3.2 Peak Velocities Measured on Experimental Test Floor

Measurement location	Peak velocity amplitude, δ
Center of the floor	1.383 in/sec
Support 1	0.261 in/sec
Support 2	0.304 in/sec
Support 3	0.263 in/sec
Support 4	0.213 in/sec
Average of supports	0.260 in/sec

The following calculation is a derivation for an estimate of the first natural frequency of the system neglecting support movement.

Equivalent single degree-of-freedom system:

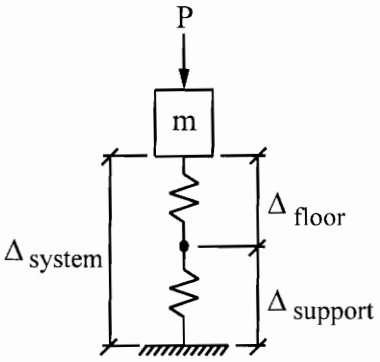

$$\Delta_{system} = \Delta_{floor} + \Delta_{support}$$

$$f_{system} = \sqrt{\frac{k_{system}}{m}}$$

$$k_{system} = \frac{P}{\Delta_{system}} = f_{system}^2 \bullet m$$

$$P = f_{system}^2 \bullet m \bullet \Delta_{system}$$

$$k_{floor} = \frac{P}{\Delta_{floor}} = \frac{m \bullet f_{system}^2 \bullet \Delta_{system}}{\Delta_{system} - \Delta_{support}}$$

$$f_{floor} = \sqrt{\frac{k_{floor}}{m}} = f_{system}\sqrt{\frac{\Delta_{system}}{\Delta_{system} - \Delta_{support}}}$$

$$= f_{system}\sqrt{\frac{\delta_{system}}{\delta_{system} - \delta_{support}}} = 7.3\sqrt{\frac{1.383}{1.383 - 0.260}} = 8.1 \text{ Hz.}$$

The frequency estimated with the support movement removed compares more favorably with the 8.5 Hz. estimated in the FE analysis.

Spring supports were added to the FE model to include the effects of support movement. The stiffness of these springs was adjusted to result in a model first natural frequency of 7.3 Hz. The first six natural frequencies and corresponding mode shapes, as computed by the SAP90 analysis, are presented in Figure 3.3. The mode shapes for the first five natural frequencies of the floor system are used to form the Φ matrix in the state space model.

3.2 Evaluation of Linear Control Effectiveness

In the following subsections, a discussion pertaining to the selection of the control law is presented, followed by several analytical studies of the controlled system aimed at illustrating the effect of the control scheme.

3.2.1 Selection of the control law

Many factors must be considered when designing a controller for a complex structure. Optimal control algorithms are very enticing because of their possible energy efficiency and systematic approach to design. Problems begin to arise when these algorithms are implemented experimentally. While reduced-order models and controllers are necessary for practical implementation, they often result in control forces which can lead to instabilities or spillover into uncontrolled modes. Because optimal control usually requires full state feedback, a great deal of information is required about the structure. A

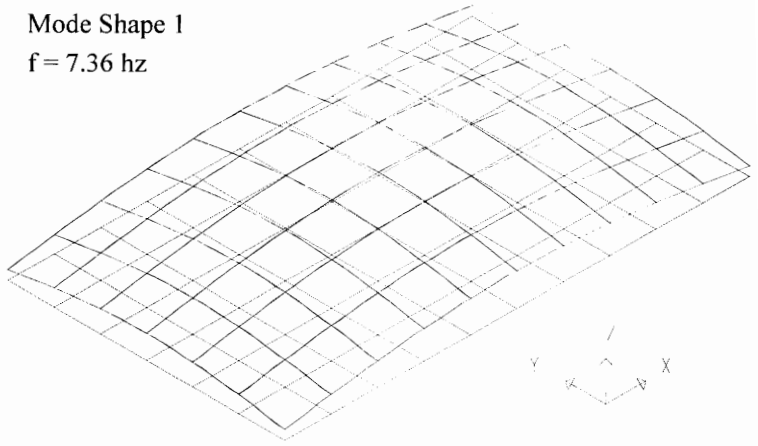

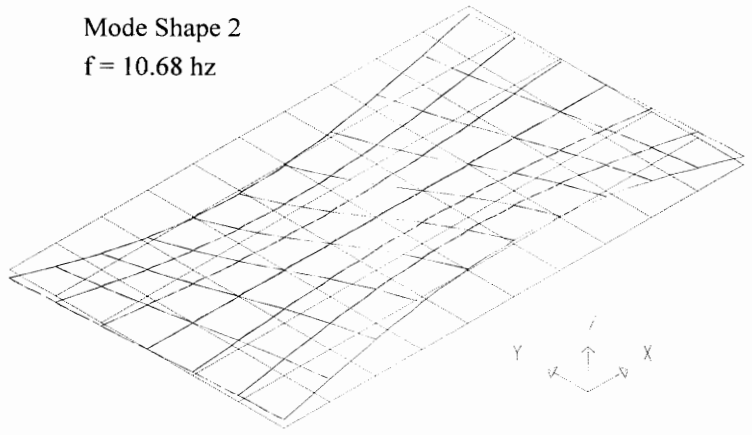

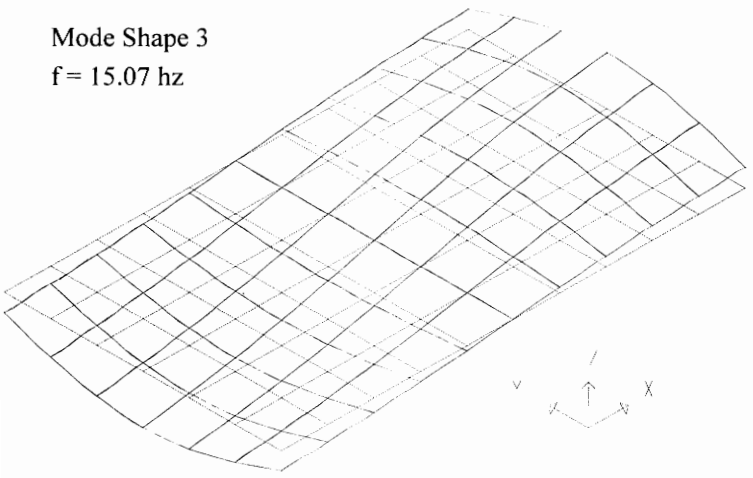

Figure 3.3 Mode Shapes from SAP90 Analysis

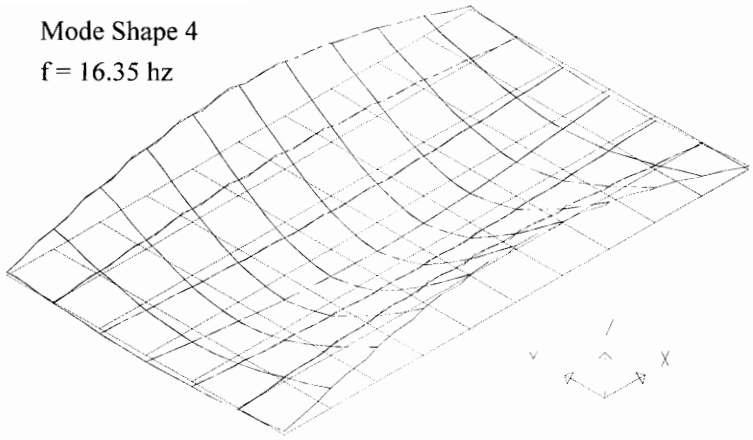

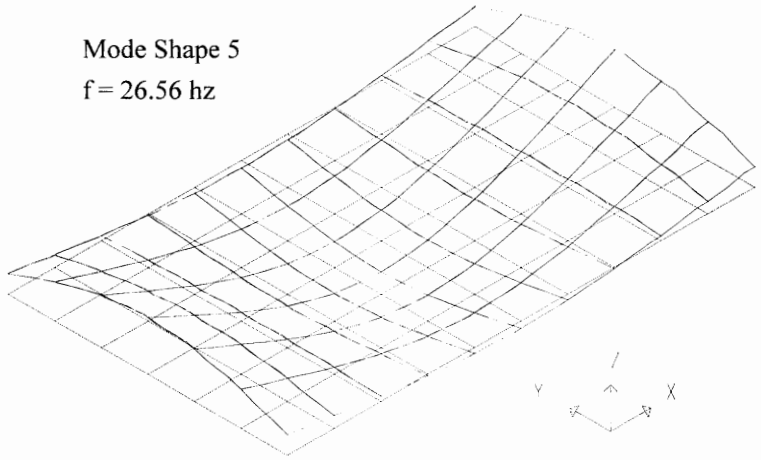

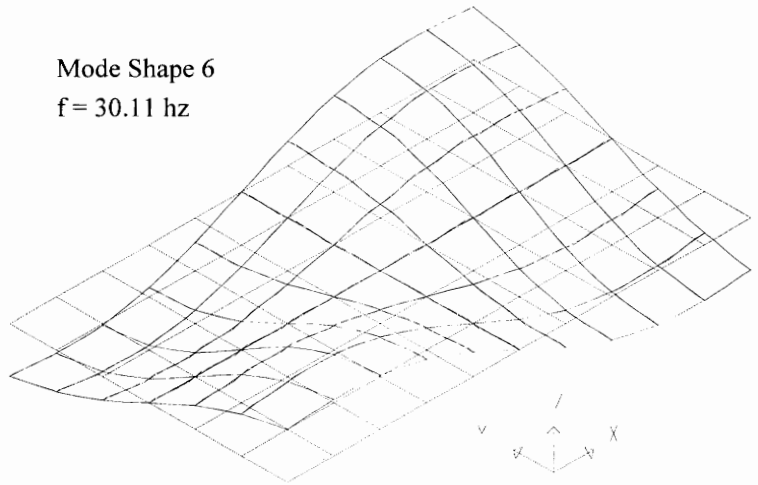

Figure 3.3 (continued) Mode Shapes from SAP90 Analysis

large number of sensors in addition to a very accurate model of the structure is necessary. When these factors are combined with those noted in the previous section, optimal control is not necessarily synonymous with "best" control.

The best control is different for every application. For application in floor systems, the controller must be robust to system uncertainties and changes. Because human perception to floor vibrations is very acute, the best controller should not increase the response of higher modes in order to control lower modes. As illustrated in Figure 1.1, perceptible displacement amplitudes of vibration decrease as the frequency increases. In light of the many complex factors involved in actively controlling a floor system, the ultimate assessment of the control scheme depends on the question: Does the floor feel better?

As noted in the Background of Chapter 1, an objectionable floor system can be improved by adding damping to the structure. A commonly utilized control law, direct velocity feedback (collocated rate feedback), was selected for experimental implementation because of its ability to add damping to the system while providing the necessary robustness. In this method, velocity sensor output is multiplied by gains and fed back to collocated force actuators. The merit of this method is that the spillover is always stabilizing. In fact, in the absence of actuator and sensor dynamics, direct velocity feedback is unconditionally stable (Balas 1979b).

For a single actuator/sensor pair, as is the case in this research, this control law is expressed as $F_a = -g \cdot \dot{y}_s$, where $\dot{y}_s$ is the velocity measured by the velocity sensor and g is the control gain.

3.2.2 Linear system roots and the root locus

In a single-input/single-output control scheme, classical control techniques are very helpful in understanding the system behavior. The root locus, in effect, maps the complex linear system roots for control gains ranging from zero to infinity. The first mode of vibration was selected as the main target of control. To control this mode, the actuator and velocity sensor are placed at the center of the test floor defined in the finite element model as spatial node 39 noted in Figure 3.2.

The multi-input/multi-output system, described by Equations 3.10 and 3.11, is reduced to a single-input/single-output system by redefining the following vectors:

$$U = F_a$$

$$B^T = \left[\begin{array}{cccccc} 0_{mx1} & 0 & \dfrac{\Phi_a^T}{M^* + M_a^*} & \dfrac{-1}{M^* + M_a^*} & 0 & 0 \end{array} \right]^T$$

$$C = \left[0_{mx1} \quad 0 \quad \Phi_s \quad 0 \quad 0 \quad 1 \right]$$

where $\Phi_s = \Phi_a = \Phi_{39}$.

The root locus of the open loop transfer function, computed from the state space variables A, B, C, and D, is plotted in Figure 3.4. This diagram illustrates the effect of the control gain selection on the complex linear system roots. The desired effect of the

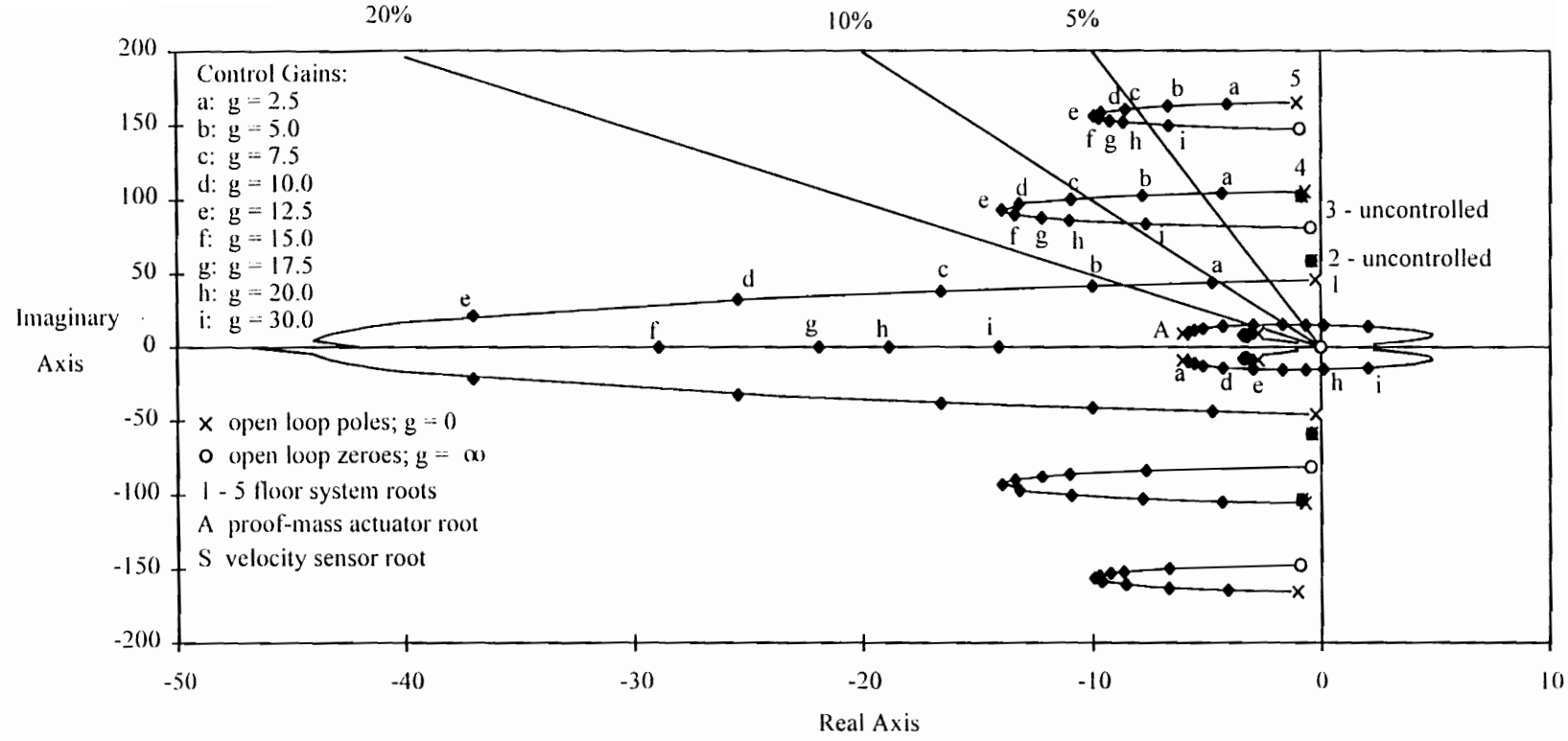

Figure 3.4 Root Locus Diagram for Collocated Velocity Feedback

control force is to change the roots of the floor system such that they possess a higher degree of damping, i.e., the ratio of the real part of the root to the imaginary part of the root becomes larger while the real portion of the root remains negative. The straight lines labeled with percentages plot this ratio expressed as a percent. A root which lies on the line labeled 10% can be said to have 10% damping. A root which possesses a positive real portion is unstable.

The lines which connect the open loop poles and zeroes are the possible values of the linear system roots for a positive control gain between zero and infinity. The open loop poles represent the system roots for the uncontrolled (zero gain) system. The lines connecting the open loop poles and zeroes map possible root locations as the control gain increases from zero to infinity. Individual root locations corresponding to nine specific control gains are plotted. The control gains, ranging from 1.25 to 30, are noted a-i in Figure 3.4. Two of the linear system roots are unaffected by the gain selection. These roots correspond to modes 2 and 3 for the floor system which have zero amplitude at the sensor/actuator location. In order to control these modes, the collocated actuator/sensor would have to be moved to a floor location where these modes are observable.

The system root labeled A, the proof mass actuator root, is of particular concern in the controlled system because it is possible to select a gain value for which the real portion of this complex root becomes positive, thus creating unstable behavior in the actuator. This clearly illustrates the fact that, with the inclusion of actuator dynamics, the direct velocity feedback control scheme is no longer unconditionally stable. Careful

selection of the control gain does, however, produce a stable, robust, and effective control system. The first, fourth and fifth, modes of vibration (closed loop poles) show an increase in damping for each of the selected gain values. The improvement in the dynamic floor properties is reflected in the analytical results presented in the next section.

3.2.3 Linearly controlled heel drop response

The control system can also be evaluated by studying the transient response of the controlled and uncontrolled systems. Using MATLAB, the system response was computed using a theoretical heel drop impact (decreasing ramp function) to excite the floor. The impact, control force (actuator), and velocity measurement were located at node 39. Ten different cases were computed using various control gains. The time histories and corresponding frequency spectra are plotted in Figure 3.5. As the control gain is increased, the transient responses of the floor modes are further reduced. This is indicated by a leveling of the sharp peaks noted in the frequency transformation of the velocity time history. The mode around 2 Hz., corresponding to the actuator mass, is destabilized by increasing gains. This destabilization begins to have a significant effect on the floor response at gains above 10. The system becomes unstable at a gain of 20 as illustrated previously in the root locus diagram. Control gains between 5 and 10 provide the best performance for controlling the transient response at the center of the floor.

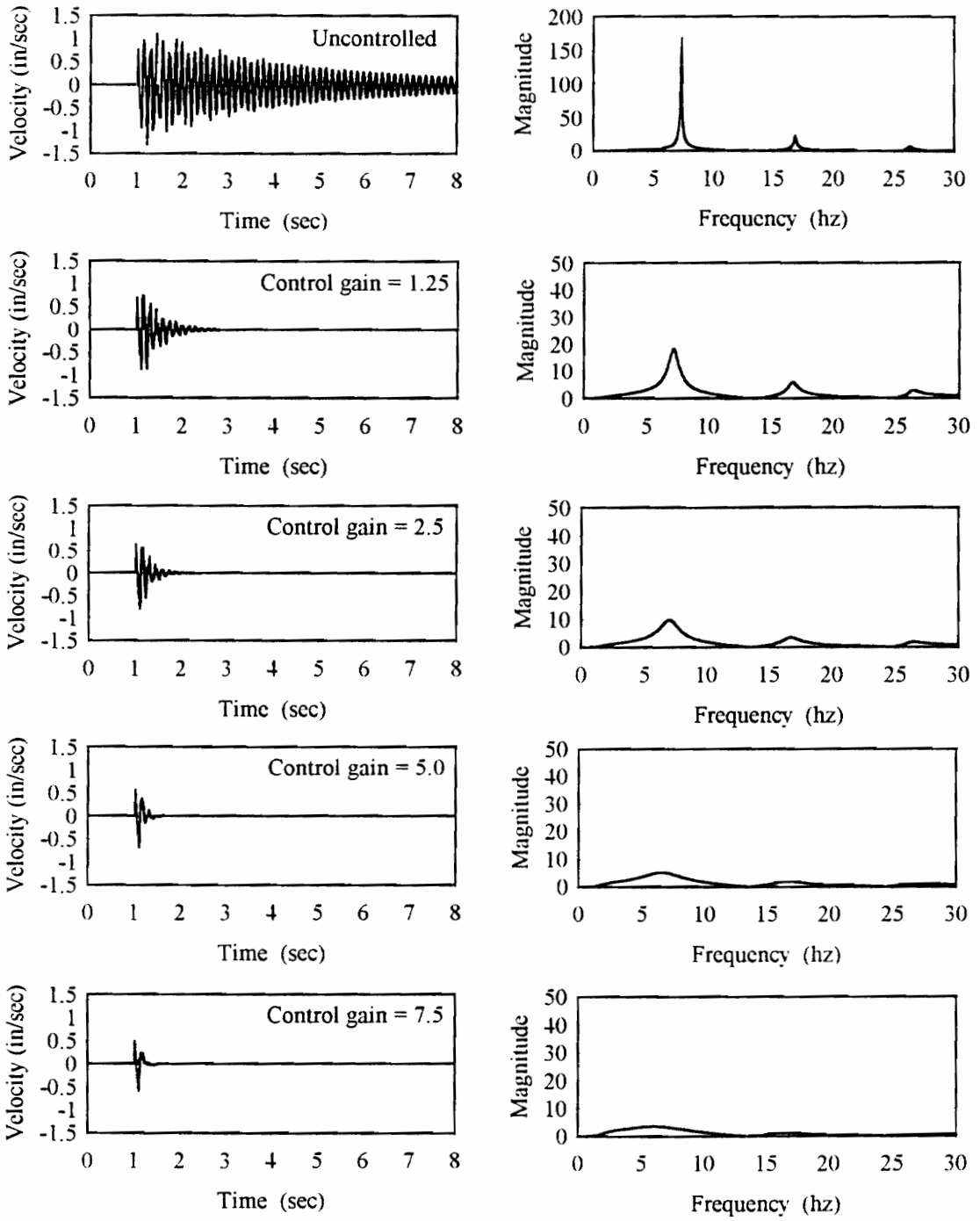

Note: The graphs labeled Magnitude vs. Frequency represent the frequency transform of the adjacent velocity time history

Figure 3.5 Uncontrolled and Controlled Floor Response Due to a Heel Drop Excitation

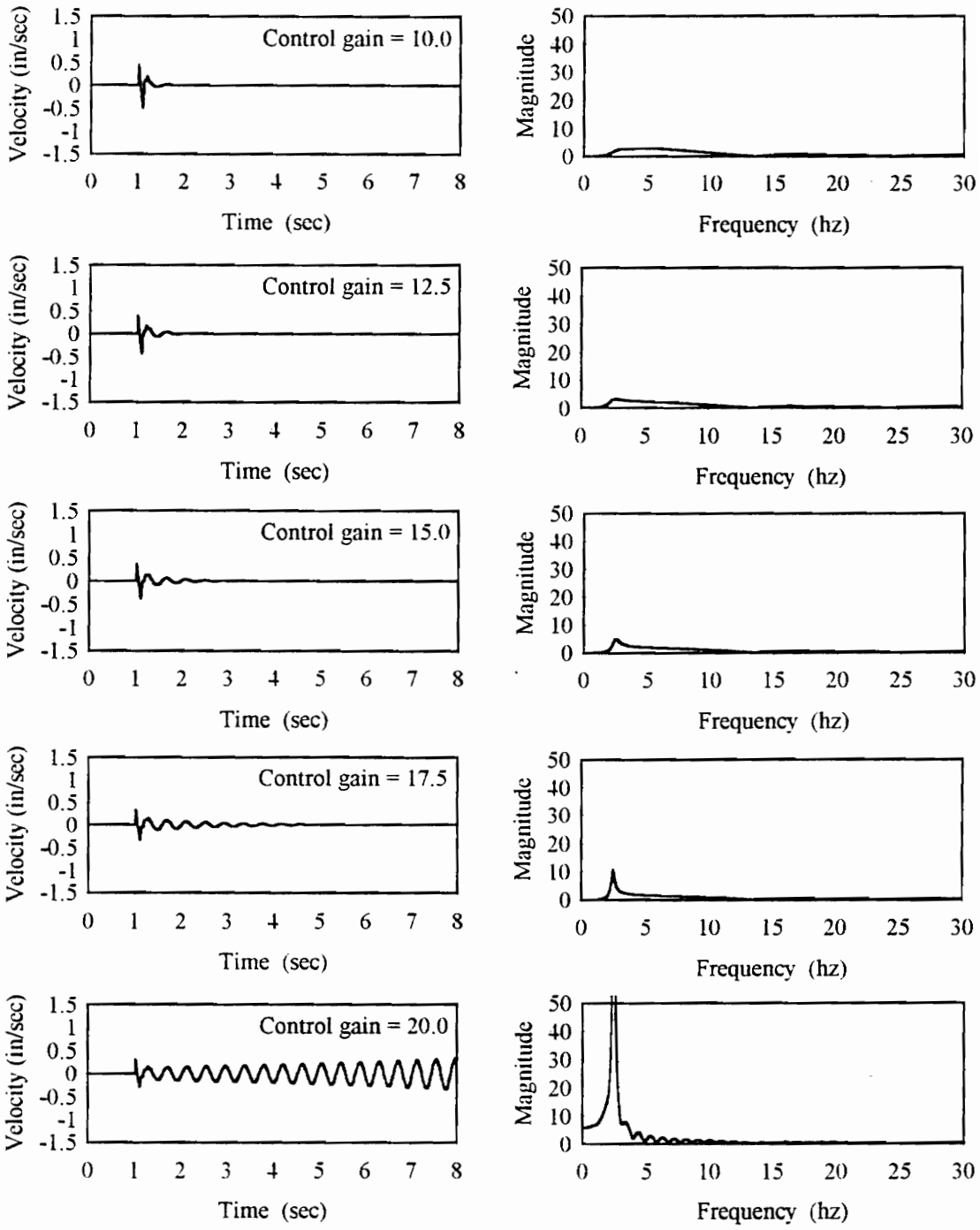

Note: The graphs labeled Magnitude vs. Frequency represent the frequency transform of the adjacent velocity time history

Figure 3.5(continued) Uncontrolled and Controlled Floor Response Due to a Heel Drop Excitation

3.3 Analytical Comparison of a Tuned Mass Damper

The most closely related traditional repair measure to the active device being studied is the tuned mass damper (TMD). An analytical study was undertaken to compare the active and passive systems with respect to controlling floor vibrations. In this study, analytical simulations of the floor response are computed to illustrate the benefits of active control over a passive device. Two tuned mass damper designs were used with the analytical model of the experimental floor to compare their relative effectiveness with that of the active control implementation. The excitation studied in the comparison is a theoretical heel drop. The control force or TMD, the excitation force, and the floor response are at the center of floor, node 39 in the finite element model.

3.3.1 Design of the tuned mass dampers

The Shock and Vibration Handbook (Reed 1988) provides equations for designing and optimizing the parameters of a tuned mass damper. This procedure is outlined in Figure 3.6. Using this procedure, two tuned mass dampers were designed for implementation in the analytical model. One damper was designed to illustrate the TMD control effectiveness using a passive reaction mass (67 lb.) equivalent to that of the active control. The second TMD was designed to provide 20% equivalent damping in the first mode of vibration of the floor system. This performance is achieved in the active system with a control gain of 5.

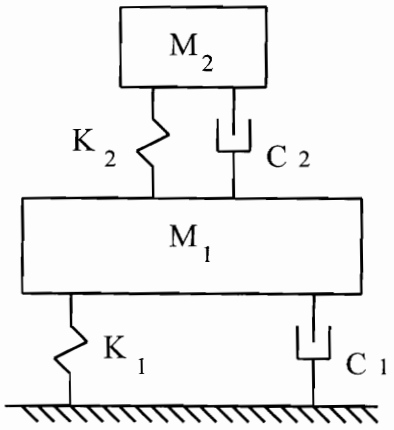

Equations for TMD parameter optimization:

(ref. Reed 1988)

$$\omega_n = \sqrt{\frac{K_1}{M_1}}$$

$$\mu = \frac{M_2}{M_1}$$

$$\omega_{opt} = \omega_n \frac{1}{1+\mu} = \frac{K_2}{M_2}$$

$$\zeta_{opt} = \sqrt{\frac{\mu}{2(1+\mu)}} = \frac{C_2}{\sqrt{K_2 M_2}}$$

where

M_1, C_1, K_1 are the single-degree-of-freedom floor system parameters for mass, damping, and stiffness, respectively

M_2, C_2, K_2 are the tuned mass damper parameters for mass, damping, and stiffness, respectively

Figure 3.6 Design and Optimization of Tuned Mass Damper Properties

Determination of floor system parameters:

The parameters from the first mode in the analytical model at spatial coordinate 39 are used to determine the floor system parameters.

$M_1 = 1/\Phi_{mn}^2 = 1/(0.2428)^2 = 16.96$ (6554 lb)

where m = the mode being controlled (in this case m = 1) and n = the spatial coordinate for the tuned mass damper location

$C_1 = 2\zeta_1\omega_1 M_1 = 2(0.0047)(46.4)(16.96) = 7.40$ lb/(in/sec)

$K_1 = \omega_1^2 M_1 = (46.4)^2(16.96) = 36514$ lb/in

$\omega_n = \omega_1 = 46.4$ rad/sec

Design of TMD #1: Equivalent mass

$M_2 = 67 / 386.4 = 0.0173$

$\mu = 0.173 / 16.96 = 0.0102$

$$\zeta_{opt} = \sqrt{\frac{0.0102}{2(1+0.0102)}} = 0.07$$

$$\omega_{opt} = (46.4)\frac{1}{1+0.0102} = 45.93 \text{ rad/sec}$$

$K_2 = (45.93)^2(0.0173) = 364.9$ lb/in.

$C_2 = 2(0.071)\sqrt{(0.173)(364.9)} = 1.128$ lb/(in/sec)

Design of TMD #2: Equivalent damping, 20%

$M_2 = 30(0.0173) = 5.19$ (2005.4 lb)

$\mu = 5.19 / 16.96 = 0.306$

$$\zeta_{opt} = \sqrt{\frac{0.306}{2(1+0.306)}} = 0.342$$

$$\omega_{opt} = (46.4)\frac{1}{1+0.306} = 35.53 \text{ rad/sec}$$

$$K_2 = (35.53)^2(5.19) = 6551 \text{ lb/in.}$$

$$C_2 = 2(0.342)\sqrt{(5.19)(6551)} = 126. \text{ lb/(in/sec)}$$

3.3.2 Floor response to heel drop excitation with TMD control

The floor response due to a heel drop impact was computed for the uncontrolled system, the actively controlled system, the TMD # 1 controlled system, and the TMD #2 controlled system. The excitation, control force (active or TMD), and the measurement were located at spatial coordinate 39. The time histories and corresponding frequency spectra are plotted in Figure 3.7.

3.3.3 Conclusions from TMD study

Results from the analytical study show that a tuned mass damper possessing an equivalent reactive mass, TMD #1, to the active system increases the damping in the first mode from 0.5% to 3.8%. The TMD designed to provide 20% damping in the first mode of vibration, TMD #2, is very effective but has 30 times the weight of the active mass and more than 30% of the primary mass of the mode being controlled. This amount of weight would be impractical for installation on a floor.

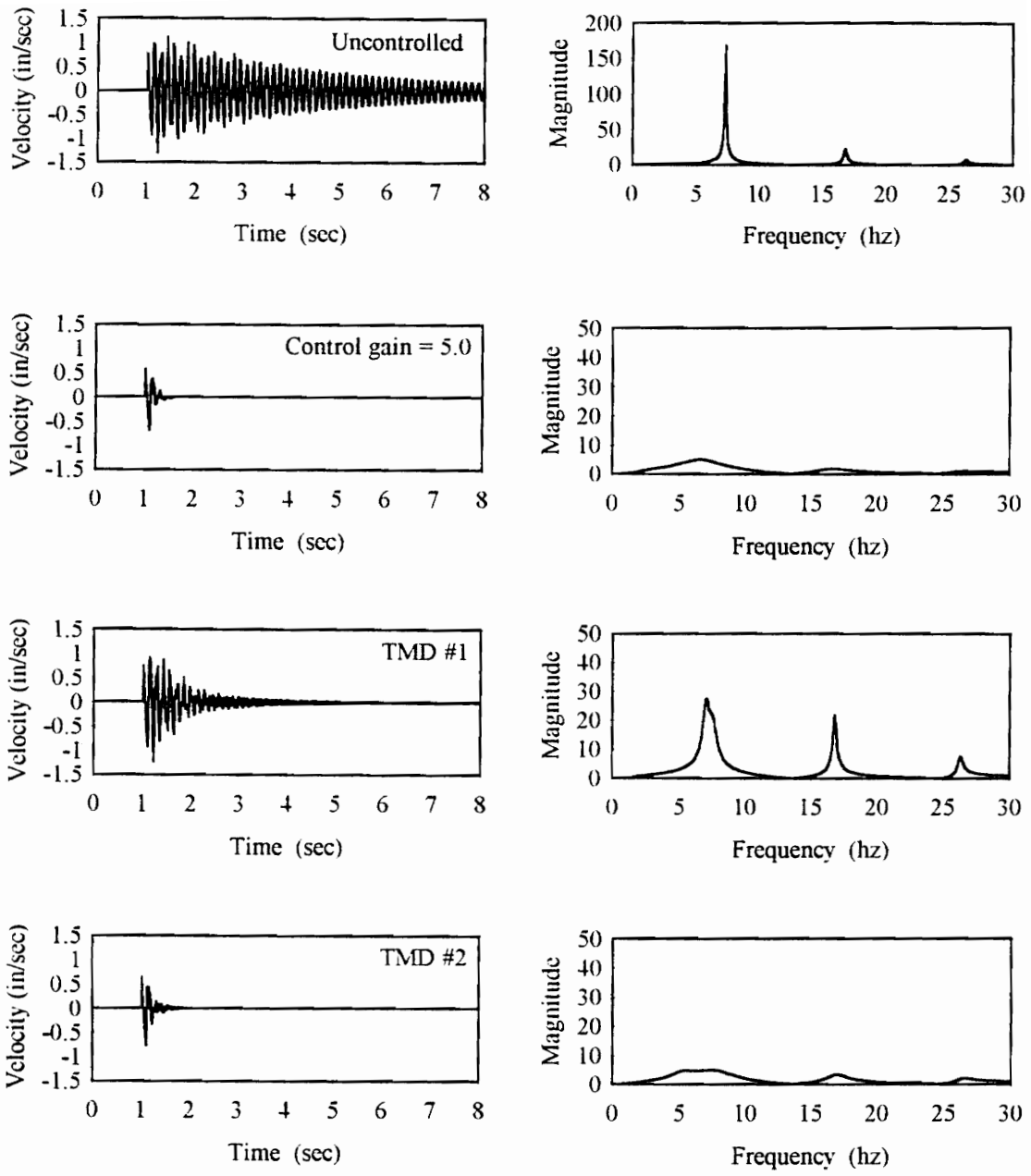

Note: The graphs labeled Magnitude vs. Frequency represent the frequency transform of the adjacent velocity time history

Figure 3.7 Analytical Comparison of Tuned Mass Damper and Active Control

3.4 Development and Evaluation of Non-Linear Control Circuit

The studies of the linear control scheme assumed the actuator has an unlimited stroke length and the actuator is unlimited in its ability to produce a control force. Neither case is true. The maximum command input to the amplifier/actuator for random excitation is limited to 0.5 volts, as discussed in Chapter 2. This results in a maximum control force of 30 lb. Figure 3.8 shows the control force and the actuator displacement using the linear controller and excitation studied in the previous section. The control gain selected to illustrate linear control behavior was 7.5. Inspection of the control force graph in Figure 3.8 reveals that a 263 lb. control force is required to achieve the linear control effectiveness illustrated in the figure.

For the actuator selected, a linear feedback law, such as direct velocity feedback, will result in a command input which will overload the amplifier in the case of a heel drop excitation. The most straightforward approach to prevent overloading the amplifier is to build a command limiter into the control algorithm. This would result in a non-linear control law in the following form:

$$\text{Voltage command} = \begin{cases} v_{max} & \text{for} \quad \dot{y}_s > \dfrac{v_{max}}{\text{gain}} \\ \dot{y}_s \cdot \text{gain} & \text{for} \quad \dfrac{v_{min}}{\text{gain}} < \dot{y}_s < \dfrac{v_{max}}{\text{gain}} \\ v_{min} & \text{for} \quad \dot{y}_s < \dfrac{v_{min}}{\text{gain}} \end{cases} \tag{3.12}$$

where v_{max} and v_{min} are the limits of the voltage command to prevent overloading. The graphs in Figure 3.9 illustrate the effect of this non-linear control law on the control

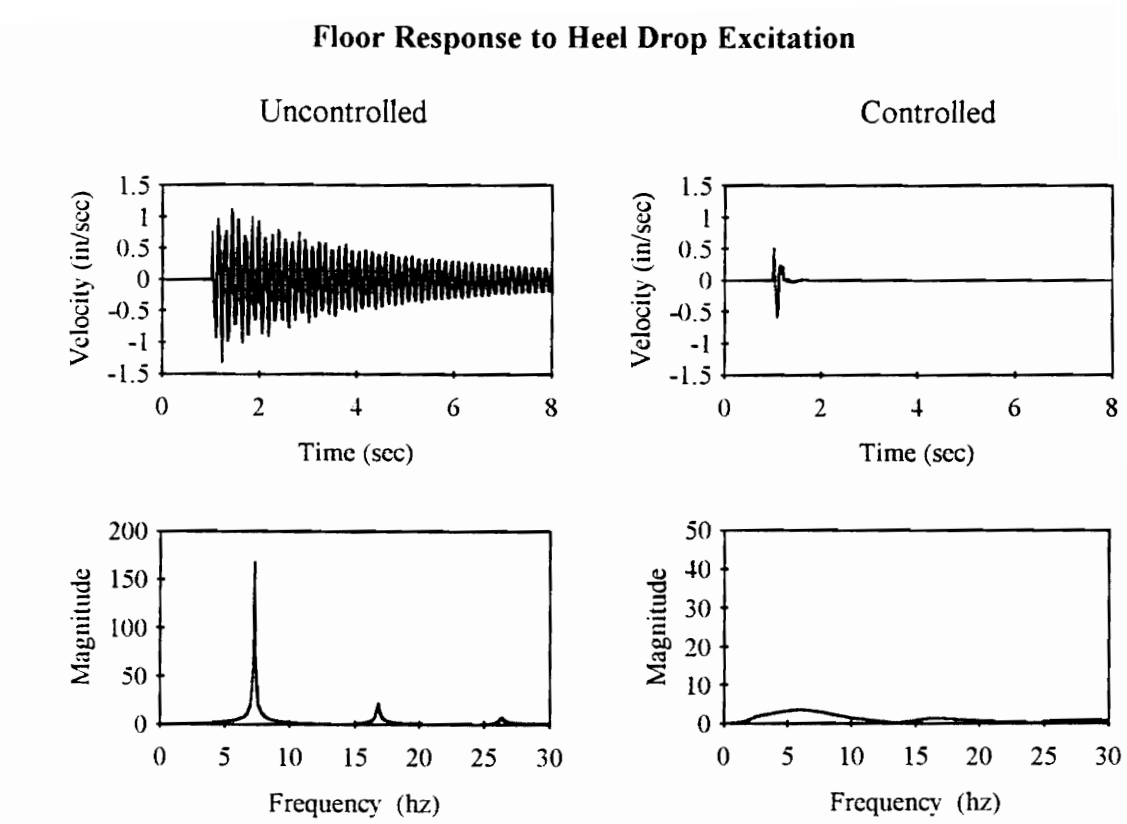

Note: The graphs labeled Magnitude vs. Frequency represent the frequency transform of the velocity time history above

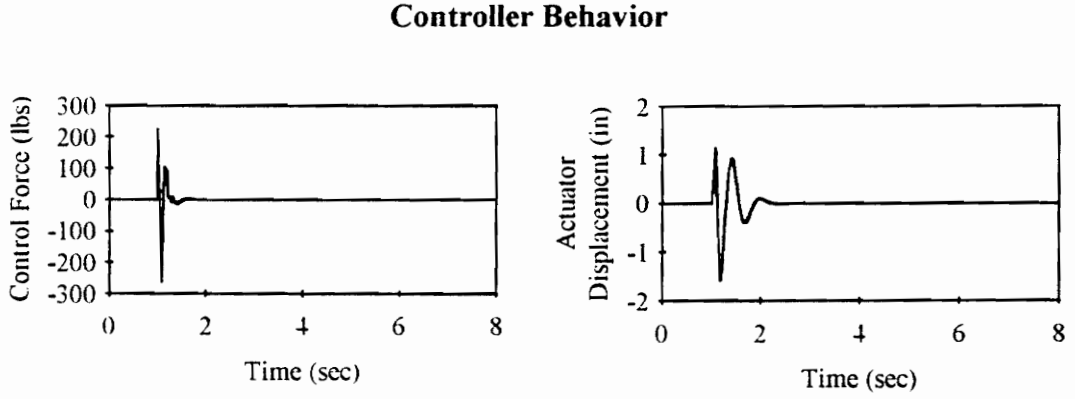

Figure 3.8 Floor Response and Linear Controller Behavior Due to Heel Drop Excitation

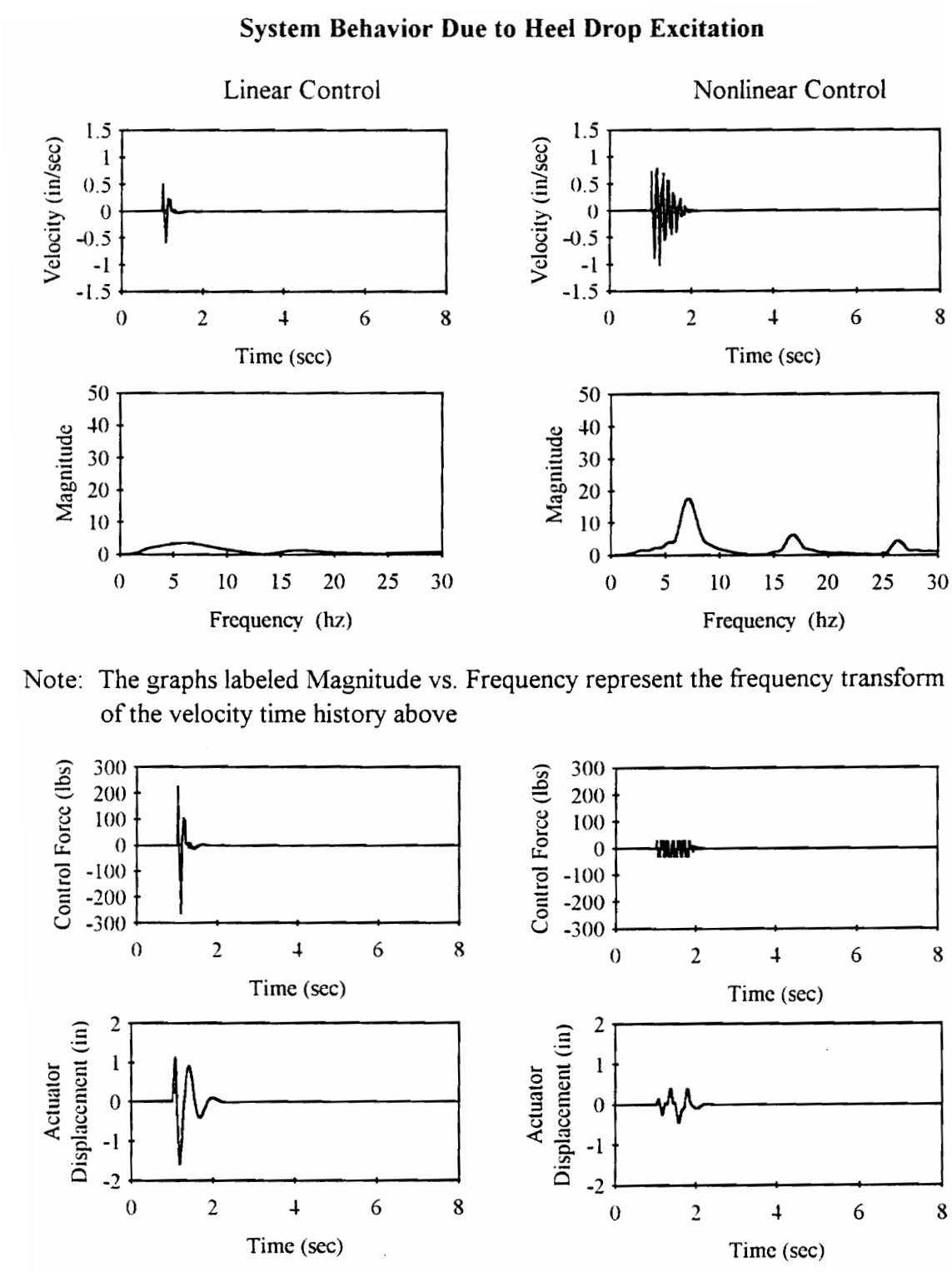

Note: The graphs labeled Magnitude vs. Frequency represent the frequency transform of the velocity time history above

Figure 3.9 System Behavior Due to Heel Drop Excitation for Linear and Nonlinear Control

system performance for a heel drop excitation. The command limit results in a control law whose performance is dependent on the magnitude of the excitation and floor response. Even with the reduced control performance imposed by the actuator limitations, the floor response due to a heel drop impact is significantly improved over the uncontrolled response illustrated in Figure 3.8.

The floor excitation produced by walking is significantly less than that of a heel drop. Floor excitations which produce maximum control forces in the linear region of the control law will exhibit the same control effect noted in the linear control studies. The command limit will be shown in Chapter 4 to have little effect on the control performance for walking-induced vibrations.

CHAPTER 4

EXPERIMENTAL VERIFICATION OF ACTIVE CONTROL ON TEST FLOOR

The analytical evaluation of Chapter 3 supports the concept that active control using a proof mass actuator can considerably improve the dynamic behavior of a floor structure. The experimental implementation of the control scheme serves two purposes. First, uncontrolled and controlled system behavior are verified using a measured excitation. Comparisons of analytical simulations and experimental results confirm the understanding of system behavior. These studies indicate that, given an accurate analytical model of the uncontrolled system, a reasonable prediction of control effectiveness can be made.

The second purpose of the experimental implementation is the verification of system effectiveness for various excitations, control gains, and actuator locations. Experimental comparisons of uncontrolled and controlled system responses provide data to support the theory that an actively controlled system using a proof mass actuator does greatly improve the floor system behavior.

4.1 Verification of Analytical Model for Uncontrolled Floor System

To verify the analytical model, different types of measurements were recorded at several locations on the floor. The first type was a frequency response function. The input variable was a random voltage input to the shaker and the output measurement was

from the velocity transducer. This measurement was made using a dynamic signal analyzer. A similar measurement can be simulated in MATLAB using the "bode" function and the analytical model developed in Chapter 3. The experimental and simulation results for a sample measurement are shown in Figure 4.1. The actuator and sensor were both located at the center of the floor. The experimental measurement consisted of 20 averages. The results in Figure 4.1 illustrate a fairly accurate simulation of the frequency response.

The second type of measurement, and perhaps more relevant to the verification of the analytical model, was a time domain measurement at various floor locations. For these measurements, a heel drop excitation force was recorded using the force plate discussed in Chapter 2 and the floor response was measured using the velocity transducer. Because the response of the floor system is dependent on the excitation, a reasonable comparison of experimental floor response and simulated floor response must use the experimentally measured excitation. Otherwise discrepancies between the experimental and simulated response may be due to differences in the excitation rather than inaccuracies in the analytical model.

It was anticipated that small changes in the analytical model would produce only small changes in the simulated response of the floor system. To test this assumption, analytical simulations were conducted for two floor models. The floor system models were identical except the first natural frequency in Model A was 0.1 Hz. higher than that of Model B. The input excitation used was a theoretical heel drop. The results from

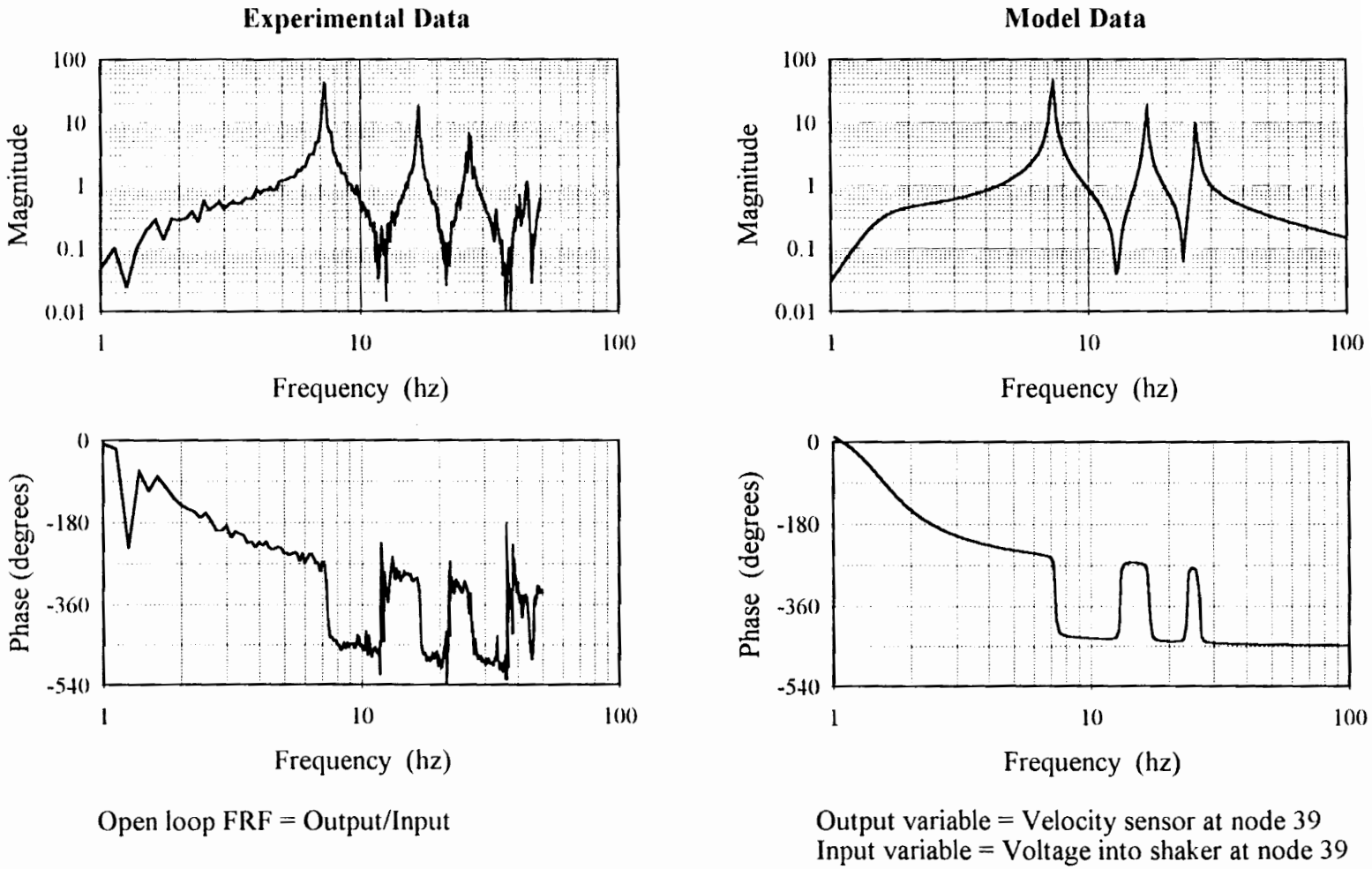

Figure 4.1 Experimental and Model Frequency Response Functions at Center of Test Floor

these analytical simulations are shown in Figure 4.2. As anticipated, there is little difference between time histories for Models A and B.

The use of the measured heel drop impact, rather than the theoretical heel drop impact, in the simulation of the floor response produced an unanticipated phenomenon. The time histories simulated in Figure 4.3 use the same floor system models as those in Figure 4.2. The excitation used was from an experimental measurement of a heel drop performed at the center of the test floor. The computed responses using the experimentally measured force are drastically different from each other for Models A and B.

This phenomenon is explained by inspection of the excitation time history in Figure 4.3. After the initial impact, there is an oscillating force present in the measurement. This force is actually caused by the motion of the floor system. As the floor moves, the mass and damping effect of the person standing on the plate is measured by the force plate. In the simulation this force is independent of the floor motion; it is imposed on the structure rather than created by it. Slight differences in the model frequencies can therefore produce dramatic differences in the simulated response, as illustrated in Figure 4.3. The floor model is similarly sensitive to estimates of floor system damping.

The simulated floor response due to the experimentally measured response in not particularly sensitive to the floor system matrix Φ. The methods for determining model parameters in Chapter 3 were strongly driven by their effects on the simulation. Because

Simulated Response at the Center of the Test Floor

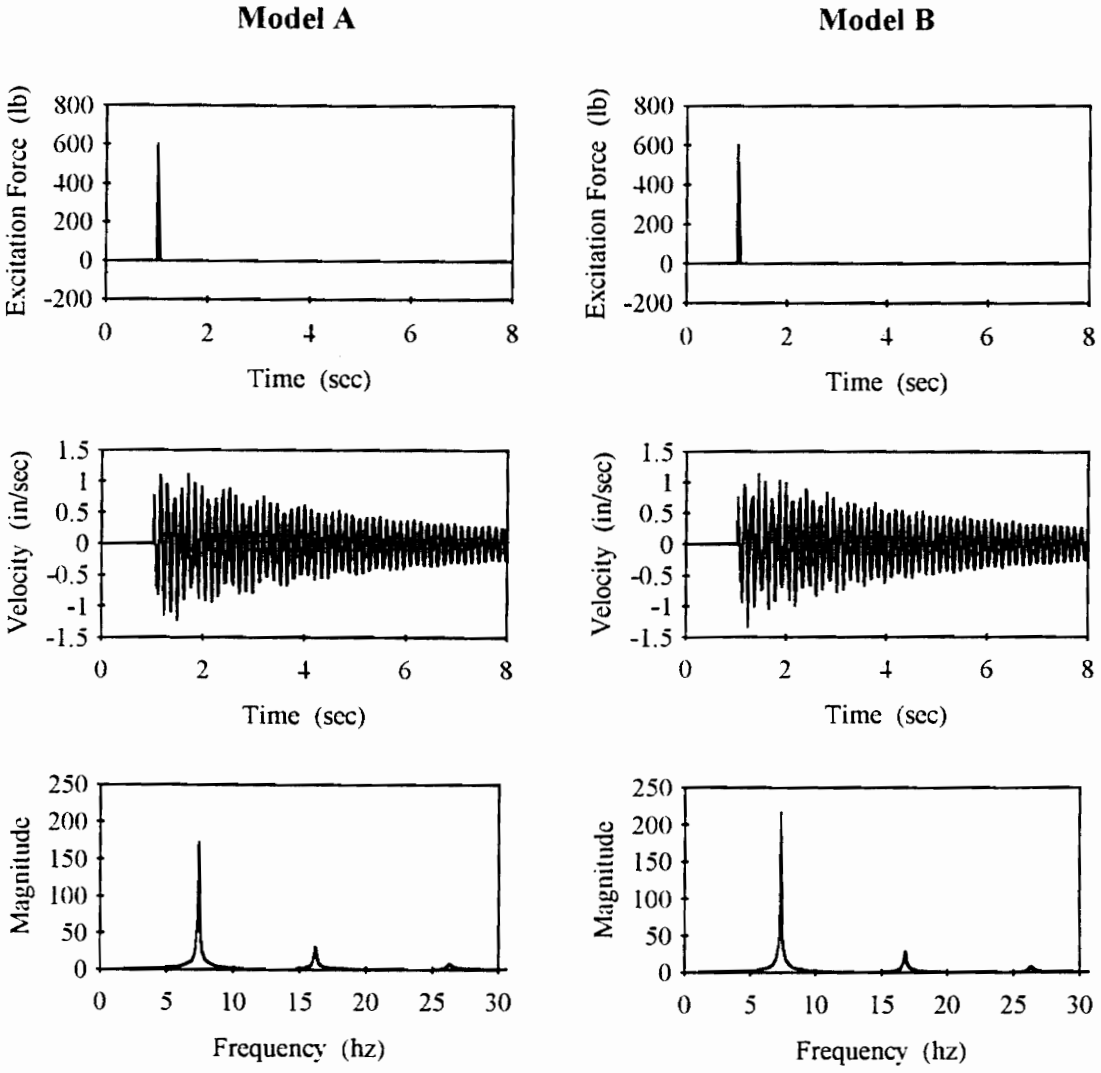

Note: The graphs labeled Magnitude vs. Frequency represent the frequency transform of the velocity time history above

Figure 4.2 Simulated Floor Response to Theoretical Heel Drop Excitation

Simulated Response at the Center of the Test Floor

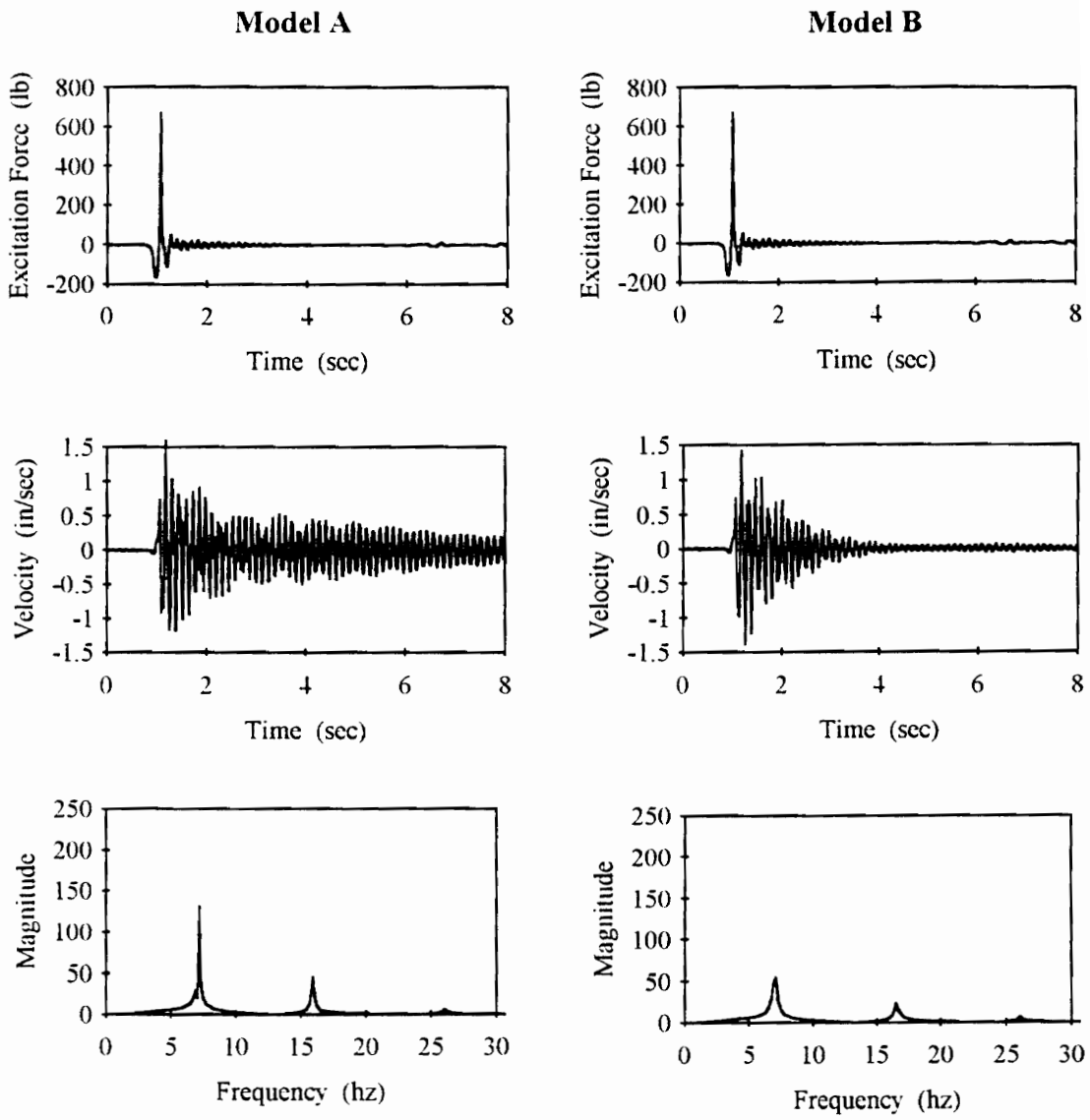

Note: The graphs labeled Magnitude vs. Frequency represent the frequency transform of the velocity time history above

Figure 4.3 Simulated Floor Response to Experimental Heel Drop Excitation

of model sensitivities, the system matrices K* and C* were determined from experimental results, while finite element results were used in determining the Φ matrix. Future research would benefit from the selection of an excitation source that is independent of the motion of the structure.

Using the finely tuned analytical model (Model B) described above, fairly accurate simulations of the uncontrolled test floor responses were achieved. Simulation and experimental data at the center of the test floor is compared in Figure 4.4. As indicated in Figures 4.1 and 4.4, the uncontrolled floor system response is accurately predicted by the analytical model at the center of the test floor. Verification of the model at this location is particularly relevant in confirming the system behavior described in the analytical studies of Chapter 3.

There is a final note of interest in Figures 4.2 and 4.4. Floor model B was used in computing the simulation results in Figures 4.2 and 4.4. The level of damping affecting the responses appears to be significantly different. The additional damping noted in Figure 4.4 is provided by the person performing the heel drop and is estimated to provide an additional 1% damping to the system. This additional damping is provided to the simulated response through the excitation force rather than the floor system parameters.

4.2 Experimental Test Setup

The control scheme is implemented digitally using a 386 personal computer and a data acquisition card with input and output channels. Many of the other components used

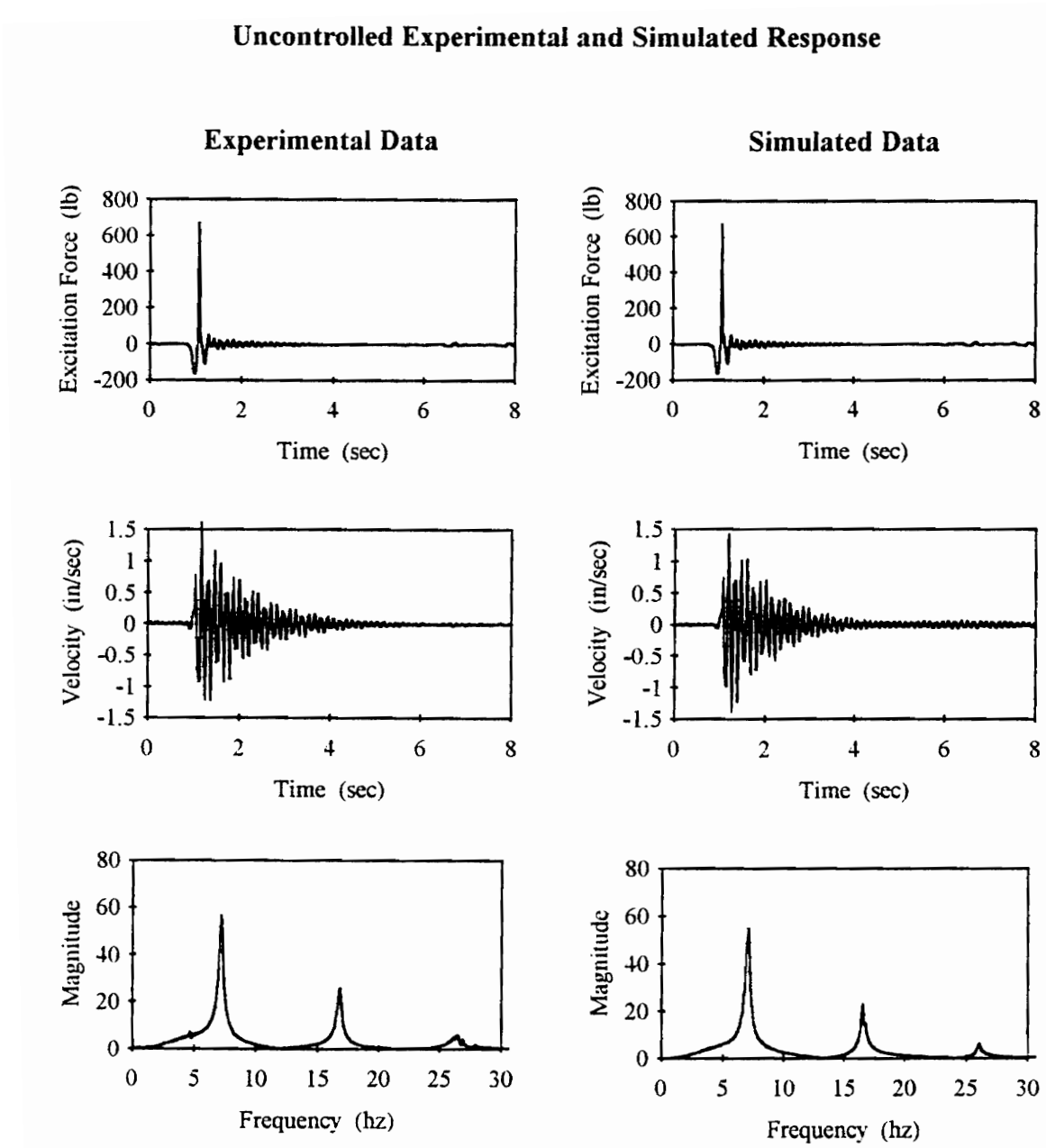

Note: The graphs labeled Magnitude vs. Frequency represent the frequency transform of the velocity time history above

Figure 4.4 Uncontrolled Experimental and Simulated Floor Response Due to Experimental Heel Drop Excitation

in the experimental implementation have already been described. The manner in which these components are integrated into a control system is illustrated in Figure 4.5.

Beginning with a disturbance input to the floor structure, the motion of the floor is measured by the velocity transducer which produces a voltage output signal proportional to the velocity. This analog voltage is input to an analog-to-digital converter and captured by the control program. A sample frequency of 2000 Hz was selected. The sample frequency was selected to be sufficiently high so as not to produce any significant time delay at the lower, more dominant frequencies while still maintaining real-time control. The control program computes an output voltage. The computation of this output voltage is based on the control law formulated in Equation 3.12. An additional computation is performed in the control program. The velocity sensor signal contains a DC offset that is corrected before the control force computation. Once computed, the output voltage is converted to an analog output signal by the digital-to-analog converter. The output voltage drives the shaker delivering the control force to the structure. It should be noted that during the operation of the continuous control loop, the only input to the amplifier/shaker is from the feedback loop.

4. 3 Evaluation of Control Effectiveness for Impact-Like Excitations

There are two purposes behind the following evaluation of control effectiveness for impact-like excitations. The first is to confirm the theoretical system behavior studied in the previous chapter. The second is to compare and evaluate the experimental results

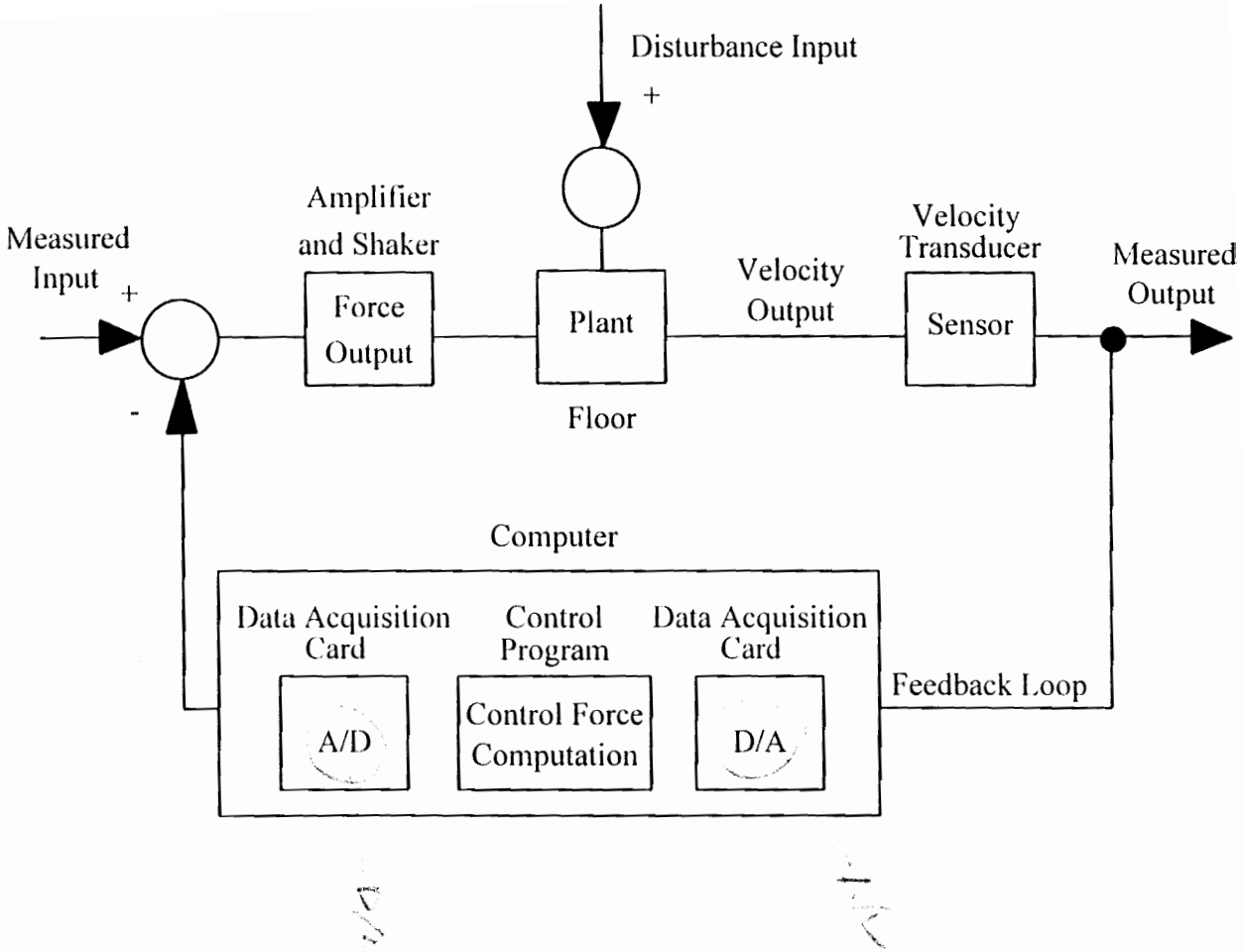

Figure 4.5 Block Diagram Illustrating Experimental Test Setup

for the controlled and uncontrolled systems when subjected to impact-like excitations. An impact-like excitation is defined here as a disturbance force of short duration with respect to the uncontrolled system response. This type of excitation is useful in evaluating the transient behavior of the system.

The simulated results presented in Figure 4.4 illustrate the effectiveness of the analytical model to predict the uncontrolled response of the floor system when subjected to a heel drop excitation. Similar experiments and simulations were conducted for the controlled system. The actuator and velocity sensor were placed at the center of the control floor. The voltage command to the shaker was limited to ±0.5 volts. The feedback gain was programmed in increments of 2.5 between 2.5 and 17.5. A heel-drop impact was performed by a person standing on the force plate next to the shaker for each gain value. Measurements were simultaneously recorded from the force plate and the velocity sensor for a period of 16 seconds. The gain producing the most significant reduction in transient vibration levels was 7.5 as it was in the analytical study of Chapter 3.

Using the experimentally measured force from the heel drop test (7.5 gain controller) as an input excitation, a simulation of the response was computed. The results from this experiment and simulation are presented in Figure 4.6. Inspection of the results reveals a very accurate prediction of the system response using the analytical model developed.

Controlled Experimental and Simulated Response

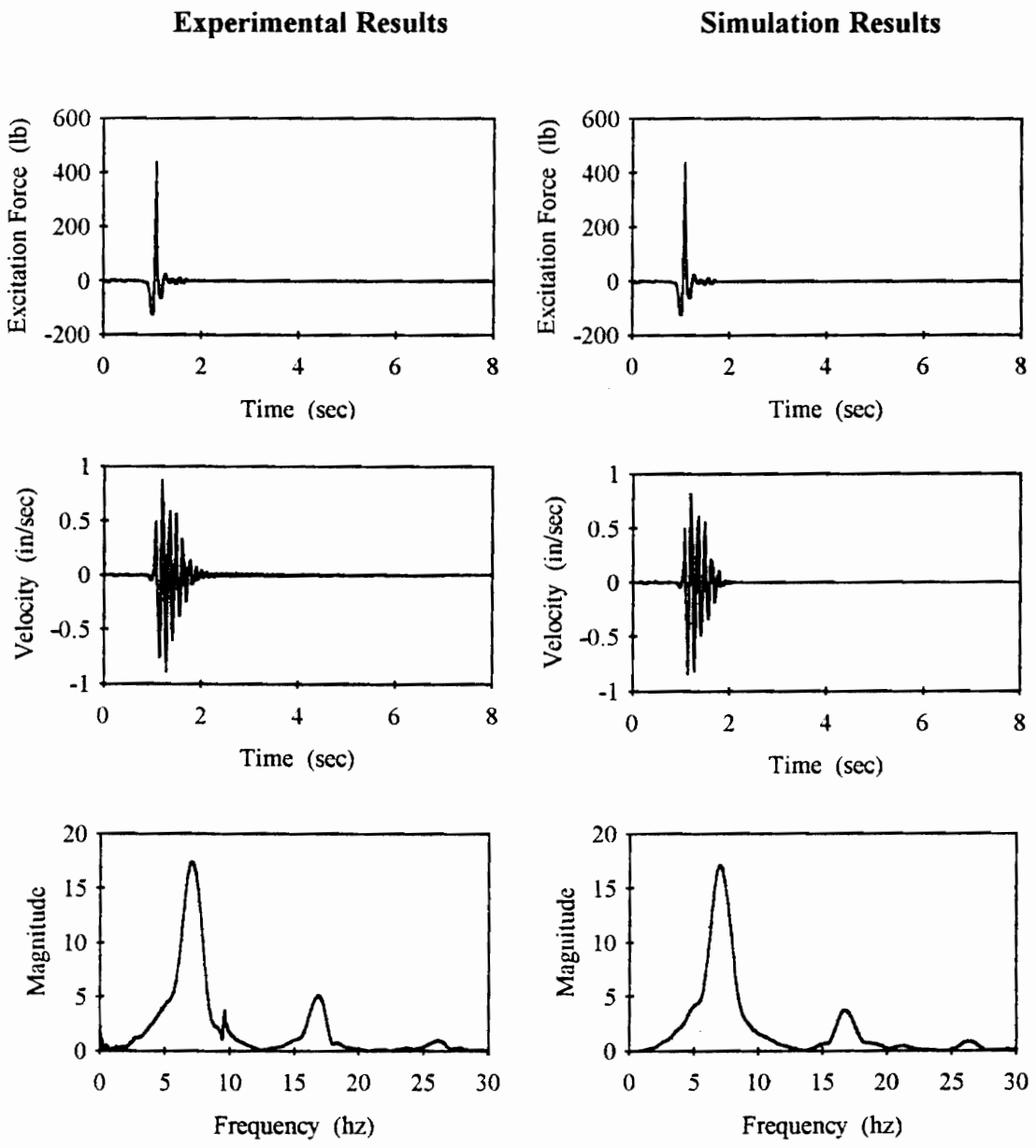

Note: The graphs labeled Magnitude vs. Frequency represent the frequency transform of the velocity time history above

Figure 4.6 Controlled Experimental and Simulated Floor Response to Experimental Heel Drop Excitation

The results presented in Figure 4.6 are very dependent on the non-linear capabilities of the controller. This concept was theoretically illustrated in Figure 3.9. A smaller impact-like excitation would provide a better indication of control system effectiveness in the range of walking excitations.

The experiments performed for the heel drop excitation were repeated using a smaller impact-like excitation. This smaller excitation was achieved by having the person standing on the plate flex their knees and then stand straight again. Results from this experiment are shown in Figures 4.7 and 4.8. Figure 4.7 presents a comparison of the experimental and simulated results for the uncontrolled system. Figure 4.8 presents a similar comparison for the controlled system. Again, the analytical model proved to be very accurate in predicting the controlled system behavior.

The results already presented can be re-evaluated to reflect control system effectiveness rather than analytical model accuracy. The concept of equivalent viscous damping is useful in assessing the non-linear control effectiveness. The method of quadrature peak picking, as described in Chapter 3, can be used to compute the equivalent viscous damping for a specific excitation level. The uncontrolled system of Figure 4.4 has 2.2% equivalent viscous damping in the first floor mode, while the controlled response of Figure 4.6 represents 9.7% equivalent damping. It should be noted that the linear control system studied in Chapter 3 possessed approximately 40% damping in the first floor mode.

Uncontrolled Experimental and Simulated Response

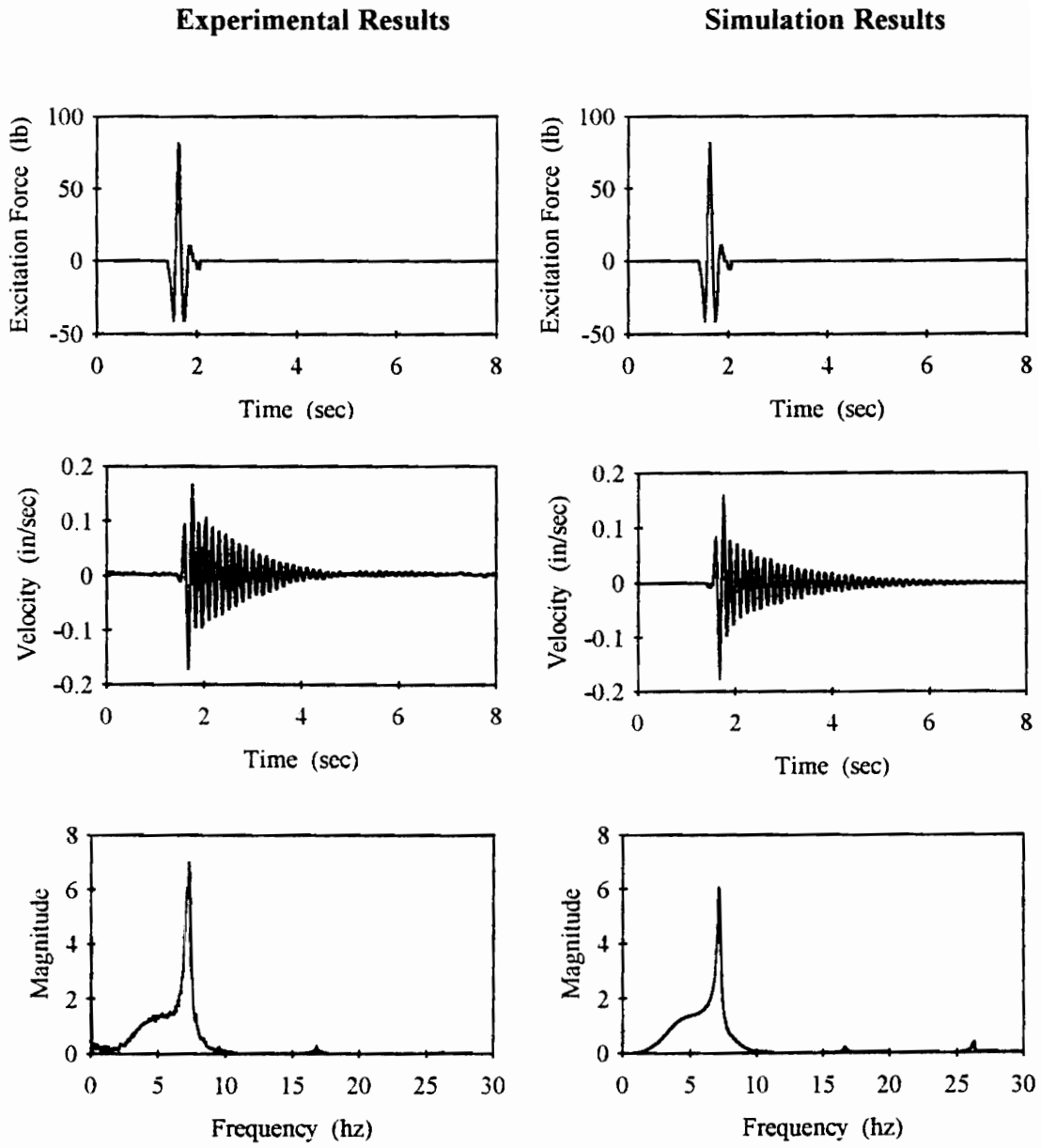

Note: The graphs labeled Magnitude vs. Frequency represent the frequency transform of the velocity time history above

Figure 4.7 Uncontrolled Experimental and Simulated Floor Response to Experimental Small Impact-Like Excitation

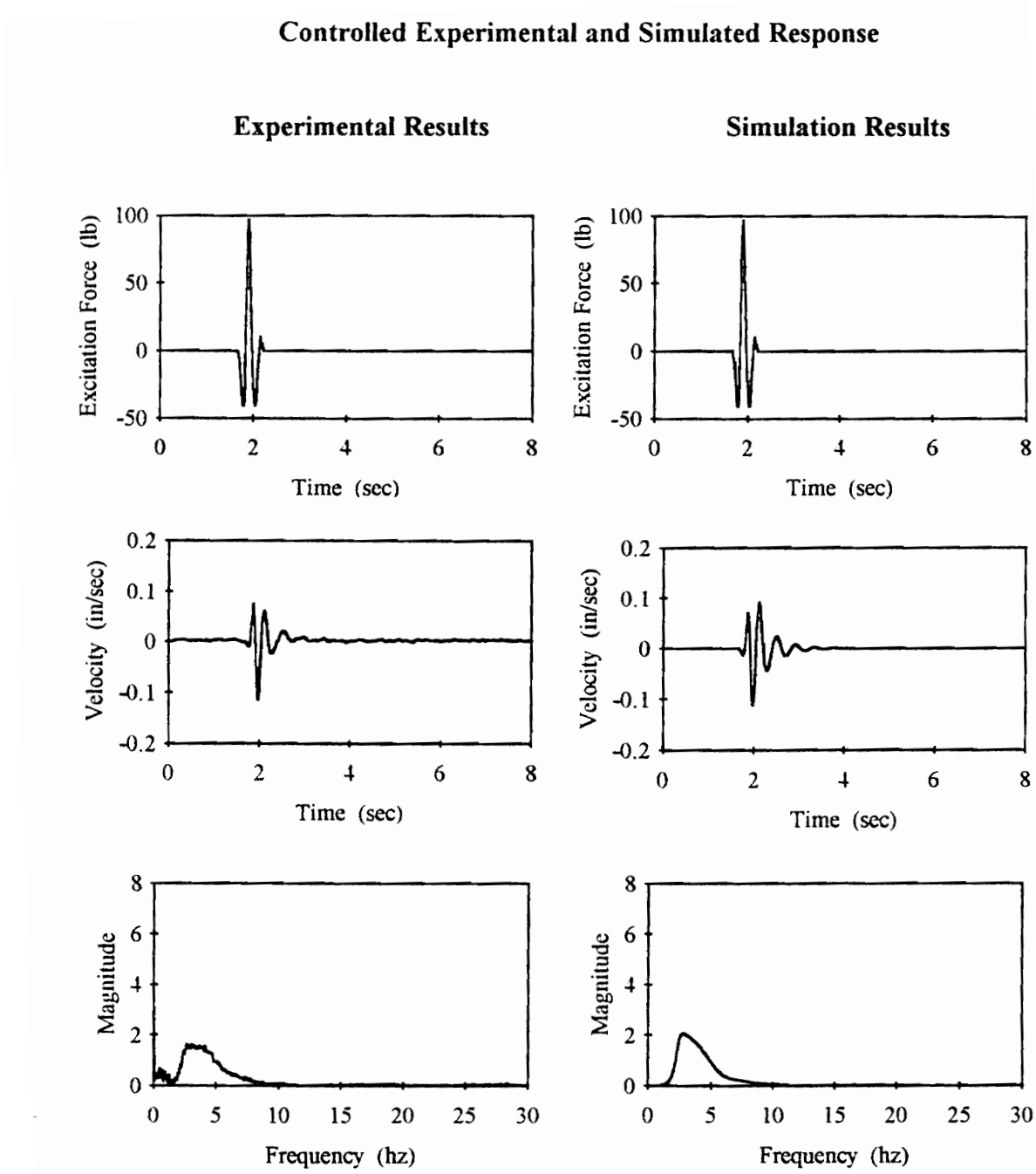

Note: The graphs labeled Magnitude vs. Frequency represent the frequency transform of the velocity time history above

Figure 4.8 Controlled Experimental and Simulated Floor Response to Experimental Small Impact-Like Excitation

The method of quadrature peak picking is only effective for predicting the equivalent viscous damping in well-spaced, lightly-damped (<20%) modes. The evaluation of the control system effectiveness for the small impact-like excitation is therefore more qualitative than quantitative. A comparison of Figures 4.7 and 4.8 reveals a nearly complete removal of the transient component in the floor response for the controlled system. This behavior reflects the effectiveness illustrated for the linear controller studies in Chapter 3. The equivalent viscous damping in the theoretical system is approximately 40% for the first floor mode.

4.4 Evaluation of Control Effectiveness for Walking Excitations

The following evaluation of control system effectiveness for walking excitations has two objectives. The first objective is to present a method by which the floor response due to walking excitations can be reasonably simulated for both the controlled and uncontrolled systems. The second objective is to evaluate the control system effectiveness by comparing the uncontrolled and controlled system responses.

4.4.1 Comparison of experimental and simulated results for walking excitations

Because the control system effectiveness is dependent on the excitation, it is helpful to study the system for the type of excitation that is to be controlled. In this case, studying the system for a walking excitation is targeted. Since the actual excitation could not be measured for use in a simulation, it was estimated using the results presented in the literature.

Many researchers have studied the forces created by occupant activities such as walking, dancing, or aerobics. The data are commonly used in formulating simplified design procedures for checking serviceability conditions. Eriksson (1994) quantifies the excitation force of an average footstep at an average step frequency. To simulate the floor response due to walking excitations, this excitation was superimposed at sequential nodes in the finite element model. The time history, Excitation A, of the walking excitation used in the simulation is plotted in Figure 4.9. The results of this simulation, Floor Response A, and the experimentally measured results are also presented in Figure 4.9 for the uncontrolled response at the center of the floor.

Comparison of the simulated (Floor Response A) and the experimental response reveals a complex phenomenon. The person's walking in the experimental response seems to be in resonance with the structure's first natural frequency rather than a random superposition of footsteps independent of the structure's motion as was simulated in floor response A. The step frequency in the analytical simulation was then altered from 1.67 Hz. to 1.48 Hz. so that a harmonic multiple (1.48 Hz. x 5 = 7.4 Hz.) of the step frequency was in resonance with the first natural frequency (7.4 Hz.) of the modeled structure. The results from this simulation are reflected in simulated Floor Response B in Figure 4.9. This simulation produces a response similar to the experimental results. Comparison of results from other people walking and other test floors, some of which are presented in Chapter 5, illustrate a similar resonance phenomenon. It appears that a person actually tunes their activity to the response of the structure.

Experimental and Simulated Response at Center of Test Floor for Walking Excitation

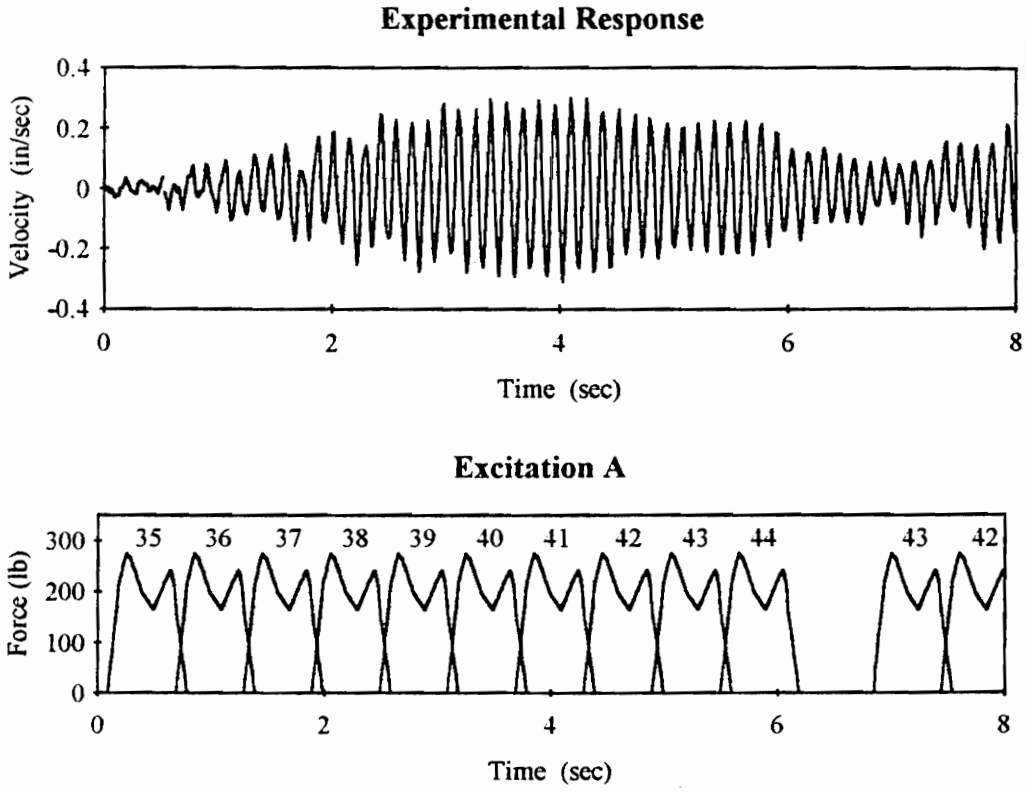

Note: Numbers in excitation time history denote the node number, defined in Figure 3.2, of the force application

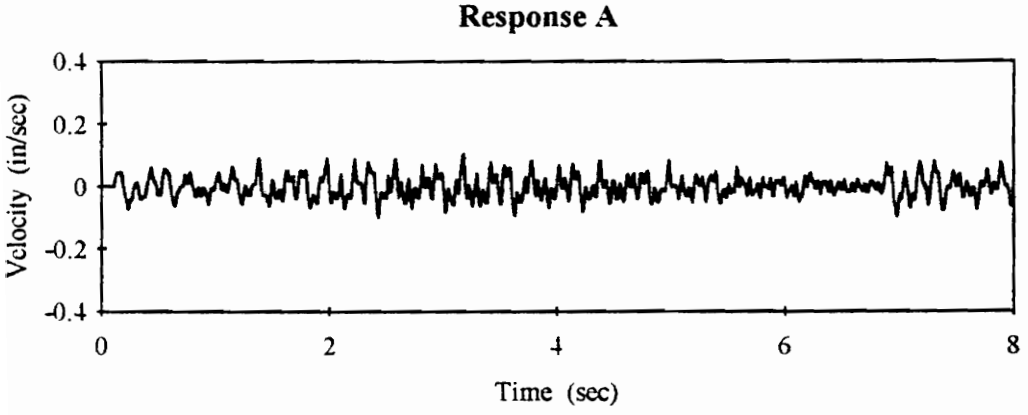

Figure 4.9 Experimental and Simulated Floor Response Due to Walking Excitation

Experimental and Simulated Response at Center of Test Floor for Walking Excitation

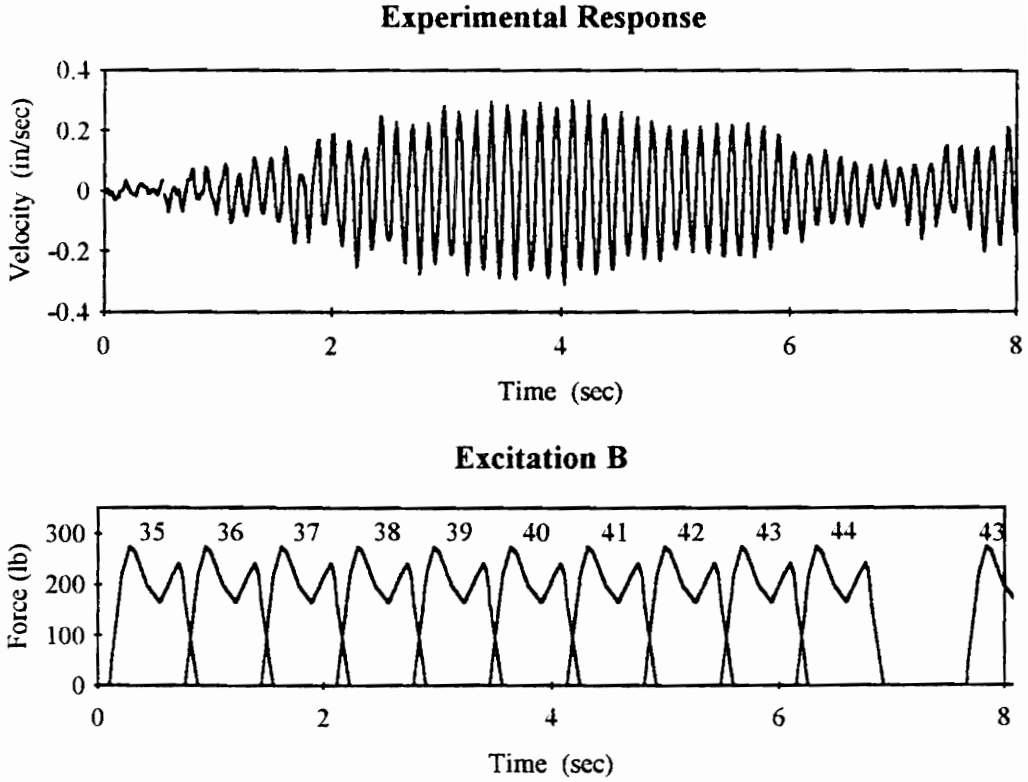

Note: Numbers in excitation time history denote the node number, defined in Figure 3.2, of the force application

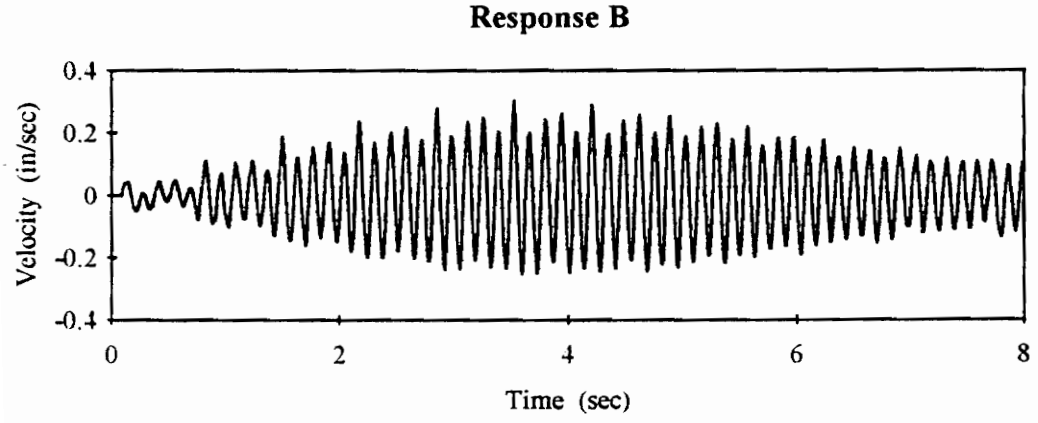

Figure 4.9 (continued) Experimental and Simulated Floor Response Due to Walking Excitation

With a reasonable simulation of the uncontrolled response, experiments and simulations were conducted to assess the ability of a similar model to predict the controlled floor response due to walking excitations. A comparison of the experimental and simulation results is shown in Figure 4.10 for the controlled response at the center of the test floor. Again, the analytical simulation produces a response similar, with respect to peak amplitudes, to the experimental results. The ability to simulate the uncontrolled and controlled floor response due to walking provides a powerful tool for control system design. Such a model could be used in predicting the improvements made to the floor system behavior before the control system is installed.

4.4.2 Comparison of experimental results for walking excitations

As noted previously, the second objective for studying the control system for walking excitations was to compare experimental results for the uncontrolled and controlled system responses. In the first set of experiments presented, the actuator and velocity sensor were located at the center of the floor. The excitation was due to a person walking parallel to the joists close to the center of the 15 ft. span. During the 16 second time measurement, the person traversed the length of the floor two times. The largest amplitudes were measured when the walker was near the center of the floor and the small amplitudes were measured as the walker turned around near each girder. In the controlled system responses, the voltage command to the shaker was limited to ±0.5 volts. The feedback gain was programmed in increments of 2.5 between 2.5 and 17.5. The results

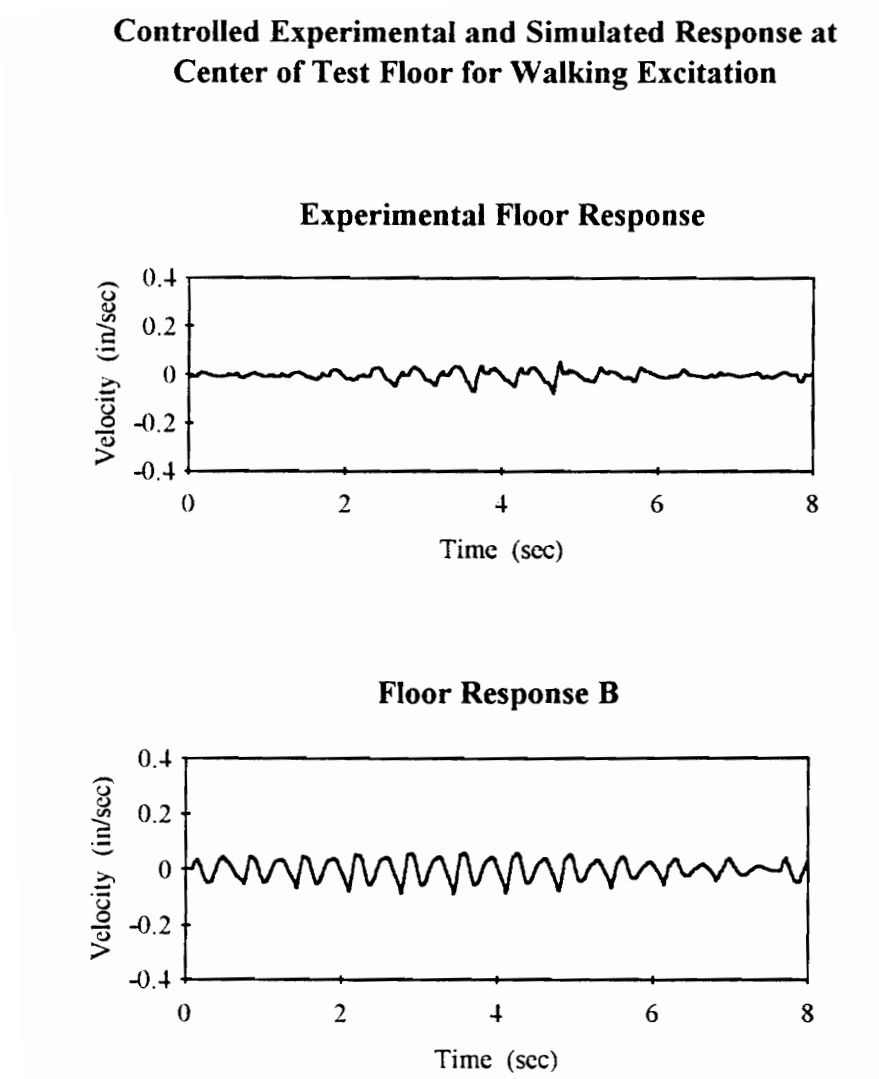

Figure 4.10 Controlled Experimental and Simulated Floor Response Due to Walking Excitation

from these experiments for the response at the center of the floor are presented in Figure 4.11. The vertical scale has been amplified for the controlled responses so subtle differences in amplitudes are noticeable. Again, the most significant effect of the controller was noted for the gain of 7.5. The peak amplitude in this controlled response represented a more than 85% reduction in amplitudes, as reflected in Figure 4.12, when compared to the uncontrolled system.

The controlled system can be evaluated, with respect to human perception, using the scale presented in Chapter 1. The peak amplitudes for the uncontrolled system are plotted on this scale in Figure 4.13. The control scheme improved the floor response, at the center of the floor, to within acceptable levels with respect to the Allen and Murray limit.

4.4.3 Effect of actuator placement in controlling floor response

Study of the uncontrolled and controlled floor system to this point has been limited to the system behavior at the center of the floor. It was noted in the root locus study of Chapter 3 that two of the significant modes of vibration are unaffected by a control actuator at the center of the test floor. In particular, mode shape 2 in Figure 3.3 is a significant component of the response at the center of either edge joist.

The following experimental study is presented to illustrate the effect of actuator placement on controlling both the center and the edge of the floor. Presented in Figure 4.14 are graphs showing the velocity time response for two floor locations. These are the

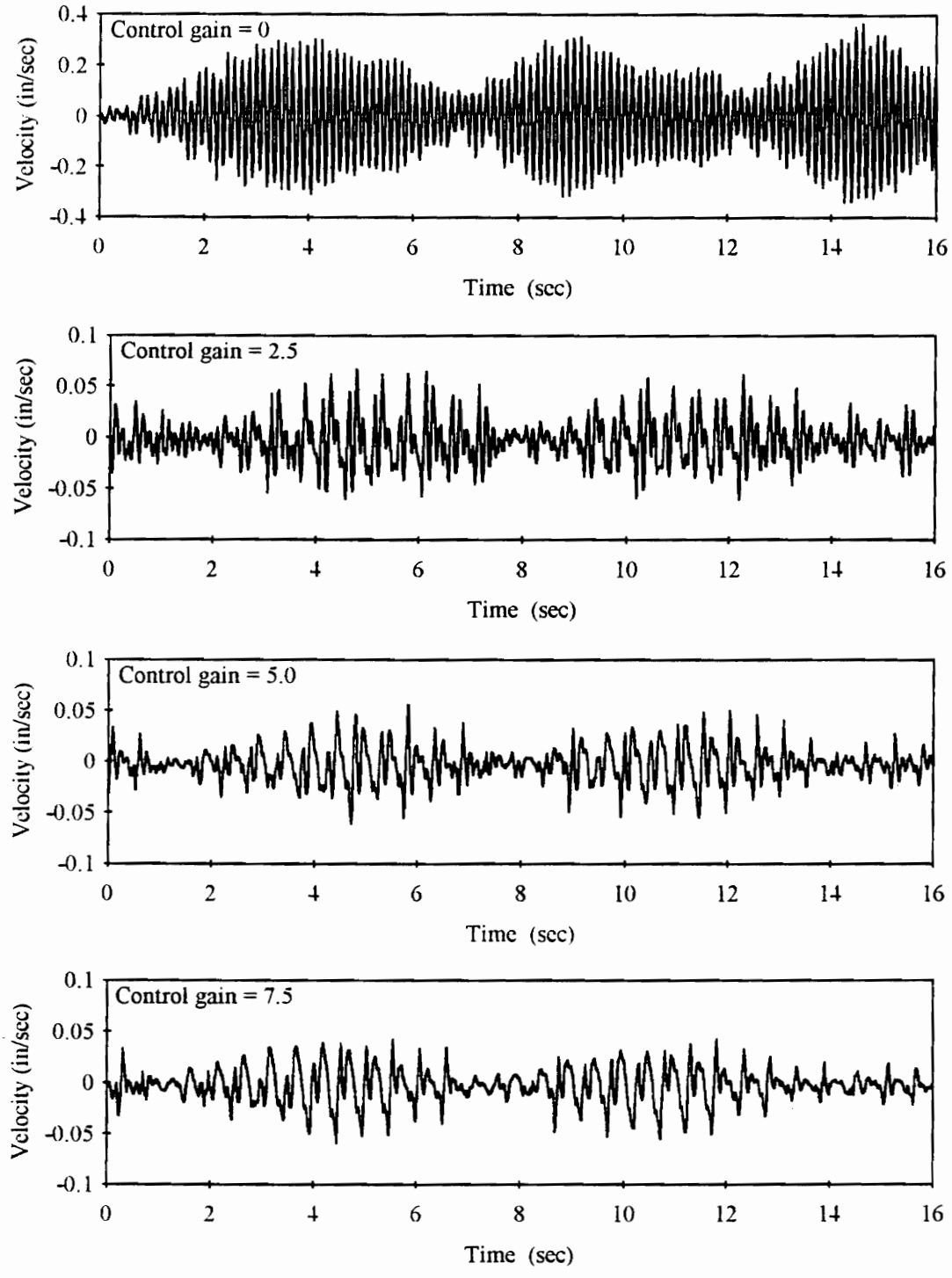

Figure 4.11 Uncontrolled and Controlled Floor Responses for Walking Excitation

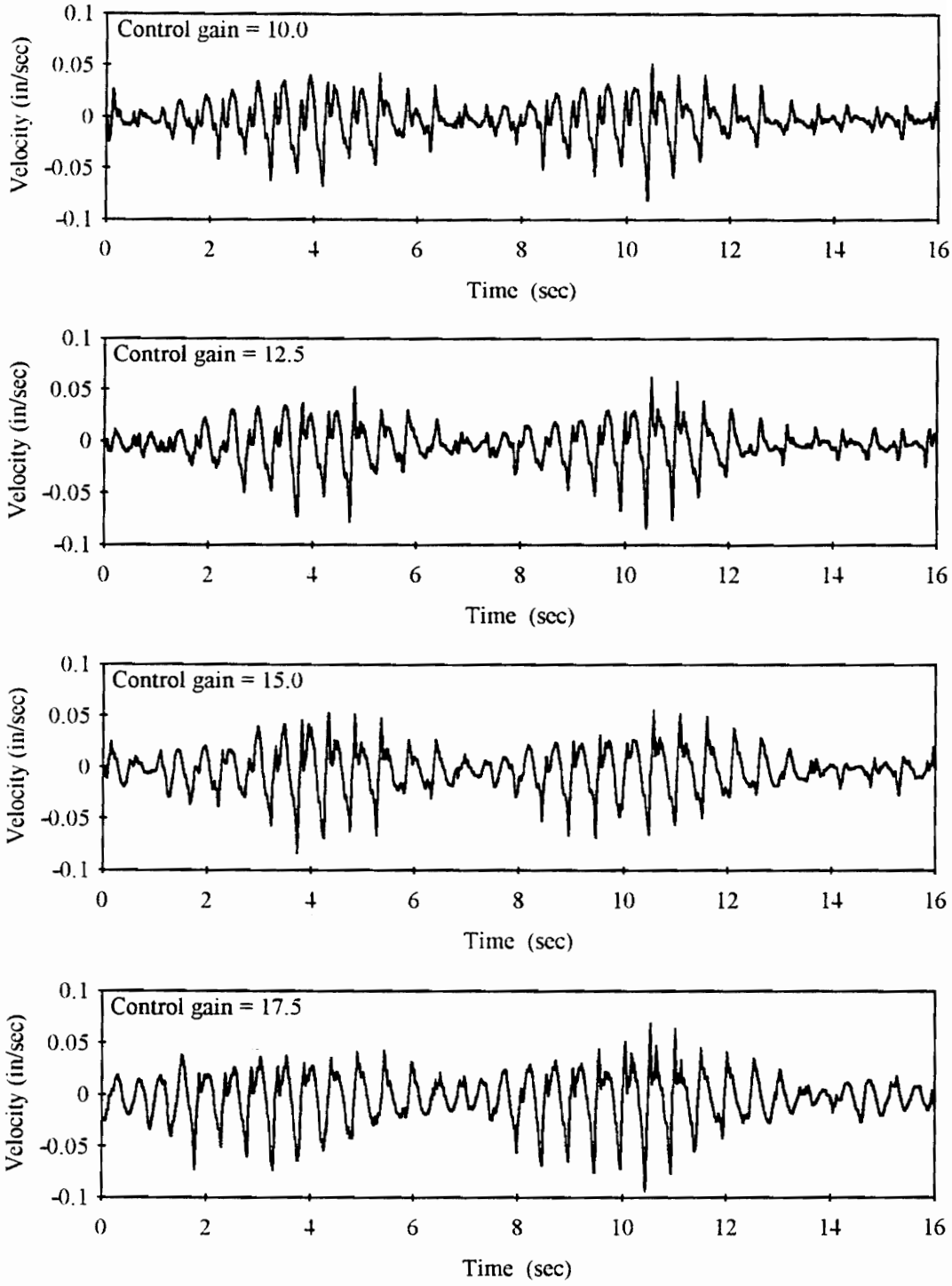

Figure 4.11(continued) Uncontrolled and Controlled Floor Responses for Walking Excitation

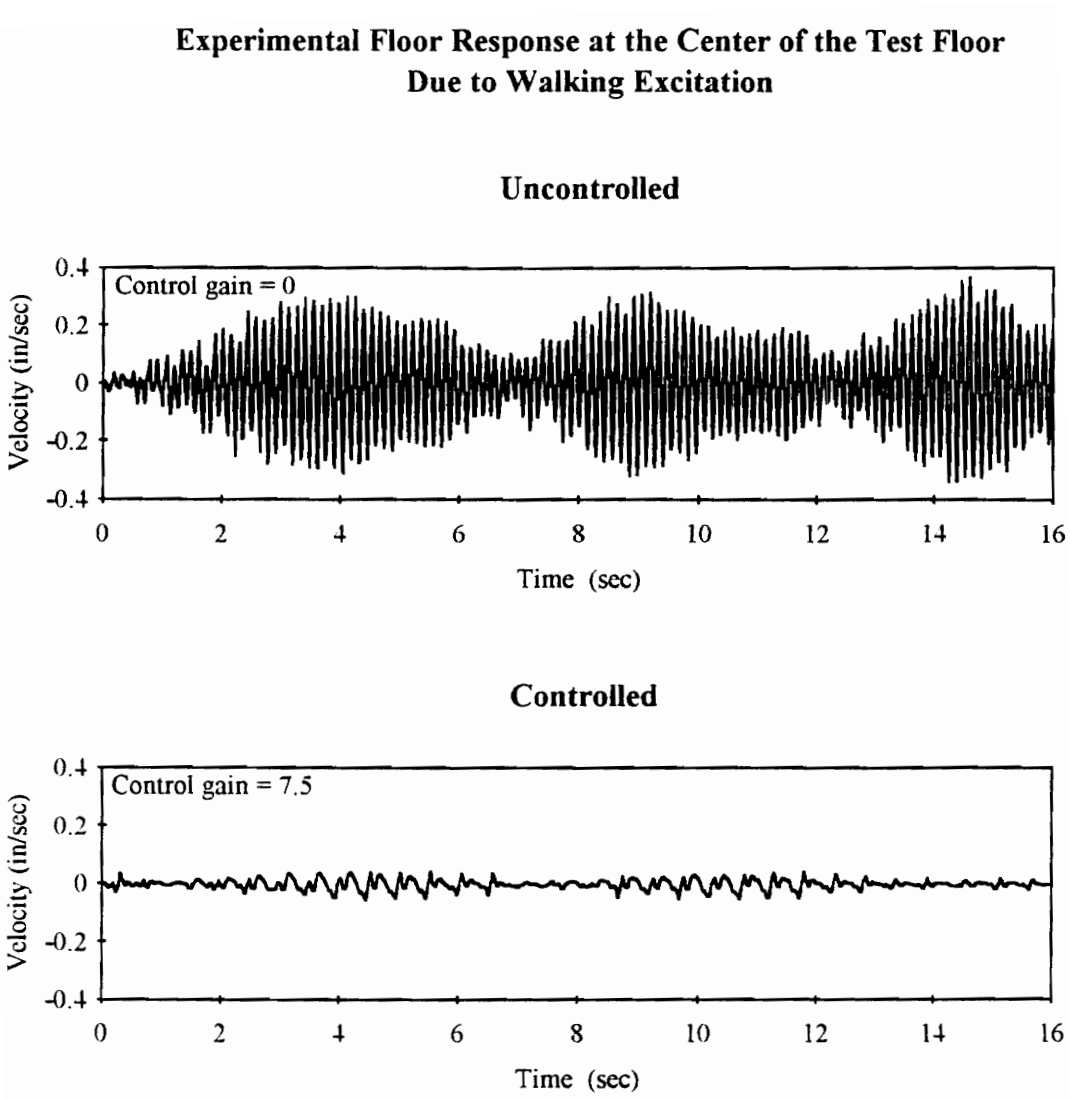

Figure 4.12 Comparison of Uncontrolled and Controlled Responses for Walking Excitation

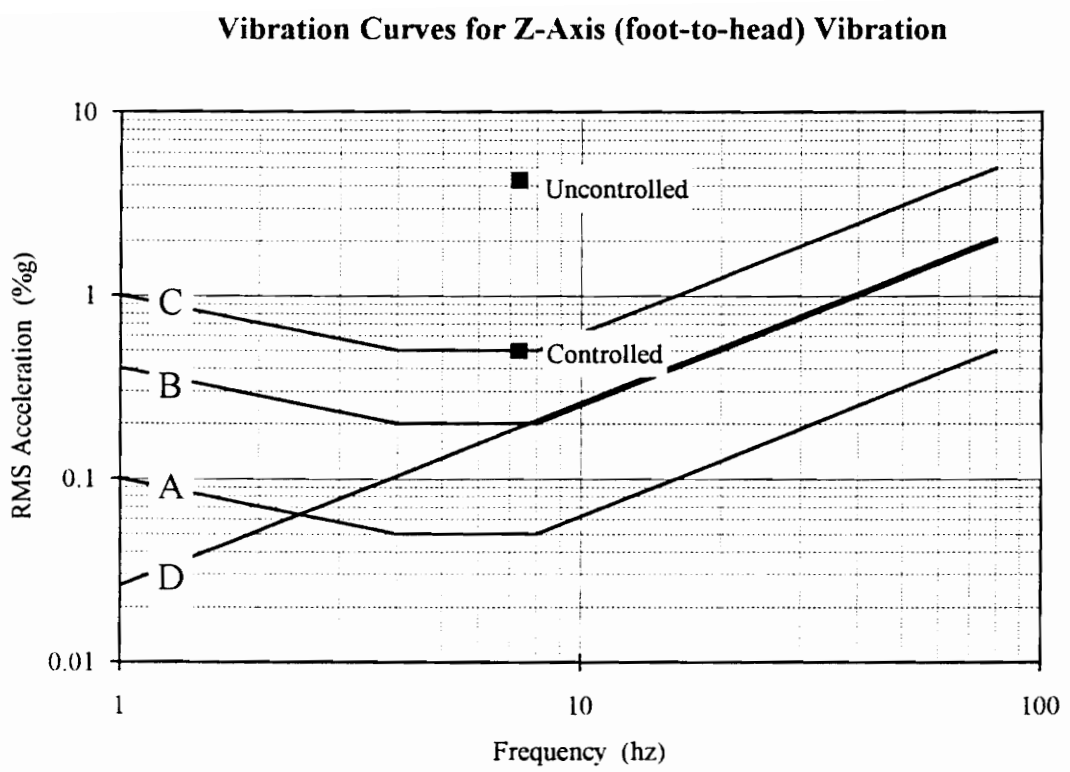

A: ISO baseline curve (ISO 1992)
B: ISO magnitude limit for satisfactory continuous and intermittant vibration in office environments (ISO 1992)
C: Allen and Murray limit for office environments (Allen and Murray 1993)
D: Ungar and Sturtz limit for peak magnitudes in office environments (Ungar et al. 1990)

Figure 4.13 Evaluation of Control Effectiveness Using Human Perception Scales

center of the test floor, node 39, and the center of the edge joist, node 6 as numbered in Figure 3.2. The excitation of the floor consisted of a person walking in a loop described by the node sequence 35-61-43-17-35. Walking in this pattern produces a floor response containing significant contributions from modes one and two. The uncontrolled response, as measured at nodes 39 and 6, is plotted in the top two graphs. The controlled responses for the control actuator located at node 39 are shown in the bottom two graphs of Figure 4.14. It should be noted that the second mode is uncontrolled for this control actuator location; therefore, very little improvement is noted for the controlled response at node 6.

To control the second mode of vibration, the control actuator must be located at a point where this mode is observable and therefore controllable. The response of the floor was recorded at nodes 6 and 39 for three other control actuator locations; these are nodes 28, 17, and 6. The results from these experiments are shown in Figure 4.15. As the control actuator is moved from the center of the floor to the edge of the floor, the response at node 6 is greatly improved, while a measure of control is sacrificed at node 39.

The experiment described above illustrates the importance of the control objectives on the location of the actuator. If the objective is to control a particular location, placing the actuator at that location will provide the best control performance when using collocated velocity feedback. If the control objective is to achieve the largest degree of control for the entire system, the actuator location must be optimized either by experimental trial and error procedures or by numerical optimization procedures. It

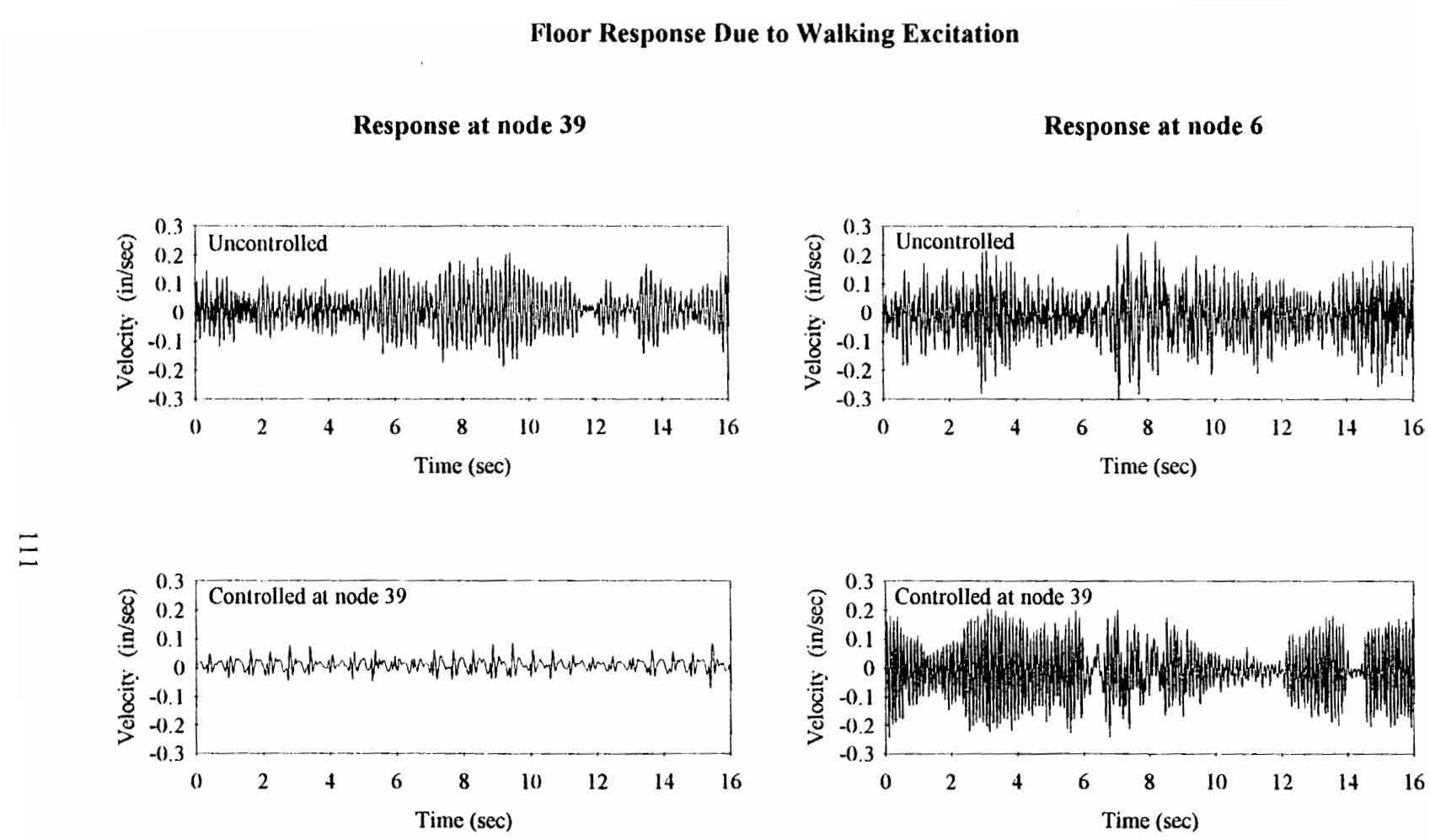

Figure 4.14 Uncontrolled and Controlled Response Due to Walking Excitation

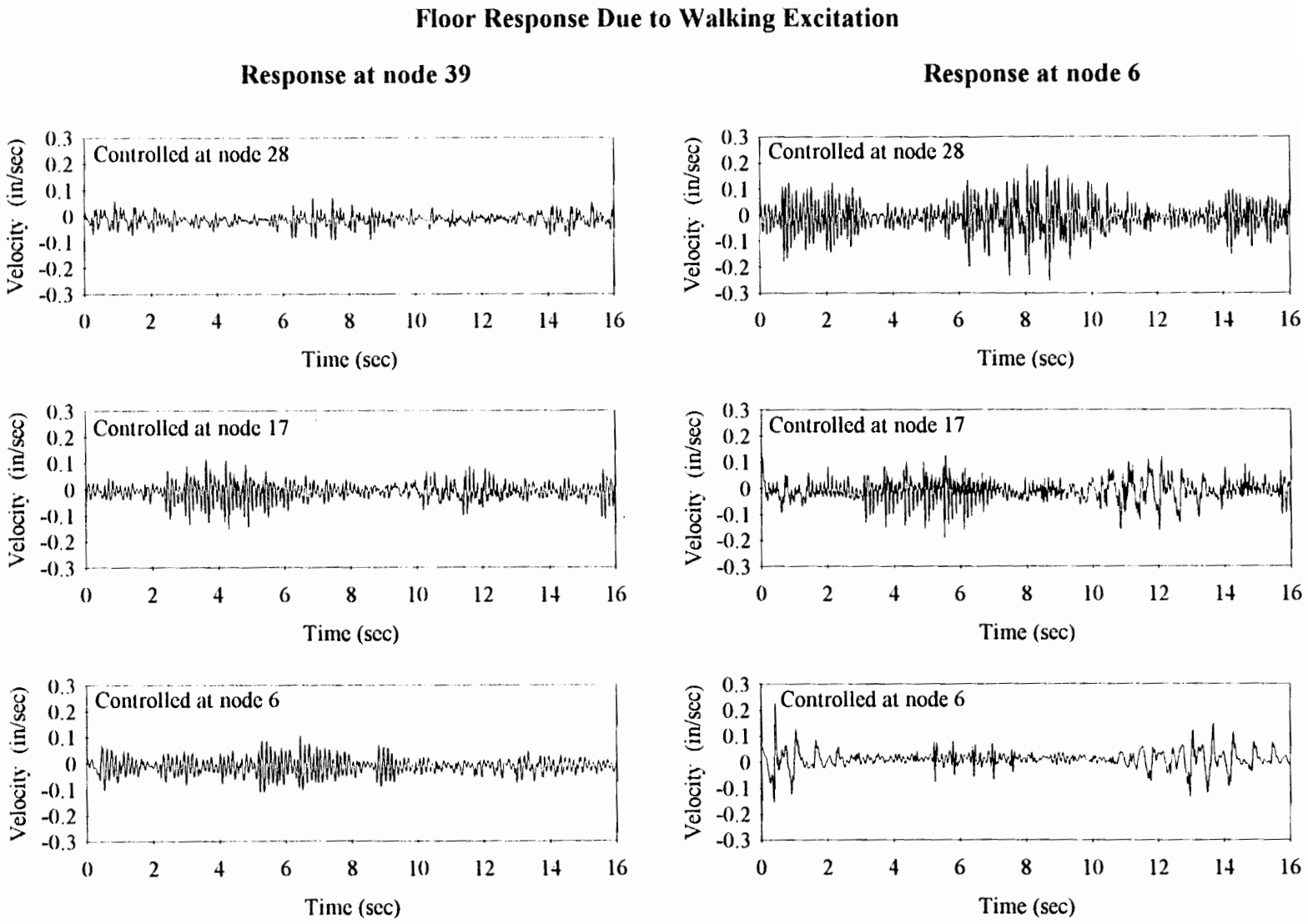

Figure 4.15 Controlled Response Due to Walking Excitation for Various Control Actuator Locations

should be noted, however, that the performance objective of controlling the entire floor system is not practical using a single control actuator and will not be explored further in this research.

4.5 Stability Evaluation of the Controlled System

Perhaps the primary concern in the implementation of active structural control is the system stability. The concept of stability was addressed in the analytical discussion of the linear system roots and the root locus in Chapter 3. As noted in this discussion, actuator dynamics can produce instabilities in the system if the control gain is not carefully selected. The purpose here is not to reiterate the discussion of Chapter 3, but rather to experimentally verify the analytical behavior with respect to stability.

For the analytical model the stable gain range was 0 to 19.53. The performance of the controller was shown to be affected by the degree of stability maintained in the actuator root. The most effective gain selection for controlling the system was not the largest possible stable gain; instead, a gain which controlled the floor response while maintaining a moderate degree of stability in the actuator root was found to provide the best control performance. This behavior was experimentally verified in the results presented in Figure 4.11. Additionally, this figure verifies experimentally that stable behavior was observed for gains up to 17.5.

Theoretically, unstable behavior is predicted for gains above 19.53. To verify this prediction, a gain selection of 20.0 was implemented experimentally. The initial

disturbance in the system was the result of electrical noise in the system. The velocity time history of the floor response (at the center of the test floor) from this experimental test is shown along with the simulated response in Figure 4.16. In the simulation, a small impact excitation was used as the initial disturbance. Within the linear range of the controller, the magnitude of the floor response increased exponentially as would be expected in the unstable system. The response then leveled off to a steady-state oscillation. This is the result of the command limiter built into the control algorithm. A destructive unstable behavior, with amplitudes increasing to failure, is not possible with the non-linear control parameters selected. In fact, the steady-state oscillation produced by a linearly unstable gain selection is found to produce only a slightly perceptible vibration level with respect to the scale in Figure 1.1.

By selecting the most effective control gain for controlling walking vibrations, a comfortable margin of stability in the linear system is maintained. Additionally, the non-linear circuit provides a safeguard against destructive behavior from an unstable gain selection.

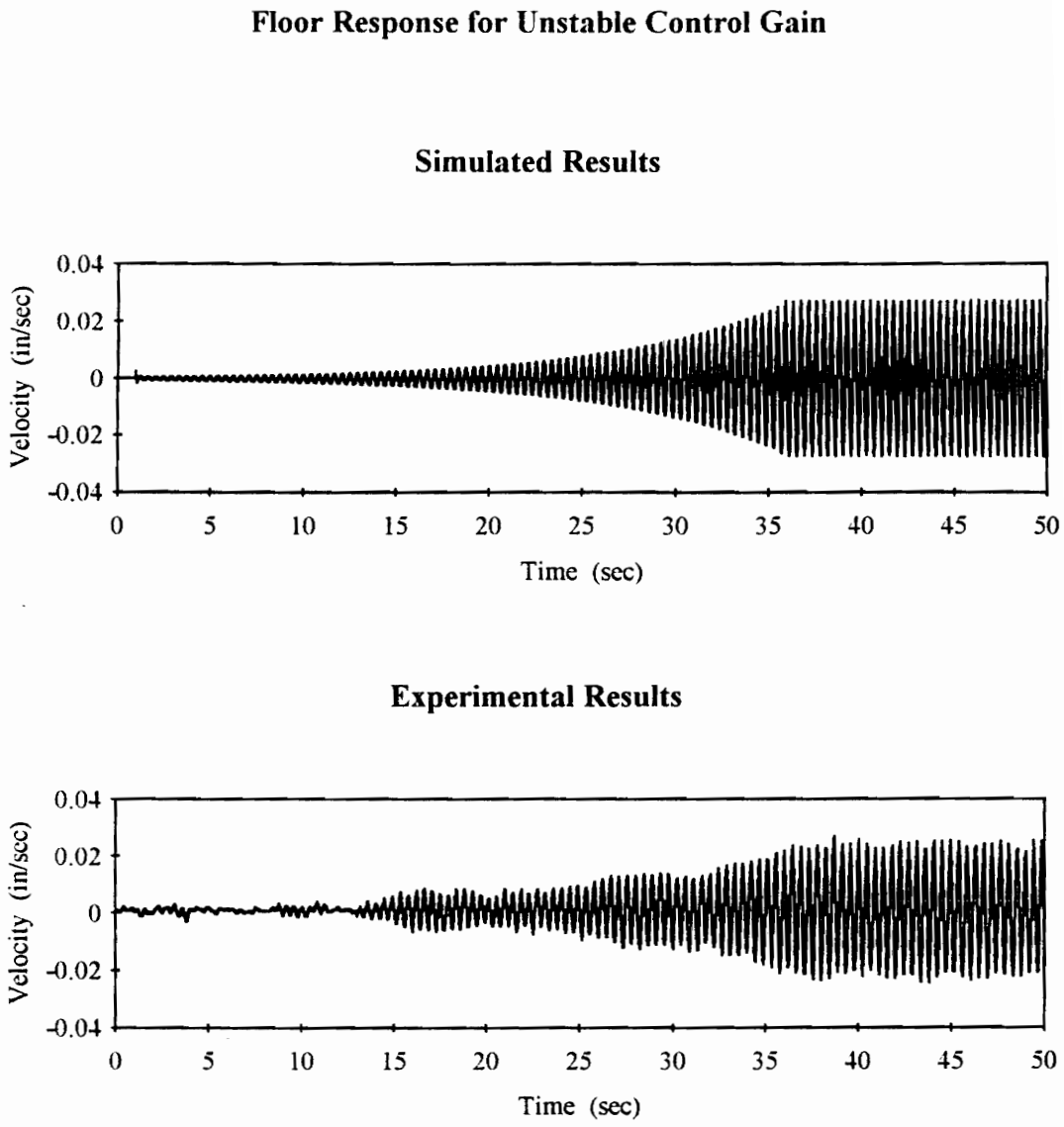

Figure 4.16 Simulated and Experimental Floor Response for Unstable Control Gain

CHAPTER 5

EXPERIMENTAL IMPLEMENTATION OF ACTIVE CONTROL ON ADDITIONAL FLOORS

Experimental tests were carried out on six additional floors to further illustrate the ability of the control scheme to reduce the levels of floor vibration. Three of the floors were full-scale test floors of varying complexity. The remaining three were occupied floors in buildings reported to have unacceptable dynamic characteristics. In the following sections, a brief description of each floor is presented along with experimental results illustrating the control system effectiveness. Finally, the results are summarized and compared in Section 5.7.

5.1 Shallow Joist Test Floor

The shallow joist test floor is a 30 ft. x 30 ft. bare test floor constructed at Virginia Tech's Prices Fork Research Center. Thirty-one 8 in. deep joists, spaced at 1 ft on center, are supported by a masonry wall as shown in Figure 5.1. The slab is lightweight concrete on metal deck with a total thickness of $2^1/_2$ in.

Two types of experimental tests were conducted to compare the uncontrolled and controlled floor system responses. In the first experimental test series, the control actuator, sensor, and force plate were all placed at the center of the test floor, noted as the controller location in Figure 5.1. A heel drop was performed on the force plate. Force and velocity measurements were recorded for the uncontrolled and controlled systems. A

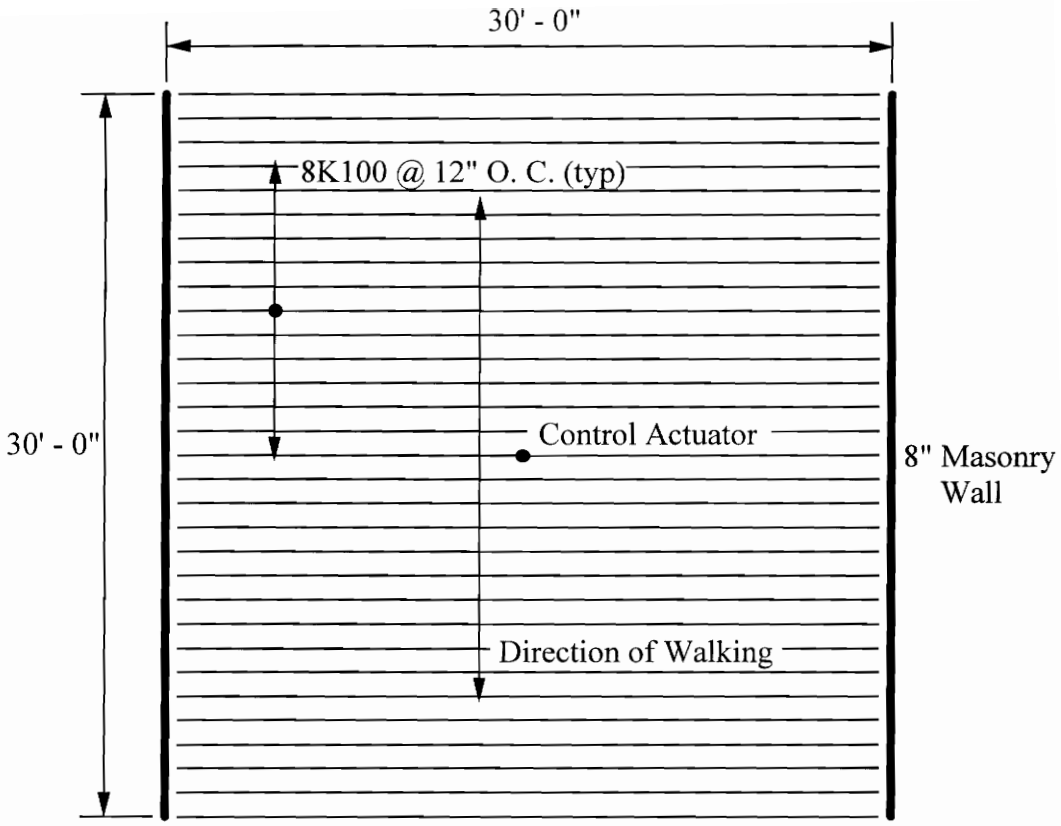

Figure 5.1 Plan of Shallow Joist Test Floor

comparison of these results is shown in Figure 5.2 From the experimental results of the uncontrolled system, the frequency and damping for the first mode of vibration are estimated to be 6.1 hz and 1.1%, respectively.

The second experimental test series measured the uncontrolled and controlled response due to a walking excitation. During a 16 second time measurement period, a person walked perpendicular to the joists as shown in Figure 5.1. The results are compared in Figure 5.3. Consistency in the walking excitation for each measurement was maintained as closely as possible to provide a relevant comparison.

As in the heel drop tests discussed in Chapter 4, the control effectiveness is largely affected by the non-linear capabilities of the controller. While significant improvements are shown in the controlled heel drop response, a better measure of the control effectiveness is computed from the responses due to walking excitation. Each measurement consists of 1024 data points measured over a period of 16 seconds. The sum of the absolute value of these data points is an indication of the vibration level present in the floor during the measured response. A ratio of the sums for the controlled and uncontrolled systems provides a quantitative measure of the control system effectiveness and can be defined as a "reduction ratio". A smaller ratio, indicates a larger degree of control effectiveness. The reduction ratio computed for the experimental measurements shown in Figure 5.3 is 0.41.

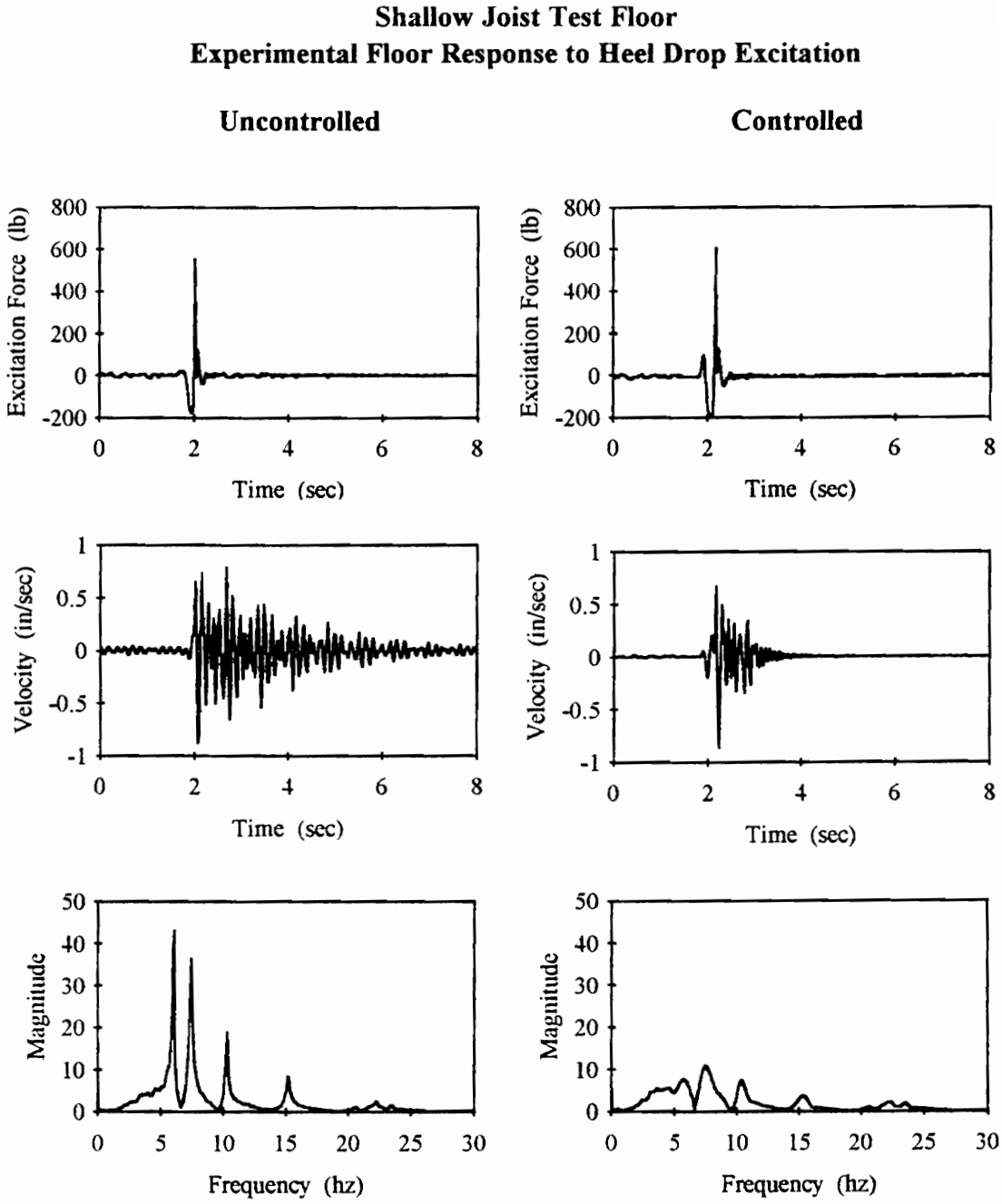

Note: The graphs labeled Magnitude vs. Frequency represent the frequency transform of the velocity time history above

Figure 5.2 Uncontrolled and Controlled Floor Response of Shallow Joist Test Floor to Heel Drop Excitation

Shallow Joist Test Floor
Experimental Floor Response to Walking Excitation

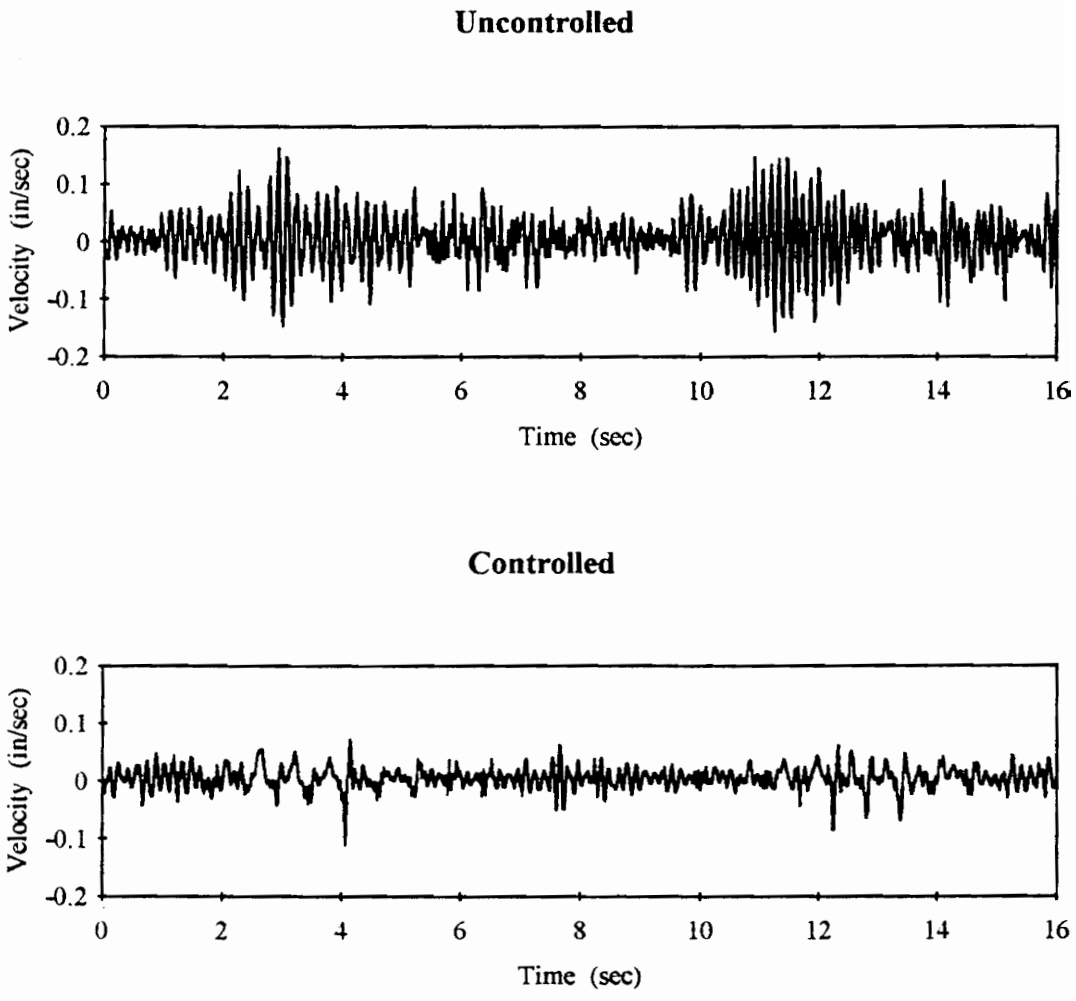

Figure 5.3 Uncontrolled and Controlled Response of Shallow Joist Test Floor Due to Walking Excitation

5.2 High Frequency Joist Test Floor

The high frequency joist test floor, also located at Virginia Tech's Prices Fork Research Center, is a 30 ft x 30 ft bare test floor. A plan of this floor is shown in Figure 5.4. Joist girders support nine 28 in. deep joist members at 48 in. on center. The slab is lightweight concrete on metal deck with a total thickness of $2^1/_2$ in. Heel drop and walking tests, as described in the previous section, were again performed. The results of these tests are shown in Figures 5.5 and 5.6. The frequency and damping for the first mode of vibration in the uncontrolled system are 6.9 hz and 0.76%, respectively. The reduction ratio, as described in the previous section, is 0.21.

5.3 Two Bay Test Floor

The two bay test floor, located at Virginia Tech's Prices Fork Research Center, is the roof of a small building. The 25 ft. x 60 ft. floor is a two bay system constructed of joists, spanning 30 ft, and joist girder members framing members as shown in Figure 5.7. The slab is normal weight concrete on metal deck with a total thickness of $2^1/_2$ in. The control actuator, sensor, and force plate were placed at the center of one bay. Results comparing the uncontrolled and controlled responses, due to heel drop and walking excitations, are shown in Figures 5.8 and 5.9. The frequency and damping for the first mode of vibration in the uncontrolled system are 5.1 hz and 2.7%, respectively. The reduction ratio, computed from results in Figure 5.9, is 0.44.

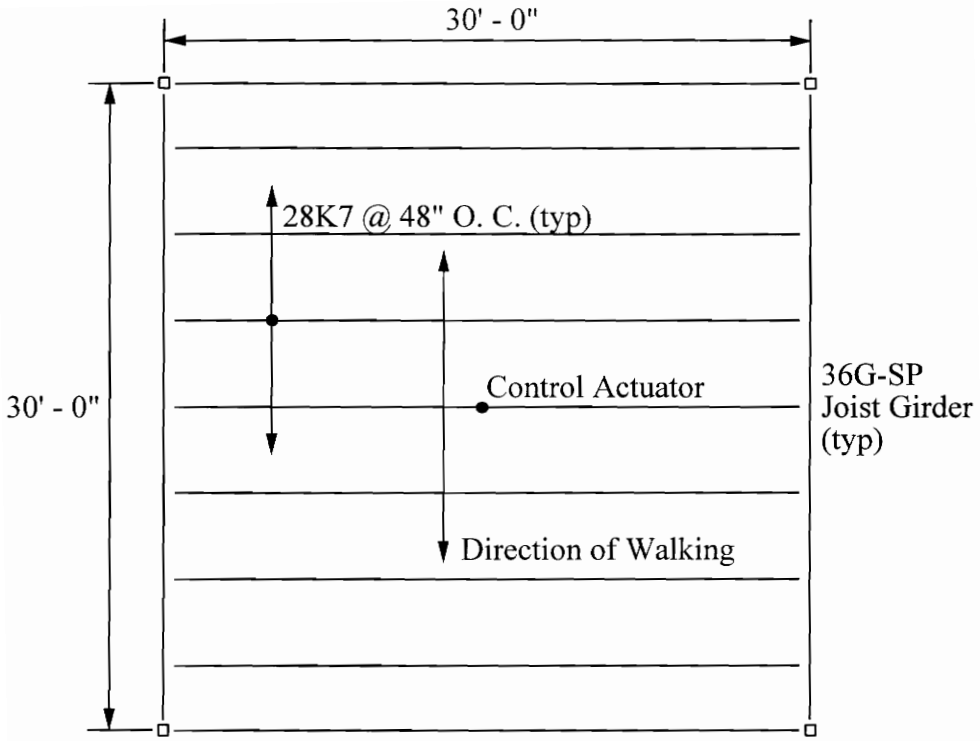

Figure 5.4 Plan of High Frequency Joist Floor

High Frequency Joist Test Floor
Experimental Floor Response to Heel Drop Excitation

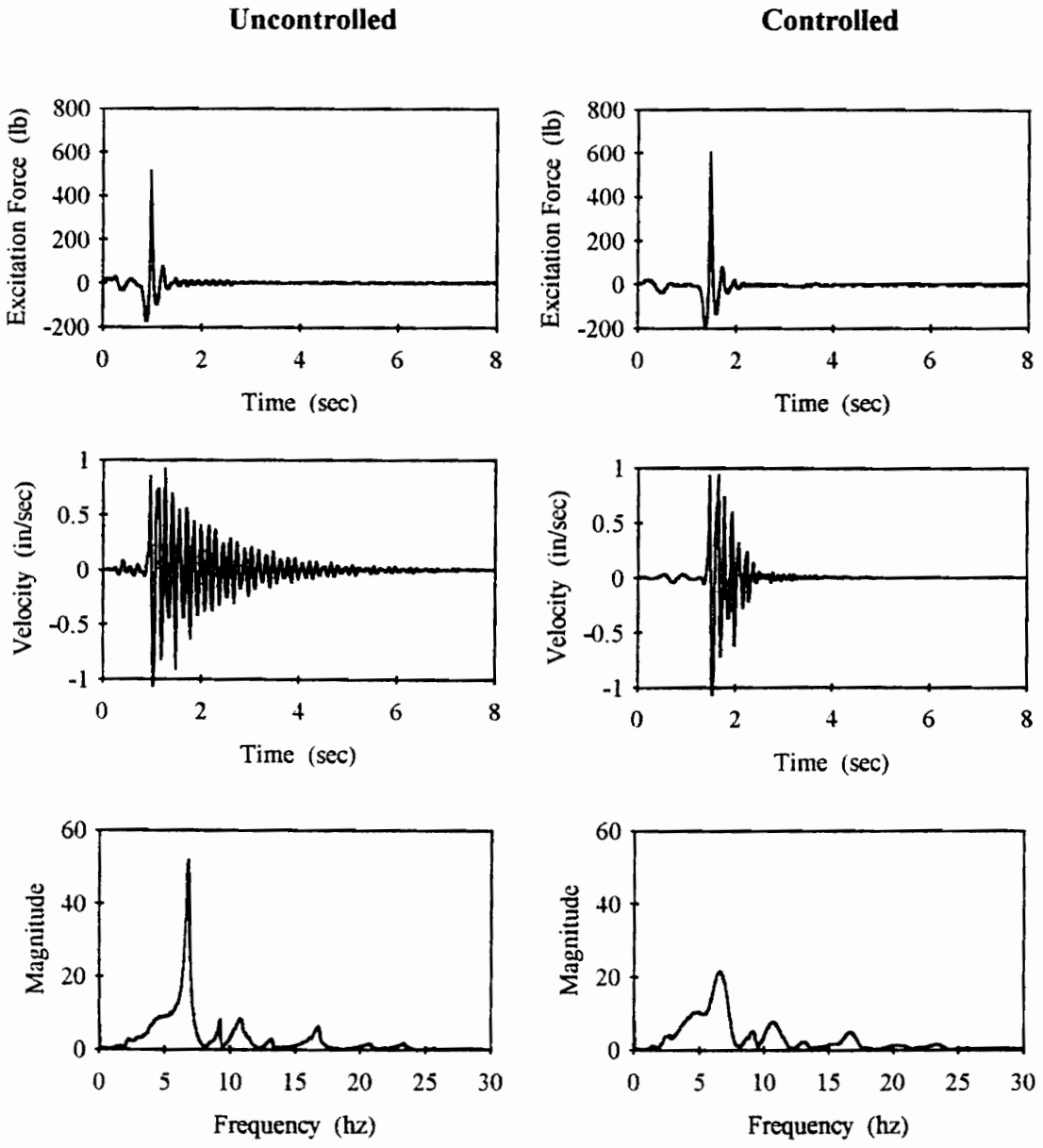

Note: The graphs labeled Magnitude vs. Frequency represent the frequency transform of the velocity time history above

Figure 5.5 Uncontrolled and Controlled Floor Response of High Frequency Test Floor Due to Heel Drop Excitation

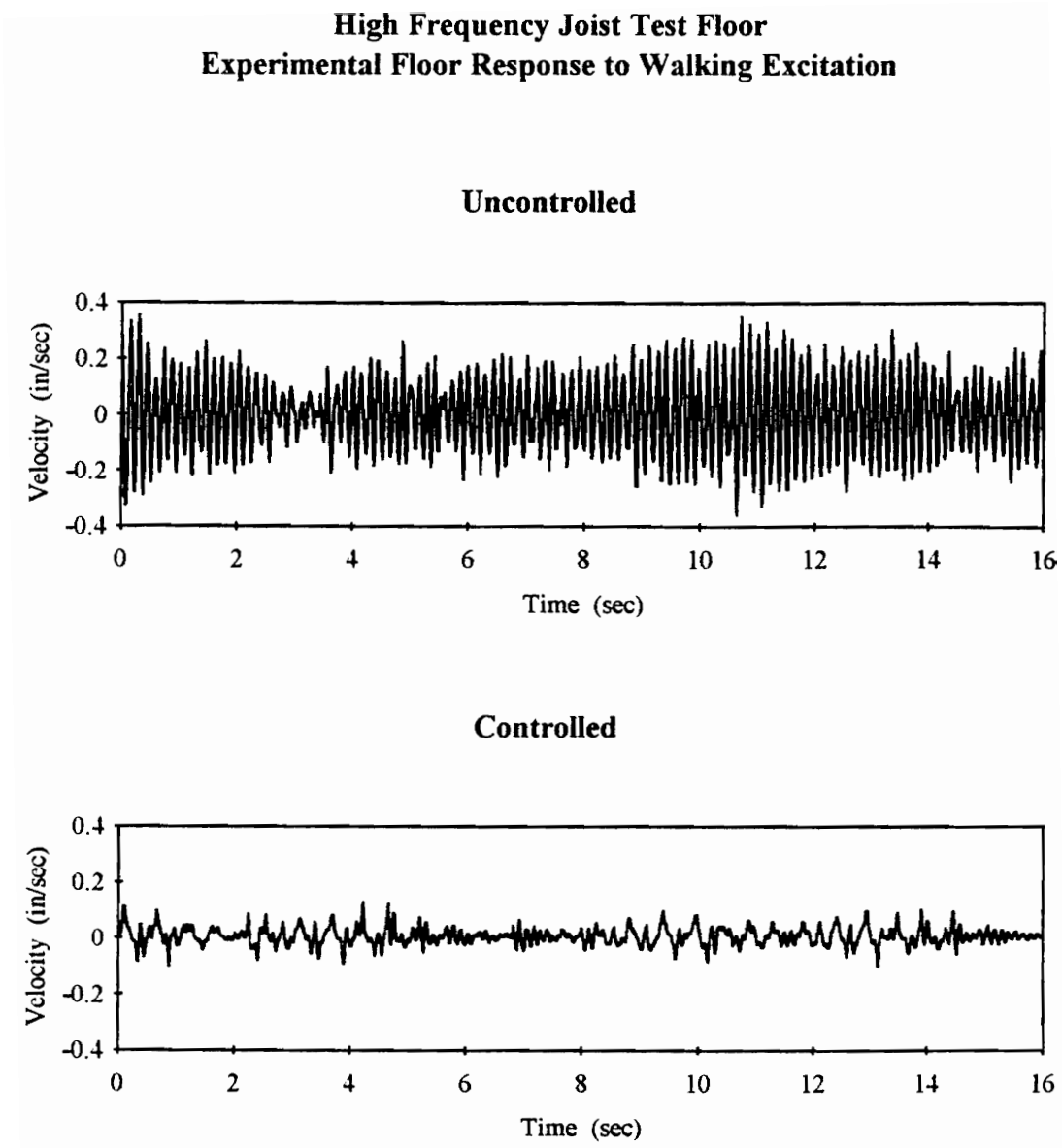

Figure 5.6 Uncontrolled and Controlled Response of High Frequency Joist Test Floor Due to Walking Excitation

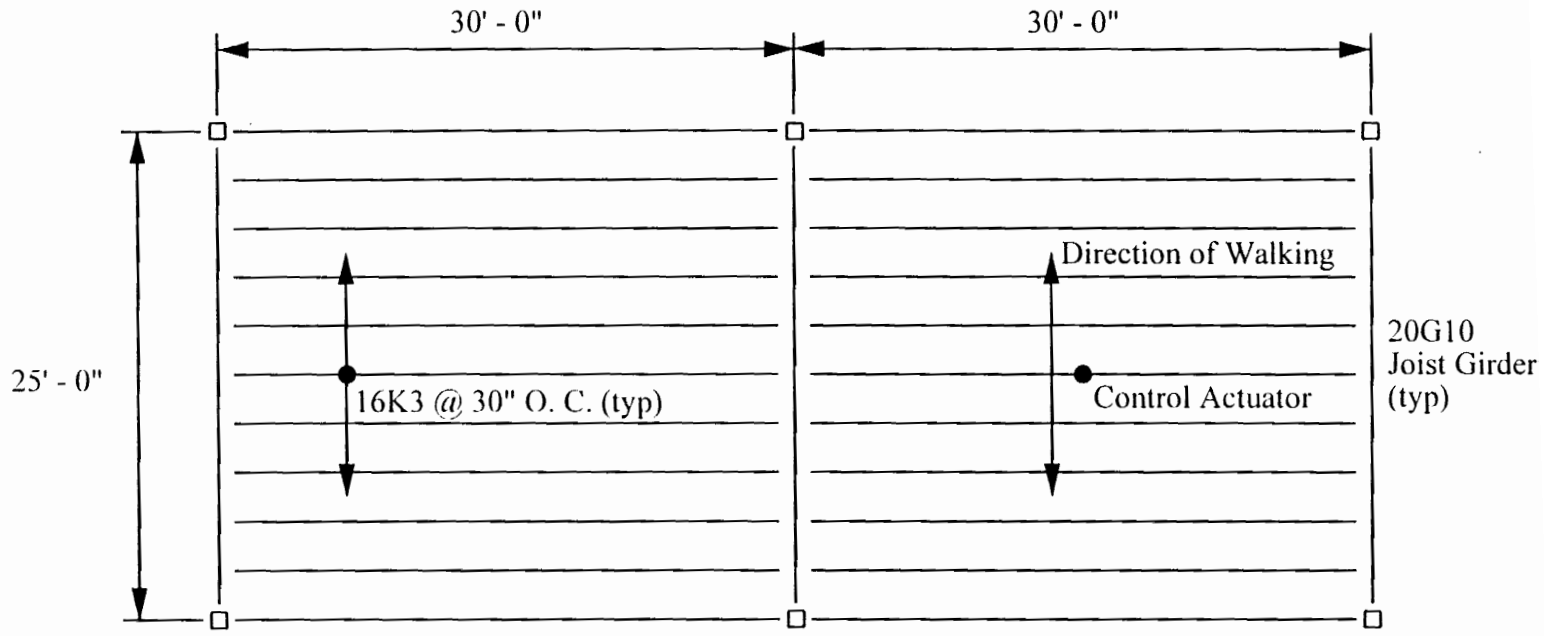

Figure 5.7 Plan of Two Bay Test Floor

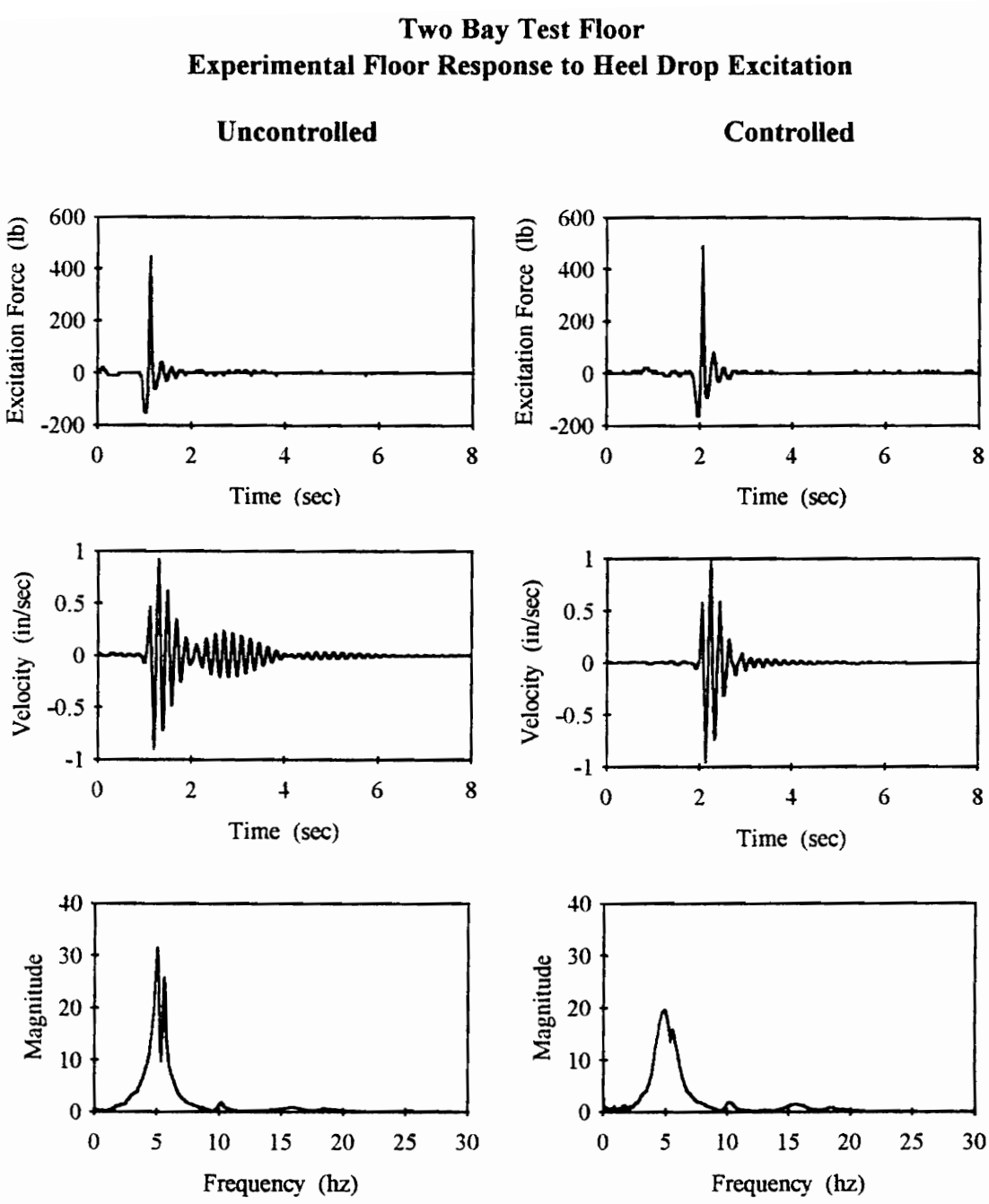

Note: The graphs labeled Magnitude vs. Frequency represent the frequency transform of the velocity time history above

Figure 5.8 Uncontrolled and Controlled Floor Response of Two Bay Test Floor Due to Heel Drop Excitation

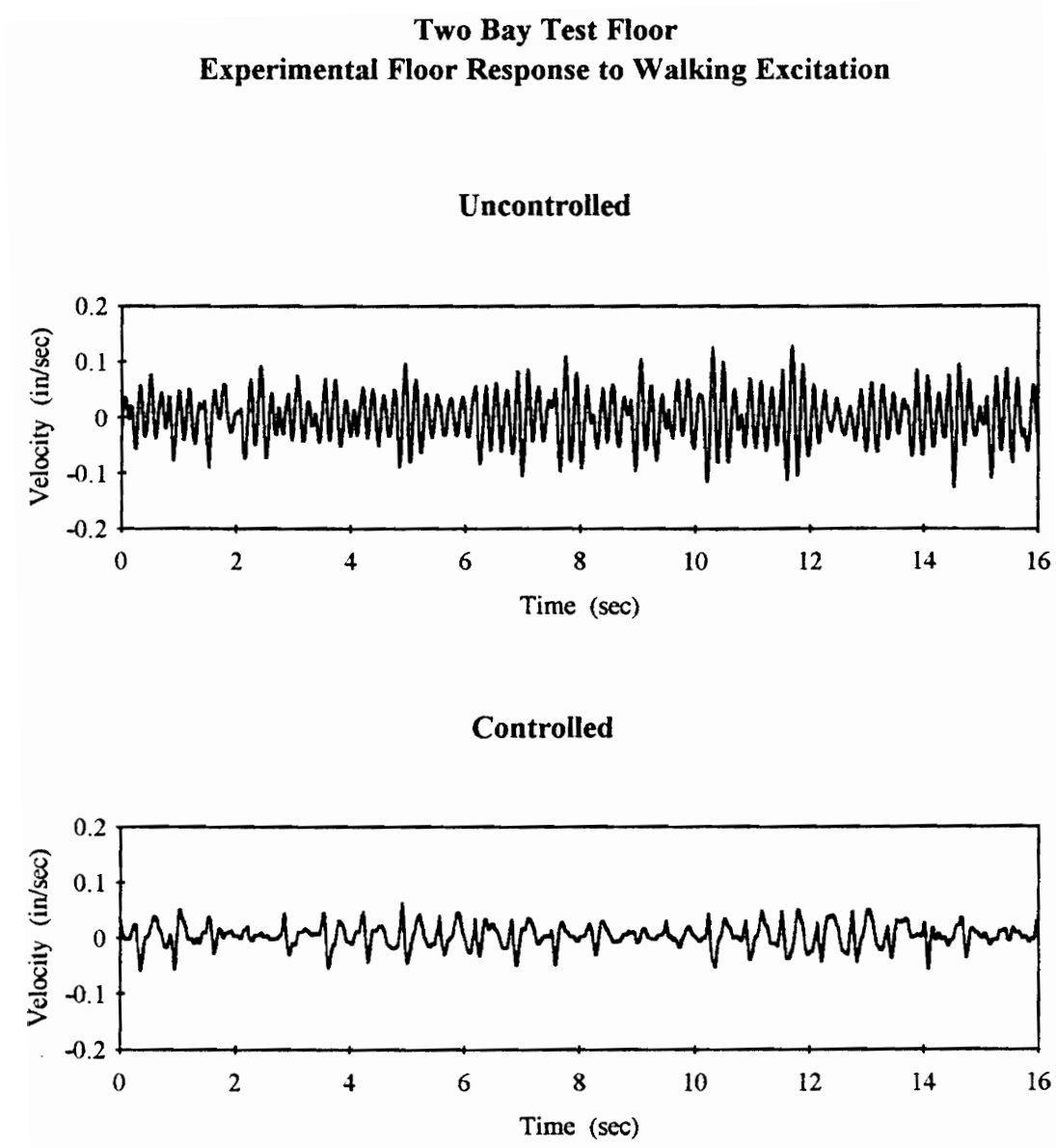

Figure 5.9 Uncontrolled and Controlled Response of Two Bay Test Floor Due to Walking Excitation

5.4 St. Louis Office Floor

An office floor in a light manufacturing facility, located in St. Louis, Missouri, was reported to have annoying levels of occupant induced floor vibrations. A plan of this floor is shown in Figure 5.10. The construction of this floor consists of a $2^1/_2$ in. lightweight concrete slab on metal deck supported by joist framing members as indicated on the plan. The 28 ft. - 4 in. span was found to be the problem area. In this span, two long rows of desks are separated by an aisle near the center of the span. This open office area is used primarily for order processing with personal computers on nearly every desk. Walking in the aisle causes computer monitors to rock, thus intensifying the degree of annoyance. One particularly disturbing characteristic of this floor is that annoying levels of vibration are felt even when the occupant movement is several bays away.

An attempt was made to actively control the floor movement at a location where the problem was particularly acute. The control actuator, sensor, and force plate were placed at the controller location noted in Figure 5.10, and heel drop tests were performed. A comparison of the results for the uncontrolled and controlled system is shown in Figure 5.11. Force plate measurements were not available for these experiments. The floor response due to a person walking in the aisle between the desks was also measured for the uncontrolled and controlled system. These results are presented in Figure 5.12. The reduction ratio for the controlled and uncontrolled system responses is 0.27.

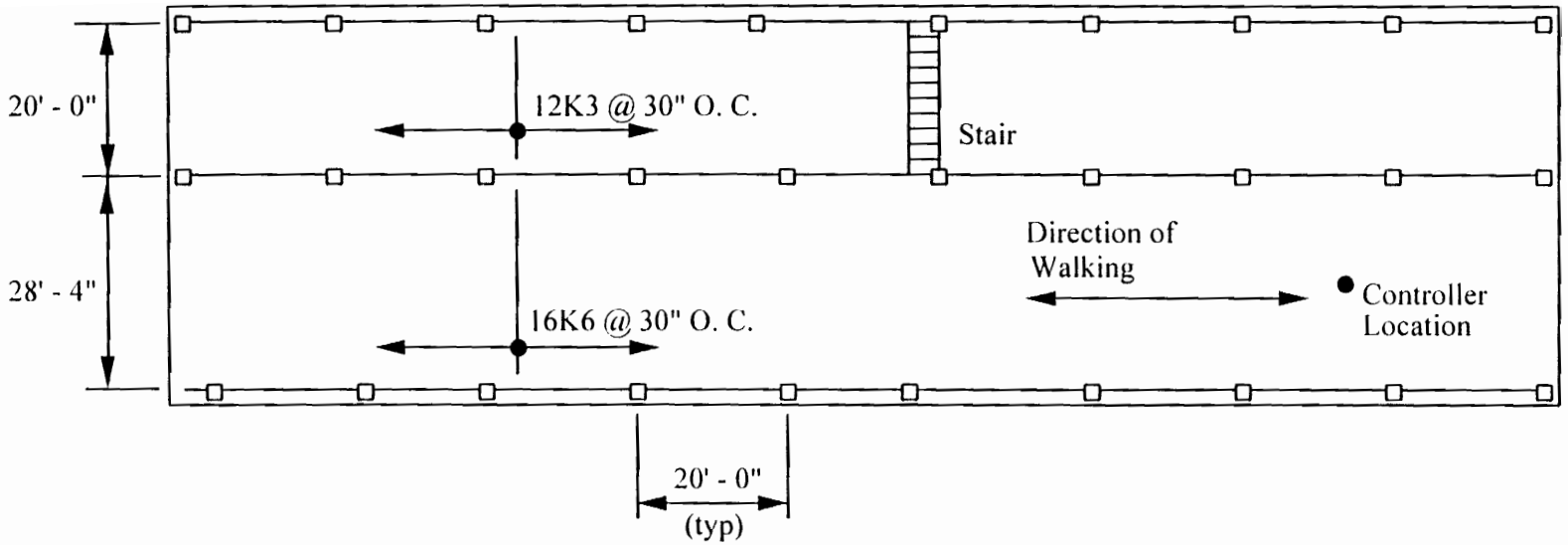

Figure 5.10 Plan of St. Louis Office Floor

St. Louis Office Floor
Experimental Floor Response to Heel Drop Excitation

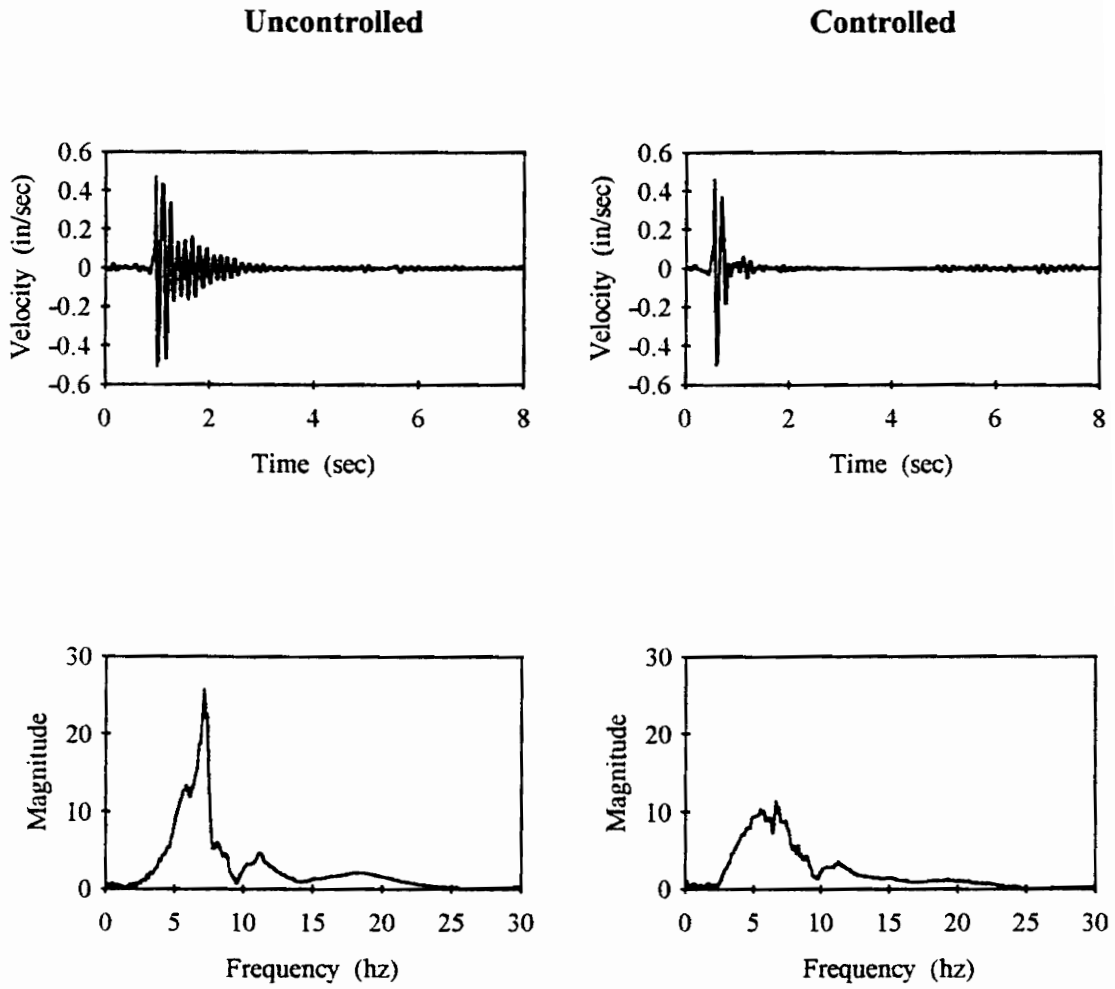

Note: The graphs labeled Magnitude vs. Frequency represent the frequency transform of the velocity time history above

Figure 5.11 Uncontrolled and Controlled Floor Response of St. Louis Office Floor Due to Heel Drop Excitation

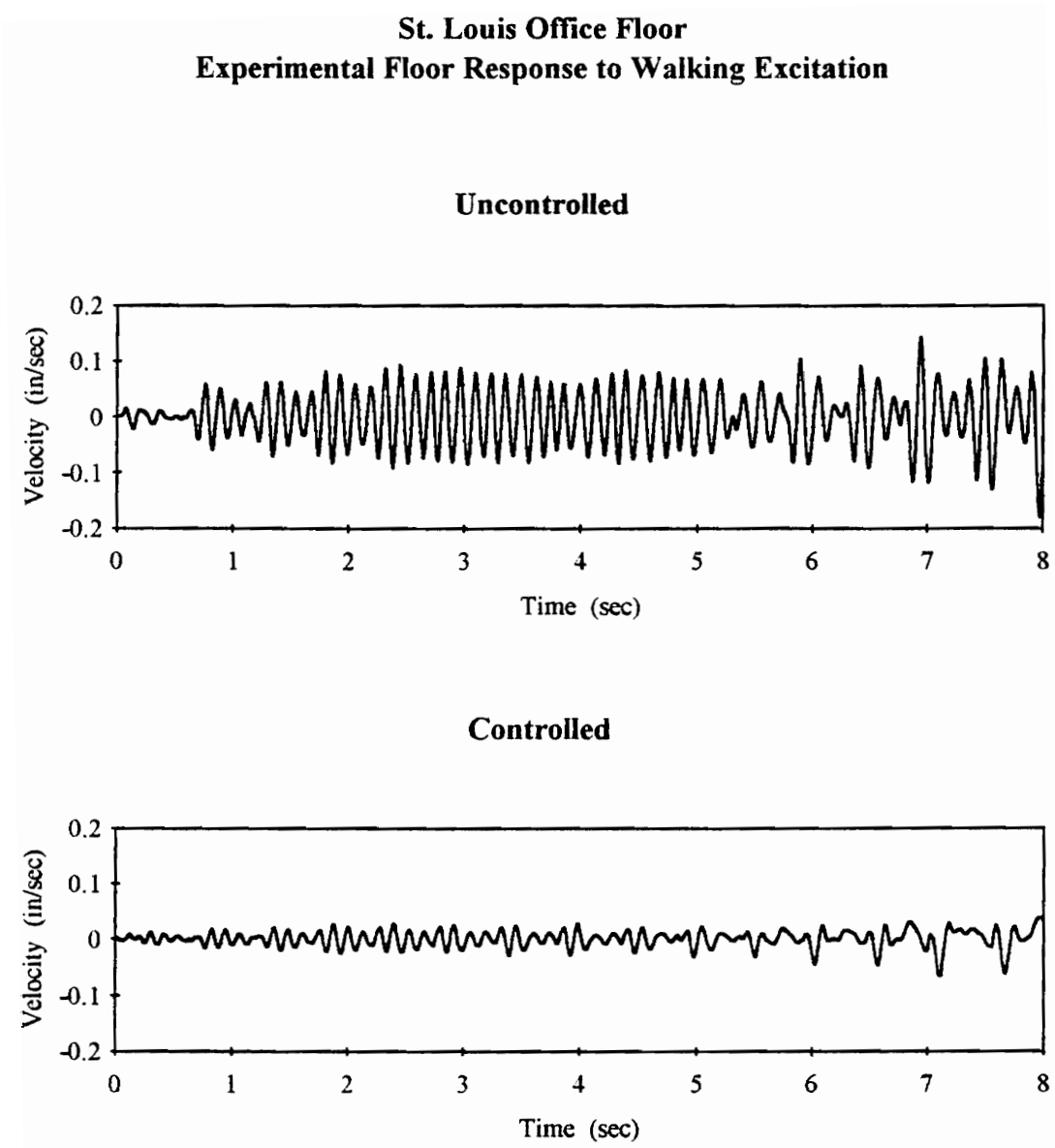

Figure 5.12 Uncontrolled and Controlled Response of St. Louis Office Floor Due to Walking Excitation

5.5 Kentucky Office Floor

A problem area, with respect to annoying levels of floor vibration, was reported for an open plan office floor in Kentucky. The floor construction is $4^1/_2$ in concrete on a 2 in composite metal deck supported by long span joist members as shown in Figure 5.13. Annoying levels of vibration in the 52 ft. span resulted from occupant movement in the aisles separating the desks. The active control scheme was implemented to reduce the occupant induced vibration levels. Heel drop and walking tests were again performed to assess the ability of the control scheme to control the floor. Results from these tests are shown in Figures 5.14 and 5.15. The frequency and damping in the first mode of the uncontrolled system are 5.1 hz and 2.6%, respectively. The reduction ratio is 0.56.

5.6 Vermont Laboratory Floor

Excessive floor vibration due to occupant movement was reported to exist in a Vermont university chemistry laboratory where sensitive microscopes were in use. A partial plan of the floor system is shown in Figure 5.16. The 7 ft. span is a corridor with laboratory rooms on either side. The floor construction consists of a $3^1/_2$ in. concrete slab on metal deck supported by joist members as shown in the plan. The problem area, in the laboratory with the 28 ft.- 7 in. span, contains three island type workbenches where the function has been severely impaired due to disturbing levels of floor vibration. The active control scheme was implemented to reduce the floor motion. Heel drop and walking tests were performed to assess the impact of the control. Results from these tests

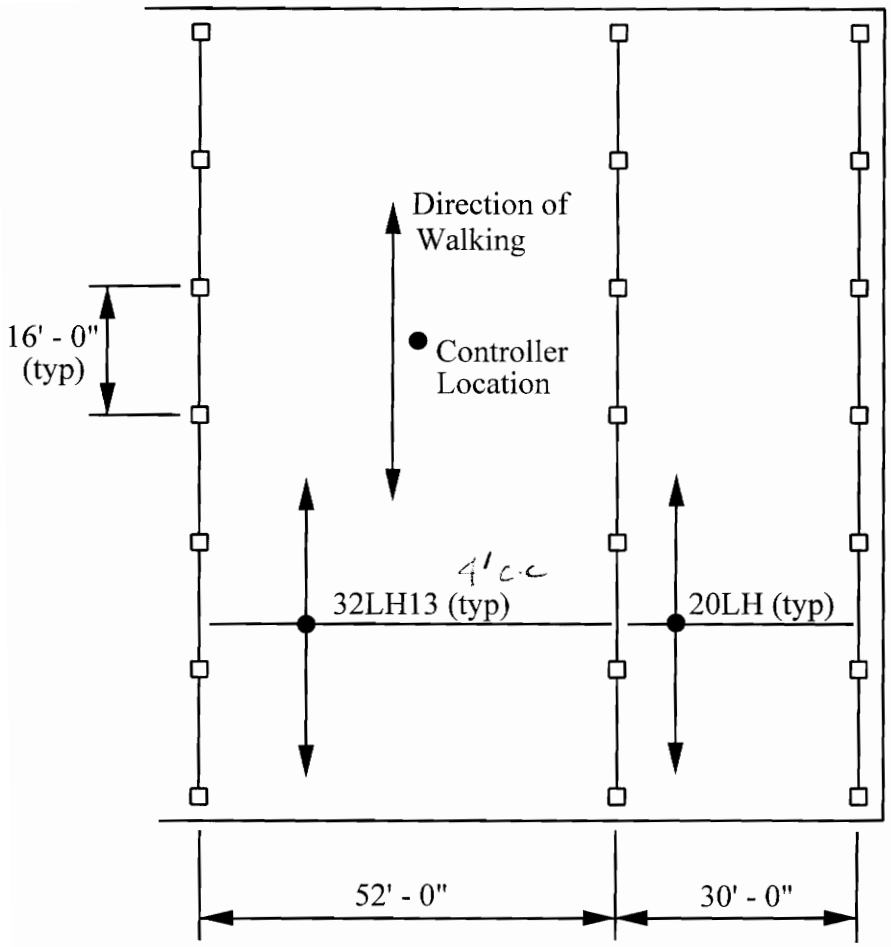

Figure 5.13 Plan of Kentucky Office Floor

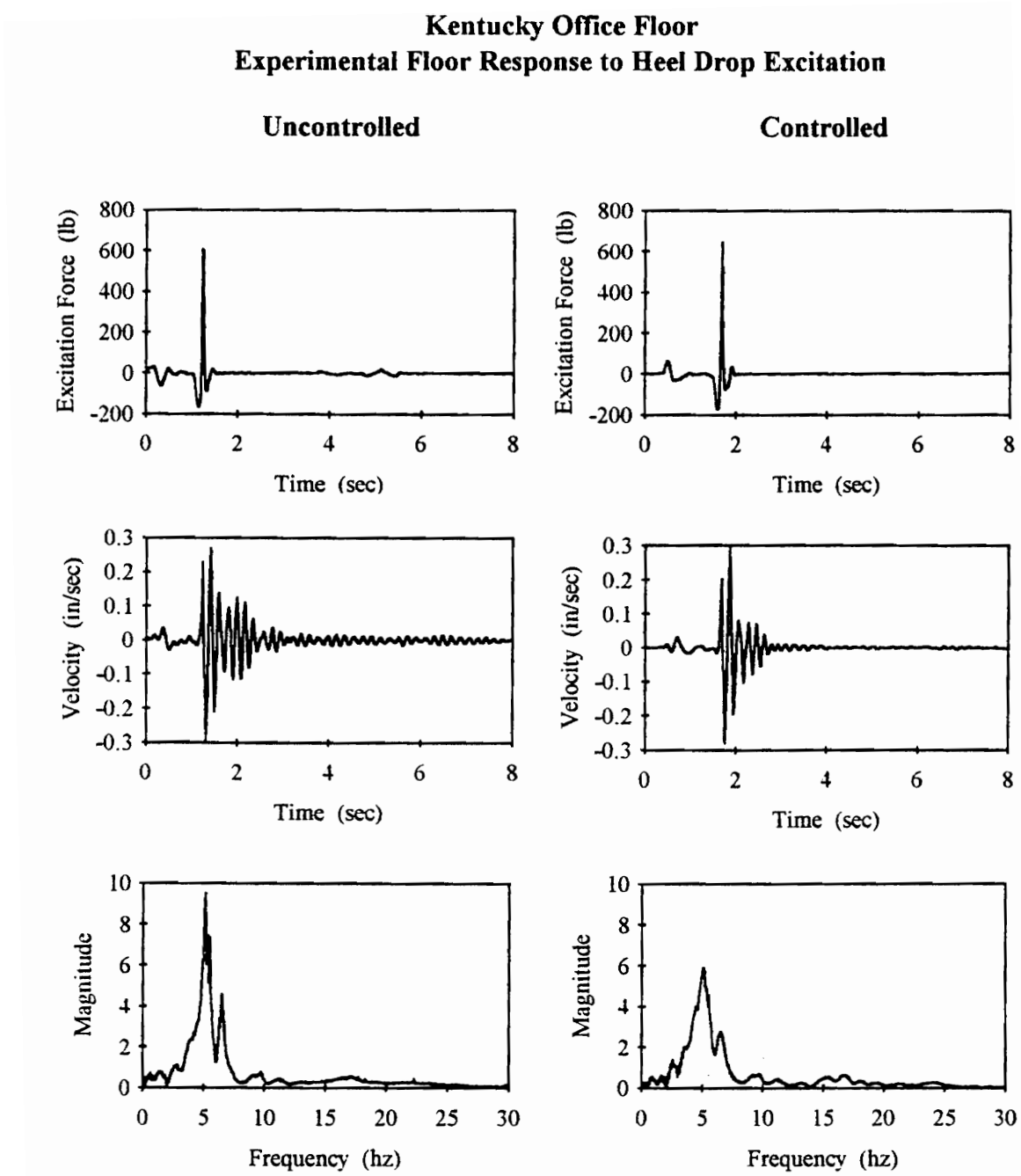

Note: The graphs labeled Magnitude vs. Frequency represent the frequency transform of the velocity time history above

Figure 5.14 Uncontrolled and Controlled Floor Response of Kentucky Office Floor Due to Heel Drop Excitation

Kentucky Office Floor
Experimental Floor Response to Walking Excitation

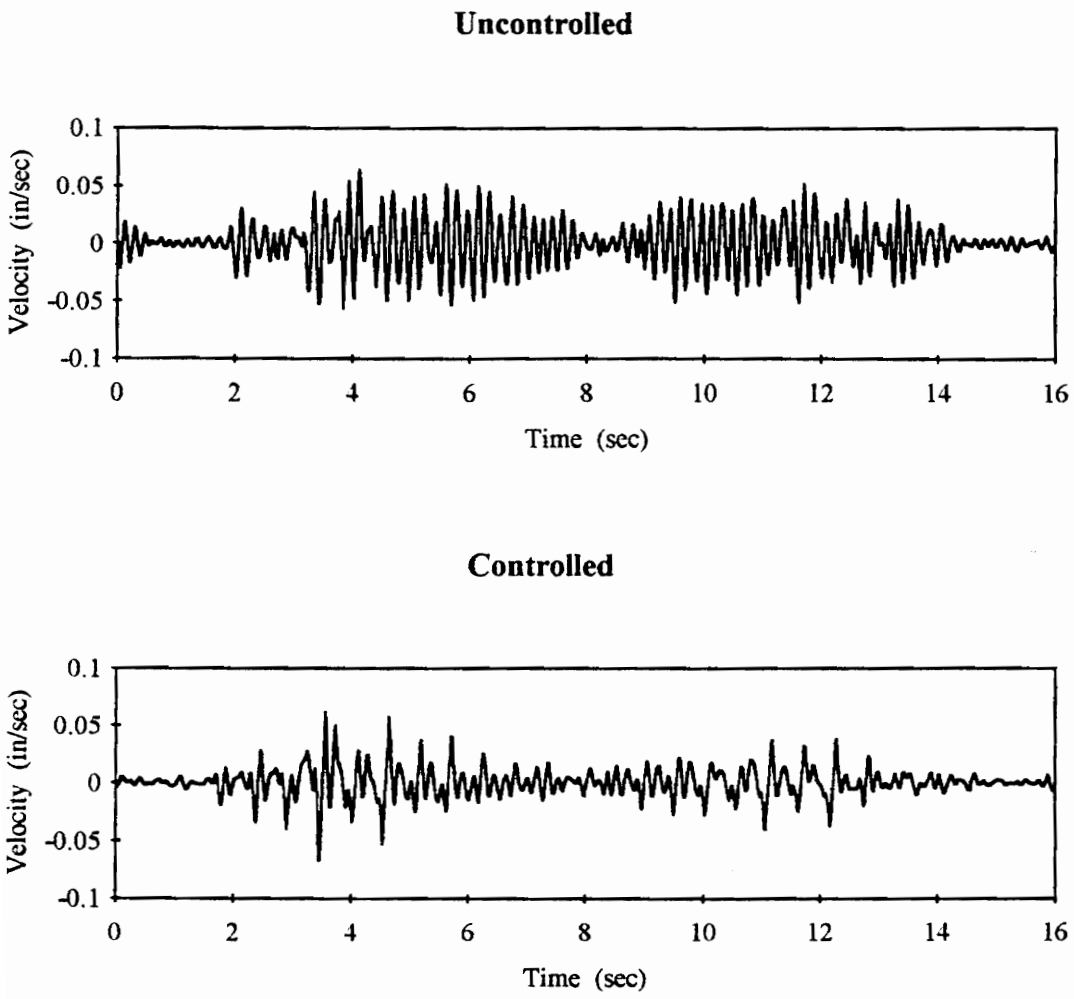

Figure 5.15 Uncontrolled and Controlled Response of Kentucky Office Floor Due to Walking Excitation

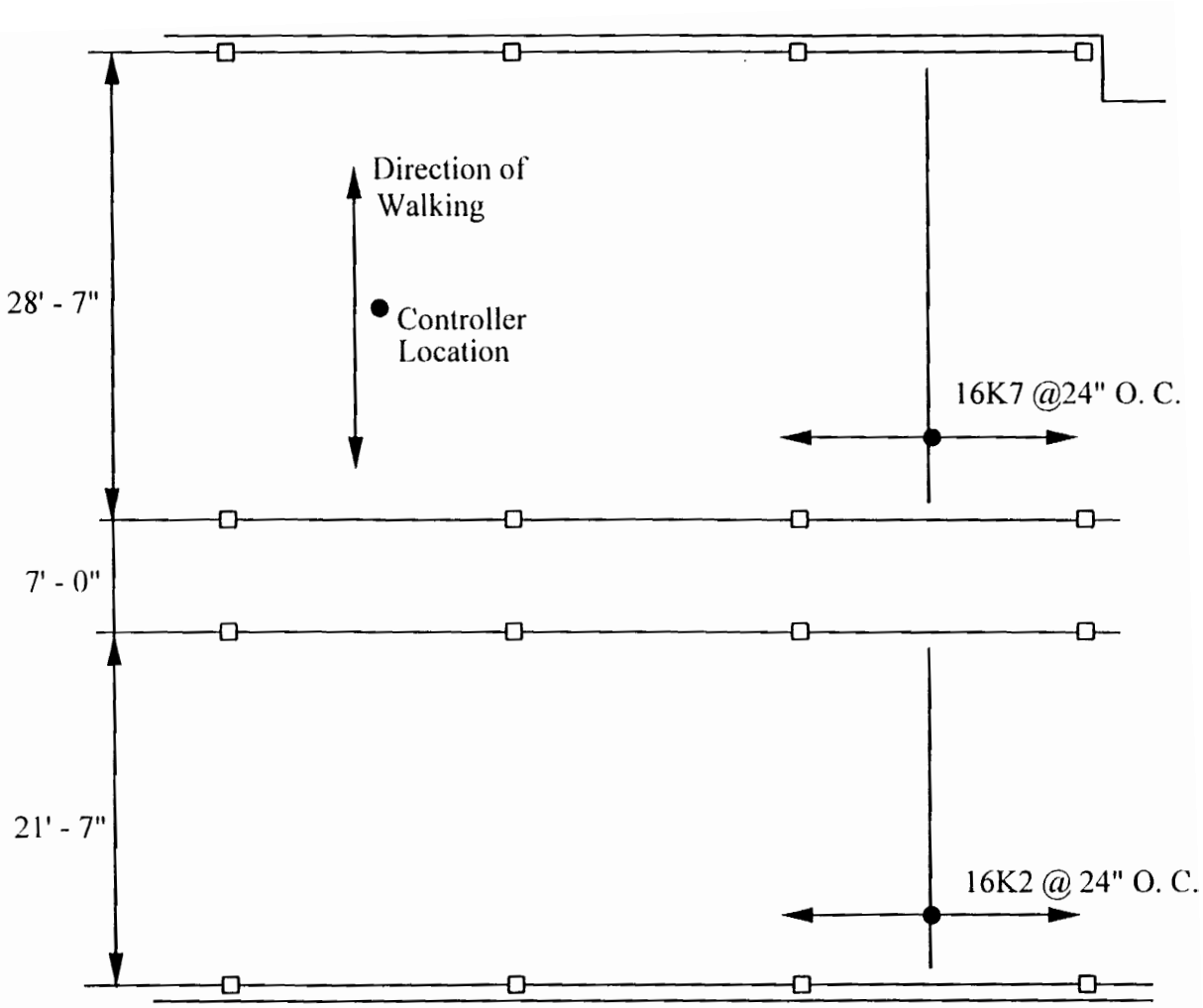

Figure 5.16 Plan of Vermont Chemistry Laboratory

VERMONT

Kentucky Office Floor

Experimental Floor Response to Heel Drop Excitation

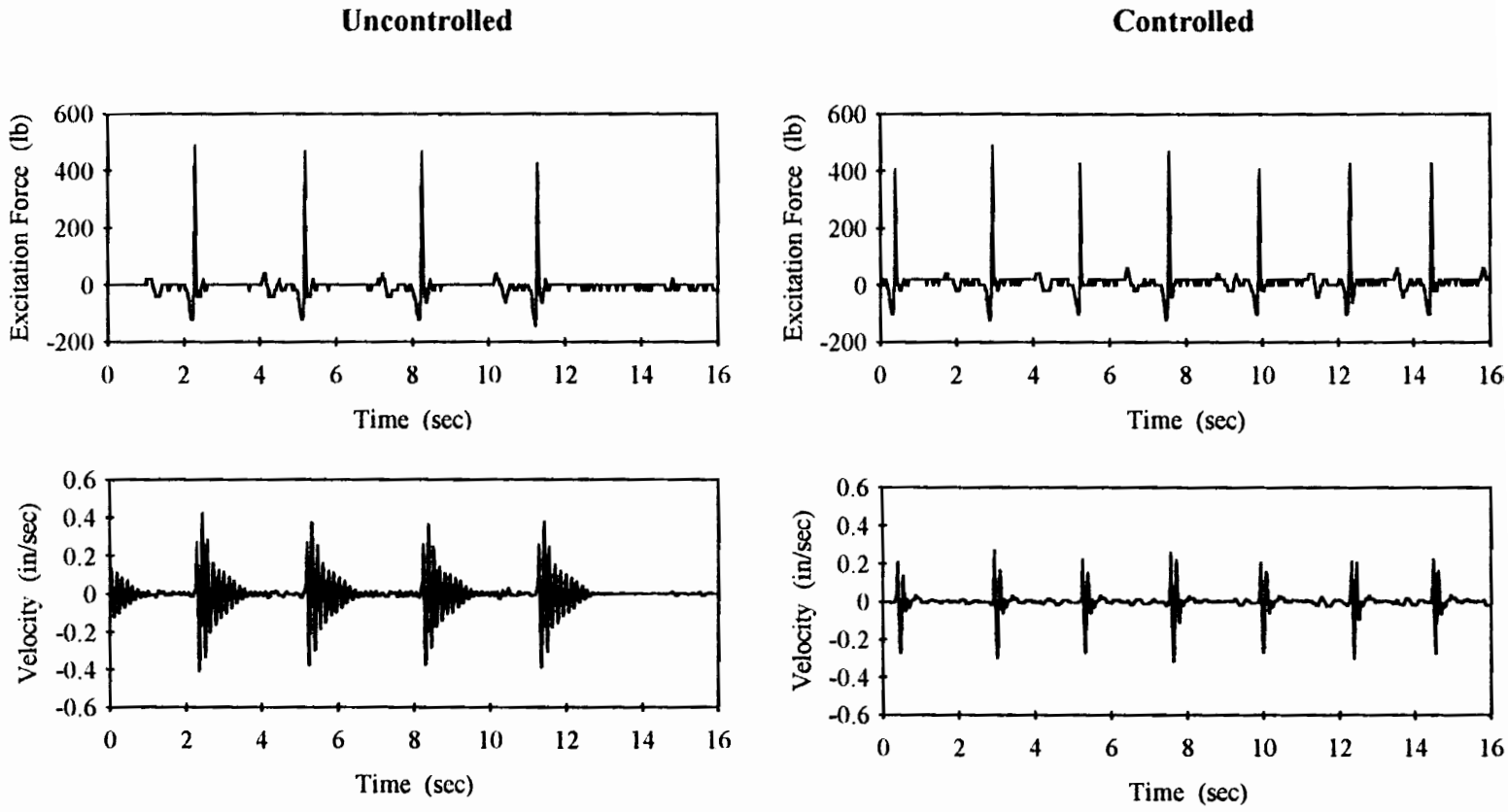

Figure 5.17 Uncontrolled and Controlled Floor Response of Vermont Laboratory Floor Due to Heel Drop Excitation

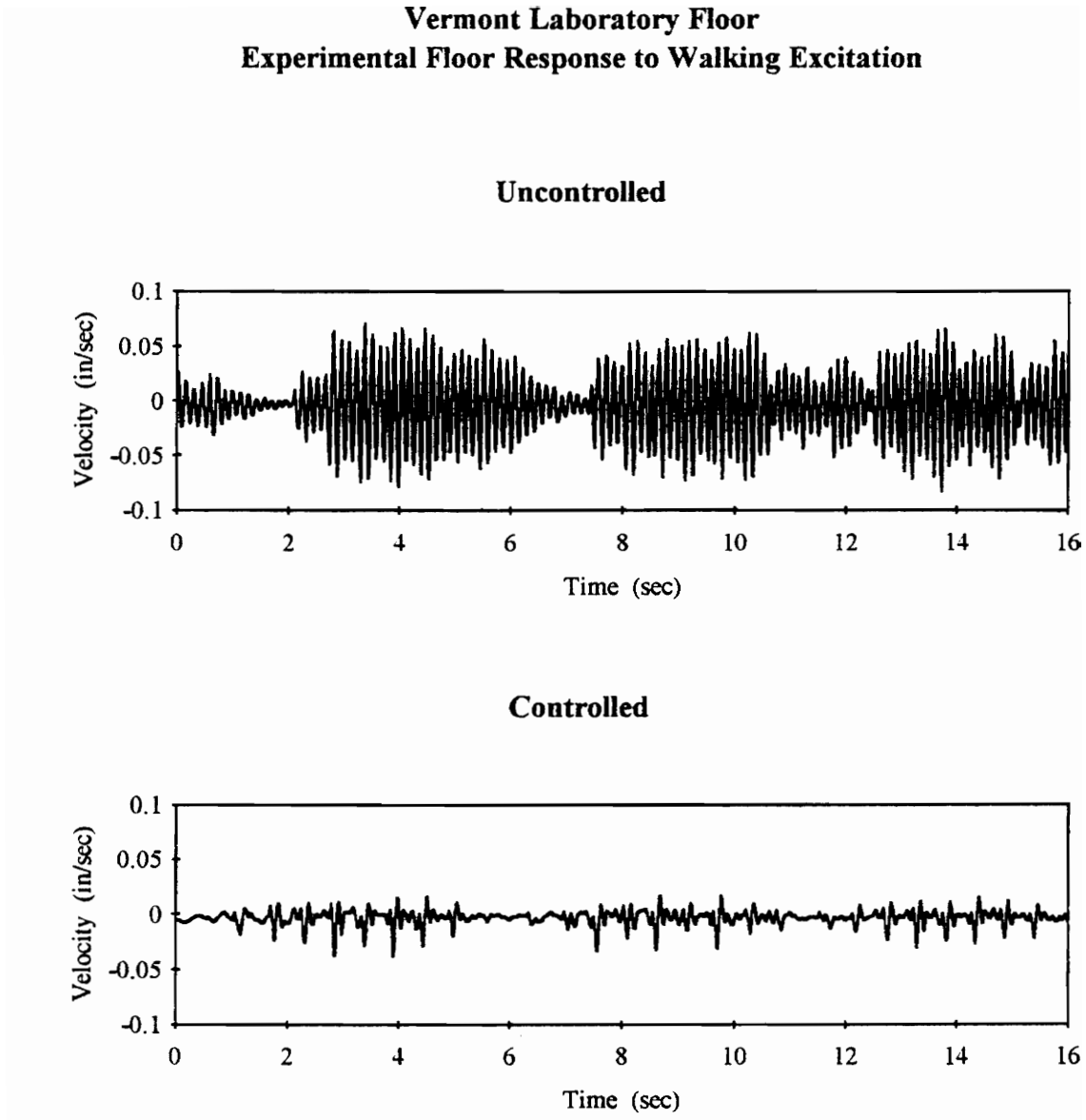

Figure 5.18 Uncontrolled and Controlled Response of Vermont Office Floor Due to Walking Excitation

are shown in Figures 5.17 and 5.18. The frequency and damping in the first mode of the uncontrolled system are 7.1 hz and 4.5%, respectively. The reduction ratio is 0.21.

5.7 Summary of Results

Improvement due to the implementation of the active control was illustrated for each of the six additional test floors studied. Results from the additional floors are summarized in Table 5.1. The results have been organized in this table according to the first natural frequency computed for the system. Information from the experimental test floor studied in Chapters 4 and 5 is also included. Clearly, there is a relationship between the first natural frequency and the reduction ratio. This relationship can be explained by the control/structure interaction described in the Literature Review of Chapter 1. Goh and Caughey (1985) note that the instabilities can occur in the system frequencies near the resonant frequency of an actuator. The proximity of the floor system frequencies to the actuator frequency has an impact on the control system effectiveness, as is illustrated by the results in Table 5.1. The actuator used in this study has a resonant frequency of 1.5 Hz. The control effectiveness on floors with natural frequencies around or below 6 Hz. is greatly dimished due to the interaction of the actuator resonant frequency. Improvement of control effectiveness for floor systems with low first natural frequencies would require a modification of the actuator parameters. This will be discussed further in the Recommendations for Future Research section of this paper.

Table 5.1 Summary of Results for Control Implementation on Additional Floors

Floor	First Natural Frequency (hz)	Reduction Ratio
Kentucky Office Floor	5.1	0.56
Two Bay Floor	5.1	0.44
Shallow Joist Floor	6.1	0.41
High Frequency Joist Floor	6.8	0.21
St. Louis Office Floor	7.1	0.27
Vermont Laboratory Floor	7.1	0.21
Experimental Test Floor	7.3	0.10

CHAPTER 6

SUMMARY, RECOMMENDATIONS, AND CONCLUSIONS

6.1 Summary

Excessive floor vibrations can produce disruption and reduced efficiency in employees and in more extreme cases can result in complete abandonment of a structure for its intended use. Floor vibration problems occur in building structures for many reasons. Often they are the result of an omission in the design phase to check this serviceability condition. When a problem floor is constructed, viable repair solutions are needed. Active control, using an electromagnetic shaker, has been shown in this research to be an effective method for improving unacceptable floor motion caused by human activity. Vibration levels due to walking excitation were reduced by 800% at the center of the experimental test floor. Dramatic improvements were also shown in the dynamic behavior of the additional floors studied.

6.2 Recommendations for Future Research

While completing the objectives of this research initiative, several subjects have been identified for future research. These subjects are reviewed briefly in the following subsections.

6.2.1 Improved actuators and algorithms for floor vibration control

Improved actuators and control algorithms are recommended for further study in the implementation of active control. The actuator used in the current research has severe maintenance and performance problems. During the two years of research, the amplifier had to be returned two different times for major repairs. Additionally, only 30% of the maximum output force specified in the manufacturer's data could be consistently achieved. This reduced force output limit severely impairs the actuator's ability to control large excitations. More rugged and reliable actuators are recommended for future research.

In the absence of actuator and sensor dynamics, structural control by means of collocated direct velocity feedback is unconditionally stable (Balas 1979b). When using a proof-mass actuator to apply the control force, the dynamics of the proof-mass are introduced into the control loop. The introduction of these dynamics can result in controller-induced instabilities. Goh and Caughey (1985) note the controller-induced instabilities in collocated velocity feedback resulting from second-order actuator dynamics. The unstable controlled system frequencies were found near the resonant frequency of the actuator. The region of stable control gains for collocated velocity feedback is dependent on the dynamic characteristics of the actuator and the structure being controlled. Parameters of the actuator (stiffness and damping) play an important role in defining the stable operating region of an actuator. Methods of analysis for

optimizing these parameters are presented by Linder *et al.* (1993) and are recommended for application in future research to improve the performance of the proof-mass actuator.

In addition to the stability issue, the actuator has limitations on the magnitude of control force it can generate. As described previously, these limitations create a nonlinearity in the controller which imposes a constraint on the operating region of the actuator (Linder *et al.* 1992). Several non-linear control schemes are presented by Linder *et al.* (1992) to account for actuator limitations. The most straightforward solution is the command limiter used in this research; that is, limit the input force to the actuator so as not to exceed either the stroke or force constraints. Other non-linear control solutions proposed by Linder *et al.* (1992) dramatically expand the operating region of the actuator. These control schemes require more feedback information to be incorporated into the control algorithm. Research to study these schemes for implementation in the active control of floor vibration is recommended.

6.2.2 Experimental implementation of active control using multiple actuators

This research primarily illustrated control effectiveness for a single actuator at a single location on the floor structure. It was shown that such an installation cannot control the entire floor system. In control terms, some of the floor modes are not observable, and therefore not controllable, at a particular location on the floor. The concepts that have proven effective for controlling a single location must be expanded to

control all of the problem modes of vibration that exist in a floor system. This requires the implementation of multiple actuators and is recommended for future research.

6.2.3 Miscellaneous recommendations for future research

To study more sophisticated algorithms or to make more precise predictions of control system effectiveness, a more accurate floor system model may be necessary. As was noted in Chapter 4, experimental modal analysis could be used to derive a more accurate model of the floor system.

Design of a successful control strategy would be enhanced by the ability to mathematically simulate uncontrolled floor behavior due to occupant activities. Such a model could be used in predicting the improvements made to the floor system behavior before the control system is installed. The walking simulations of Chapter 4 prove that the development of such models is feasible. Recommendations for future research include a continuation of this analytical and experimental work including simulations for activities such as dancing and aerobics.

6.3 Conclusions

The active control scheme studied in this research presents several advantages over many of the traditional methods used in repairing problem floors. An actively controlled mass was shown in Chapter 4 to provide a larger degree of control than a passive device with an equivalent reactive mass. The active system is also less disruptive to the building function than most other repair measures. Partitions and posts are often

ruled out as repair options because of their infringement on the building space. The active device is rather compact and can be installed with relative speed and ease in the ceiling cavity present in most commercial buildings.

There are also disadvantages to the active control scheme. The cost of the components to provide a single control circuit are currently very high. The hardware components alone have a total cost of $21,300 for a single control circuit. This results in an estimated cost of $24 per square foot, assuming one actuator is necessary to control a 30 ft. x 30 ft. bay. One must keep in mind, however, that any new technology is expensive and often becomes more reasonable in time. Maintenance and reliability issues also detract from the attractiveness of a active system. These issues are not necessarily prohibitive. Maintenance and repair is necessary for many building systems. As this technology matures, maintenance and repair could be considered similar to changing a filter or overhauling a boiler.

The potential of this application far exceeds the drawbacks. The results of this research, in addition to future research, will move this technology toward acceptance as an alternative to traditional methods in repairing problem floors and provide desperate building owners a practicable solution to a very difficult problem.

REFERENCES

Allen, D. E. (1975). "Vibrational behavior of long-span floor slabs." *Canadian Journal of Civil Engineering*, 1(1), 108-115.

Allen, D. E. (1990). "Building vibrations from human activities." *Concrete International: Design and Construction,* 12(6), 66-73.

Allen, D. E., and Murray, T. M. (1993). "Design criterion for walking vibrations." *Engineering Journal, AISC*, 31(3), 117-129.

Balas, M. J. (1978). "Feedback control of flexible systems." *IEEE Transactions on Automatic Control*, AC-23(4), 673-679.

Balas, M. J. (1979a). "Direct output feedback control of large space structures." *The Journal of Astronautical Sciences*, 27(2), 157-180.

Balas, M. J. (1979b). "Direct velocity feedback control of large space structures." *Journal of Guidance and Control*, 2(3), 252-253.

Balas, M. J. (1982). "Trends in large space structure control theory: Fondest hopes, wildest dreams." *IEEE Transactions on Automatic Control*, AC-27(3), 522-535.

Bell, D. H. (1994). "A tuned mass damper to control occupant induced floor motion." *Proceedings* from the 18th Annual Meeting of the Vibration Institute, Willowbrook, Illinois, 181-186.

Bouten, H., and Meyr, H. (1985). "Control design for ADC-girder." *Structural Control*, H. H. E. Leipholz, ed., Proceedings of the Second International Symposium on Structural Control, University of Waterloo, Canada. Martinus Nijhoff Publishers, 199-214.

Brogan, W. L. (1974). *Modern Control Theory*, Quantum Publishers, New York, N.Y.

Chung L. L., Lin, R. C., Soong, T. T., and Reinhorn, A. M. (1989). "Experimental study of active control for MDOF seismic structures." *Journal of Engineering Mechanics, ASCE*, 115(8), 1609-1627.

Chung L. L., Reinhorn, A. M., and Soong, T. T. (1988). "Experiments on active control of seismic structures." *Journal of Engineering Mechanics, ASCE*, 114(2), 241-255.

Chung L. L. (1987). "Analyses and experiments for practical applications of active structural control." Thesis presented to the State University of New York at Buffalo, N.Y., in partial fulfillment of the requirements for the degree of Doctor of Philosophy.

Dyke, S. J., Spencer, B. F., Quast, P., and Sain, M. K. (1993). "Protective system design: The role of control-structure interaction." *Proceedings* of International Workshop on Structural Control, USC Publication No. CE-9311, Los Angeles, 100-114.

Eriksson, P. E. (1994). *Vibration of Low Frequency Floors - Dynamic Forces and Response Prediction*, Chalmers University of Technology, Goteborg, Sweden.

First World Conference on Structural Control, Final Program and Abstracts (1994). Los Angeles, Ca.

Franklin, G. F., Powell, J. D., and Workman, M. L. (1990). *Digital Control of Dynamic Systems*, 2nd ed., Addison-Wesley Publishing Company, Reading, MA.

Goh, C. J. (1982). "Analysis and control of Quasi-distributed parameter systems." Dynamics Laboratory report DYNL-82-3, California Institute of Technology.

Goh, C. J., and Caughey, T. K. (1985). "On the stability problem caused by finite actuator dynamics in the collocated control of large space structures." *International Journal of Control*, 41(3), 787-802.

Grace, A., Laub, A. J., Little, J. N., and Thompson, C. M. (1992). *Control System Toolbox,* The Math Works, Inc., Natick, MA.

Hanes, R. M. (1970). "Human sensitivity to whole body vibration: A literature review." Silver Springs, MD, Applied Physics Laboratory, The Johns Hopkins University.

Ibidapo-Obe, O. (1985). "Active performance enhancement for reduced order model of large scale systems." *Structural Control*, H.H.E. Leipholz, ed., Proceedings of Second International Symposium on Structural Control, University of Waterloo, Canada. Martinus Nijhoff Publishers, 318-328.

Inman, D. J. (1990). "Control/structure interaction: Effects of actuator dynamics." *Mechanics and Control of Large Structures*, Junkins, J. L., ed., Progress in Astronautics and Aeronautics, 29, 507-533.

Inman, D. J. (1994). *Engineering Vibration,* Prentice-Hall, Englewood Cliffs, NJ.

Inoue, Y., Tachibana, E., and Mukai, Y. (1993). "Recent developments in active structural control in Japan." Proceedings of International Conference on Structural Control, USC Publication No. 9311, Los Angeles, CA, 239-247.

International Workshop on Structural Control, Proceedings (1993). Housner, G. W., and Masri, S. F., eds., USC Publication No. CE-9311, Los Angeles, CA.

ISO (1992). International Standards ISO 10137. "Basis for the design of structures - Serviceability of buildings against vibration." International Standards Organization, 41-43.

Izumi, M., Teramoto, T., Kitamura, H., and Shirasawa, Y. (1993). "Buildings with response control systems in Japan." Proceedings of International Conference on Structural Control, USC Publication No. 9311, Los Angeles, CA, 268-276.

Kobori, T., Norihide, K., Kazuhiko, Y., and Ikeda, Y. (1991a). "Seismic-response-controlled structure with active mass driver system. Part 1: Design." *Earthquake Engineering and Structural Dynamics*, 20(2), 133-149.

Kobori, T., Norihide, K., Kazuhiko, Y., and Ikeda, Y. (1991b). "Seismic-response-controlled structure with active mass driver system. Part 2: Verification." *Earthquake Engineering and Structural Dynamics*, 20(2), 151-166.

Lenzen, K. H. (1966). "Vibration of steel joist - concrete slab floors." *Engineering Journal, AISC*, 3(3), 133-136.

Lewis, F. L. (1992). *Applied Optimal Control and Estimation*, Prentice-Hall, Englewood Cliffs, NJ.

Lin, R. C., Soong, T. T., and Reinhorn, A. M. (1987). "Experimental evaluation of instantaneous optimal algorithms for structural control." Technical Report NCEER-87-0002, National Center for Earthquake Engineering Research, State University of New York at Buffalo.

Linder, D. K., Celano, T. P., and Ide, E. N. (1991). "Vibration suppression using a proof-mass actuator operating in stroke saturation." *Journal of Vibration and Acoustics*, 113(9), 423-433.

Linder, D. K., Zvonar, G. A., and Borojevic, D. (1992). "Limit cycle analysis of a nonlinear controller for a proof-mass actuator." Proceedings of the AIAA Dynamics Specialists Conference, Dallas, TX, 585-594.

Linder, D. K., Zvonar, G. A., and Borojevic, D. (1993). "Performance and control of proof-mass actuators accounting for stroke saturation." Accepted for publication in *AIAA Journal of Guidance, Control, and Dynamics*.

MATLAB (1993). *MATLAB User's Guide*, The Math Works, Inc.,Natick, MA.

Meirovitch, L. (1985). "Direct Feedback Control of Distributed Structures." Presented at the 22nd Annual Meeting for the Society of Engineering Science, University Park, PA.

Morley, L. J. and Murray, T. M. (1992). "Predicting floor response due to human activity". *Proceedings* from the International Colloquium for Structural Serviceability of Buildings, Goteborg, Sweden, 297-302.

Murray, T. M. (1979). "Acceptability criteria for occupant-induced floor vibrations." *Sound and Vibration*, Nov. 1979, 24-30.

Murray, T. M. (1991). "Building floor vibrations." *Engineering Journal, AISC*, 28(3), 102-109.

Oz, H. (1985). "Fundamental aspects of structural control." *Structural Control*, H.H.E. Leipholz, ed., Proceedings of Second International Symposium on Structural Control, University of Waterloo, Canada. Martinus Nijhoff Publishers, 505-531.

Pernica, G. (1990). "Dynamic load factors for pedestrian movements and rhythmic exercises." *Canadian Acoustics*, 18(2), 3-18.

Reed, F. E., "Dynamic Vibration Absorbers and Auxiliary Systems", *Shock and Vibration Handbook*, Harris, C., 3rd ed., Mcgraw Hill, New York, 1988.

Reiher, H., and Meister, F. J. (1931). "The effect of vibration on people." (in German). Forchung auf dem Gebeite des Ingenieurwesens, vol. 2, II, 381. (Translation: Report No. F-TS-616-RE H. Q. Air Material Command, Wright Field, Ohio)

Reinhorn, A. M., and Mangolis, G. D., (1985). "Current state of knowledge on structural control." *Shock and Vibration Digest*, 17(10), 7-16.

Reinhorn, A. M., and Mangolis, G. D., (1989). "Recent advances in structural control." *Shock and Vibration Digest*, 21(1), 3-8.

Reinhorn, A. M., Soong, T. T., Wang, A. M., and Lin, R. C. (1993). "Full scale implementation of active control-Part 2: Installation and performance." *Journal of Structural Engineering, ASCE*, 119(6), 1935-1960.

Reinhorn, A. M., and Soong, T. T. (1992). "Full scale implementation of active control braces for structural control." Proceedings of US/China/Japan Trilateral Workshop on Structural Control, Shanghai, China, 141-150.

Roorda, J. (1980). "Experiments in feedback control." *Structural Control*, H.H.E. Leipholz, ed., North-Holland Publishing Co. and SM Publications, 505-521.

Setareh, M., and Hanson, R. D. (1992a). "Tuned mass dampers for balcony vibration control." *Journal of Structural Engineering, ASCE*, 118(3), 723-740.

Setareh, M., and Hanson, R. D. (1992b). "Tuned mass dampers control vibration from humans." *Journal of Structural Engineering, ASCE*, 118(3), 741-762.

Setareh, M., and Hanson, R. D. (1992c). "Using component mode synthesis and static shapes for tuning TMD's." *Journal of Structural Engineering, ASCE*, 118(3), 763-782.

Shope, R. L., and Murray, T. M., (1994). "Multi-celled liquid dampers to eliminate annoying floor vibrations." To be presented at the Canadian Acoustical Society Symposium, Ottawa.

Skelton, R., and Likens, P. (1978). "Orthogonal filters for model error compensation in the control of nonrigid spacecraft." *Journal of Guidance and Control*, 1(1), 41-49.

Soong, T. T., Reinhorn, A. M., Wang, A. M., and Lin, R. C. (1991). "Full scale implementation of active control-Part 1: Design and simulation." *Journal of Structural Engineering, ASCE*, 117(11), 3516-3536.

Soong, T. T. (1988). "State-of-the-art review: Active structural control in civil Engineering." *Engineering Structures*, 10(2), 74-84.

Soong, T. T., Reinhorn, A. M., and Yang, J. N. (1985). "A standardized model for structural control experiments and some experimental results." *Structural Control*, H.H.E. Leipholz, ed., Proceedings of Second International Symposium on Structural Control, University of Waterloo, Canada. Martinus Nijhoff Publishers, 669-693.

Thornton, C. H., Cuocco, D. A., and Velivasakis, E. E. (1990). "Taming structural vibrations." *Civil Engineering, ASCE*, Nov. 1990, 57-59.

Ungar, E. E., Sturz, D. H., and Amick, C. H. (1990). "Vibration control design of high technology facilities." *Sound and Vibration*, July 1990, 20-27.

US/China/Japan Trilateral Workshop on Structural Control, Proceedings. (1991) Shanghai, China.

Webster, A. C., and Vaicaitis, R. (1992). "Application of tuned mass dampers to control vibrations of composite floor systems." *Engineering Journal, AISC*, 29(3), 116-124.

Wilson, E. L. and Habibullah, A. (1992). *SAP90™ Structural Analysis User's Manual*, Computers & Structures, Inc., Berkeley, CA.

Zimmerman, D. C., and Inman, D. J. (1990). " On the nature of the interaction between structures and proof-mass actuators." *AIAA Journal of Guidance, Control, and Dynamics*, 13(1), 82-88.

APPENDIX A

DESIGN CALCULATIONS FOR EXPERIMENTAL TEST FLOOR

A.1 Strength Design of Experimental Test Floor

The following calculations summarize the design of the experimental test floor with respect to strength required for a typical office floor.

Load Summary:

$3^1/_2$ in. lightweight concrete slab on 1.0C metal deck:

w = (3in/12)(115 pcf)+2 psf = 30.75 psf

where,

average concrete thickness = 3 in.

assumed concrete weight = 115 pcf

deck weight = 2 psf

Live load for office occupancy (as suggested by BOCA (1994)):

w = 60 psf

Partition load (as suggested by BOCA (1994)):

w = 20 psf

Miscellaneous dead load (mechanical, plumbing, ceiling, etc.):

w = 10 psf

Joist Design:

Joist spacing = 2.5 ft.

Superimposed load:

$$w = (30.75\ \text{psf} + 60\ \text{psf} + 20\ \text{psf} + 10\ \text{psf})(2.5\ \text{ft.}) = 302\ \text{plf}$$

Selection from Steel Joist Institute joist catalog tables:

16K4: allowable w = 314 plf

Joist properties:

weight = 7 plf

$$M_{all} = \frac{w\ell^2}{8} = \frac{(0.314\text{klf})(25\text{ft.} - 0.33\text{ft.})^2}{8} = 23.89\,\text{ft} - \text{kips}$$

$$A_{bot} = \frac{M_{all}}{(d-1)f_{all}} = \frac{23.89(12)}{(16\text{in.} - 1\text{in.})(30\text{ksi})} = 0.637\text{in}^2$$

$$A_{top} = 1.25 * A_{bot} = 1.25(0.637) = 0.796\text{in}^2$$

$$A_{chord} = A_{top} + A_{bot} = 1.433\text{in}^2$$

$$A_j = 0.85 * A_{chord} = 1.218\text{in}^2$$

$$y_c = \frac{(d-1)A_{bot}}{A_{chord}} + 0.5 = 7.168\text{in.}$$

$$I_j = 0.85 * I_{chord} = 0.85[0.637(8.332)^2 + 0.796(6.668)^2] = 67.3\text{in}^4$$

Girder Design:

Joist length = 25 ft

Girder length = 15 ft

Equivalent superimposed uniform load:

$$w = [(302\ \text{plf} + 7\ \text{plf})/2.5\ \text{ft}](25\ \text{ft}/2) + 22\ \text{plf} = 1567\ \text{plf}$$

Allowable design moment:

$$M = 1.567 \text{ klf } (15 \text{ ft})^2/8 = 44.1 \text{ ft-kips}$$

$$S_{req'd} = 22.0 \text{ in}^3 \text{ (A36 steel)}$$

Select W14X22

Girder properties:

$$S = 29 \text{ in}^3; I = 199 \text{ in}^4; A = 6.49 \text{ in}^2; d = 13.74 \text{ in}$$

Summary of Strength Design:

$3\ ^1/_2$ in. lightweight concrete slab on 1.0C metal deck

16K4 steel joists spaced at 30 in O.C.

W14X22 girder (A36 steel)

A.2 Analysis of Dynamic Behavior

The criterion proposed by Murray (1991) was developed to identify, before construction, floors which may possess annoying levels of vibration due to occupant movement. This criterion is applicable to office and residential environments. The criterion predicts an acceptable floor, with respect to floor vibrations, if the following inequality is satisfied.

$$D > 35\ A_o\ f + 2.5 = D_{req'd}$$

where

D = predicted damping for finished floor structure, % critical

A_o = maximum dynamic amplitude due to heel drop impact, in. and

f = first natural frequency of floor system, Hz.

The following calculations were performed to evaluate the proposed design. A more thorough discussion of the computational proceedure is provided in the Murray (1991) paper. An "unacceptable" floor design is desired for the experimental test floor so that improvements can be made by means of active control.

Determine first natural frequency of floor system: f

Transformed moment of inertia of joist:

The joist is assumed to act compositely with the concrete, regardless of the connection between the deck and joist. This assumption is discussed further in Section 2.5.

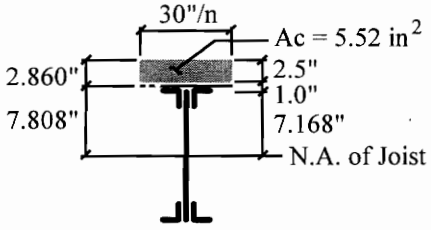

$$n = E_s / E_c = 29{,}000 \text{ ksi} / (115)^{1.5}\sqrt{3 \text{ ksi}} = 13.58$$

$$\bar{y} = \frac{(5.52)(2.5/2) + 1.218(10.668)}{5.52 + 1.218} = 2.860 \text{ in.}$$

Joist Properties

$I_j = 67.68 \text{ in}^4$

$A_j = 1.218 \text{ in}^2$

$$I_t = \frac{(30/13.58)(2.5)^3}{12} + 5.52(1.61)^2 + 67.68 + 1.218(7.808)^2$$

$$= 159.1 \text{ in}^4$$

Distributed weight on joist:

$$w = (3 \text{ in.}/12)(115 \text{ pcf})(2.5 \text{ ft.}) + 2 \text{ psf}(2.5 \text{ ft.}) + 7 \text{ plf} = 83.9 \text{ plf}$$

First natural frequency of joist: f_j

$$f_j = 1.57\sqrt{\frac{gEI_t}{w\ell^4}} = 1.57\sqrt{\frac{(386.4 \text{in./sec}^2)(29{,}000{,}000 \text{psi})(159.1 \text{in}^4)}{(83.9 \text{plf})(25 \text{ft})^4(1728)}} = 8.81 \text{hz}$$

Moment of inertia of girder and transformed slab: $I_g + I_{str}$

The selection of non-composite girder properties is discussed further in Section 2.2.3.

$$I_g = 199 \text{ in4}$$

$$I_{str} = I_s / n = \frac{(0.2 * 25\text{ft.})(12\text{in./ft.})(3\text{in.})^3}{12(13.58)} = 9.94\text{in}^4$$

Distributed weight on girder:

$$w = (3 \text{ in./12})(115 \text{ pcf})(12.5 \text{ ft.}) + 2 \text{ psf}(12.5 \text{ ft.}) + 7 \text{ plf} / (2.5\text{ft.}) + 22 \text{ plf}$$

$$= 455.3 \text{ plf}$$

First natural frequency of girder: f_g

$$f_g = 1.57\sqrt{\frac{gE(I_g + I_{str})}{w\ell^4}}$$

$$= 1.57\sqrt{\frac{(386.4 \text{ in} / \text{sec}^2)(29{,}000{,}000 \text{ psi})(199 \text{ in}^4 + 9.94 \text{ in}^4)}{(455.3 \text{ plf})(15 \text{ ft})^4(1728)}}$$

$$f_g = 12.04 \text{ Hz.}$$

Calculation of frequency of floor system: f

$$\frac{1}{f^2} = \frac{1}{f_j^2} + \frac{1}{f_g^2} = \frac{1}{8.81^2} + \frac{1}{12.04^2} = \frac{1}{7.11^2}$$

$$f = 7.11 \text{ Hz.}$$

Determine maximum dynamic amplitude due to heel drop impact: A_o

Dynamic amplitude of joist: A_{oj}

$$A_{oj} = \frac{A_{ot}}{N_{eff}} = \frac{0.0803 \text{ in.}}{5.70} = 0.0141 \text{ in.}$$

where

$$A_{ot} = (DLF)_{max} \cdot \frac{600\ell^3}{48EI_{tr}}$$

$$= 1.0976 \cdot \frac{600(25\ \text{ft} \cdot 12\ \text{in/ft})^3}{48(29{,}000{,}000\text{psi})(159.1\ \text{in}^4)}$$

$$= 0.0803\ \text{in.}$$

$(DLF)_{max}$ = value selected from table in Murray (1991)

$$N_{eff} = 1 + 2\sum \cos\frac{\pi x}{2x_o}$$

$$= 1 + 2\cos\frac{\pi(30)}{2(133.7)} + 2\cos\frac{\pi(60)}{2(133.7)} + 2\cos\frac{\pi(90)}{2(133.7)} + 2\cos\frac{\pi(120)}{2(133.7)}$$

$$= 5.70$$

$$x_o = 1.06\varepsilon\ell = 1.06\left(\frac{2136\ \text{ksi}\ (3\text{in.})^3/12}{29{,}000\ \text{ksi}\ (159.1\ \text{in}^4)/30\ \text{in.}}\right)^{0.25}(25\ \text{ft.})(12\ \text{in./ft.})$$

$$= 133.7\ \text{in.}$$

Dynamic amplitude of girder: A_{og}

$$A_{og} = (DLF)_{max} \cdot \frac{600\ell^3}{48E(I_g + I_{str})}$$

$$= 1.2861 \cdot \frac{600(15\ \text{ft.} \cdot 12\ \text{in./ft.})^3}{48(29{,}000{,}000\ \text{ksi})(199\ \text{in}^4 + 9.94\ \text{in}^4)}$$

$$= 0.0155\ \text{in.}$$

Calculate dynamic system amplitude: A_o

$A_o = A_{oj} + A_{og}/2$ girders = 0.0141 in. + 0.0155 in. /2 = 0.0218 in.

Assessment of Murray (1991) Criterion:

$$D_{req'd} = 35\ A_o\ f + 2.5 = 35\ (0.0218\ \text{in.})(7.11\ \text{Hz.}) + 2.5 = 7.94\%$$

The damping expected for the floor system is approximately 1%, much less than that required ($D_{req'd}$) for an acceptable floor system. Therefore a problem floor, with respect to walking vibrations, is predicted for this design configuration.

APPENDIX B

FORTRAN SOURCE CODE FOR ACTIVE CONTROL PROGRAM

```
$NOFLOATCALLS
$STORAGE:2
$NOTSTRICT
      INCLUDE  'pc30.fi'
       interface to function pc30_ad(c_l, n_s, b_l, f_s)
       integer*2 pc30_ad
       integer*2 c_l[REFERENCE]
       integer*2 n_s[VALUE]
       integer*2 b_l[VALUE]
       integer*2 f_s[REFERENCE]
       end
      PROGRAM CONTROL
C
C       *** uses the PC-30DS/16 a/d board ***
      INCLUDE  'pc30.fd'
       integer*2 pc30_ad [EXTERN]
      REAL*8 DCOFF
      INTEGER*2 IRT,ICHR
      INTEGER*2 ICHARR(16),INBUF(32),IVALO
      INTEGER*2 ISCCNT,IZER,IDAC(1)
      REAL*8 SFREQ,RMVOLT,RRVOLT
      REAL*8 VOMAXF
      REAL*8 VOMIN
      REAL*8 CGAIN
      REAL RVAL(1),VALO
C
C     SET UP PROGRAM
C
C     READ CONTROL PARAMETERS FROM FILE
C
      OPEN (UNIT=10,FILE='SETPAR.DAT')
      READ(10,*)SFREQ
      READ(10,*)DCOFF
      READ(10,*)VOMAXF
      READ(10,*)VOMIN
        READ(10,*)CGAIN
      CLOSE(10)
C
C     WRITE OUT AND CONFIRM PROGRAM DATA
C
      WRITE(*,1000)
```

```
      WRITE(*,1001)
      WRITE(*,1003)SFREQ
      WRITE(*,1004)
      WRITE(*,1005)DCOFF
      WRITE(*,1008)VOMAXF
      WRITE(*,1011)VOMIN
      WRITE(*,1012)CGAIN
      WRITE(*,1013)
      WRITE(*,1014)
 1000 FORMAT(////)
 1001 FORMAT(' CONTROL PROGRAM PARAMETERS',/)
 1003 FORMAT(' DATA AQUISITION FREQUENCY (HZ):',T35,F5.0,/)
 1004 FORMAT(' CONTROL PARAMETERS',T30,'ACTUATOR CIRCUIT',/)
 1005 FORMAT(' DC OFFSET: TRANSDUCER',T35,G10.4)
 1008 FORMAT(' MAXIMUM OUTPUT VOLTAGE',T35,G10.4)
 1011 FORMAT(' MINIMUM OUTPUT VOLTAGE',T35,G10.4)
 1012 FORMAT(' CONTROL GAIN',T35,G10.4,T58,G10.4,//)
 1013 FORMAT(' PRESS <ENTER> TO COMFIRM AND CONTINUE')
 1014 FORMAT(' [CTRL Y WILL END PROGRAM]',////)
 300  CONTINUE
      CALL KEYIN(ICHR,IRT)
C       check for ENTER
     IF(IRT.eq.1 .and. ichr.eq.13) goto 400
C       check for 'Cntrl Y'
     if(irt.eq.1 .and. ichr.eq.25) goto 999
      GOTO 300
 400  CONTINUE
C
C     SET UP CHANNELS
C
      ICHARR(1)=0
      ICHARR(2)=16
      IDAC(1)=0
      ISCCNT=1
C
C     SET UP BOARD INCLUDING SAMPLING FREQUENCY
C
      CALL set_base(#700)
      i=diag()
      if (i .ne. 0) THEN
       STOP 'PC-30 diagnostics report PC-30 not found or
      failed'
      END IF
      ityp=get_type()
      WRITE(*,1000)
      write(*,*) ' A/D Board Type=',ityp
      call init()
```

```
      r=2000000./SFREQ
      ipres=10
      iadpr=int(r/real(ipres))
      SFREQ=2000000./real(ipres*iadpr)
      write(*,*) ' Actual Clock Speed Used=',SFREQ,' Hertz'
      call ad_clock(ipres)
      call ad_prescaler(iadpr)
C
C     SET UP BINARY/VOLTS CONVERSION
C
      CONV1=(10./4096.)
      CONV2=-5.
      DCON1=2048.
      DCON2=2048./10.
C
C     INITIALIZE VALUES
C
      DO 610 I=1,ISCCNT
        RVAL(I)=0.0
 610  CONTINUE
        IVALO=0
        VALO=0.0
        IZER=2048
      WRITE(*,*)' Output Voltage Zeroed'
      ierr=da_out(idac(1),izer)
      WRITE(*,1000)
      WRITE(*,1000)
      WRITE(*,1022)
      WRITE(*,1014)
      ICHR=0
 640  CONTINUE
      CALL KEYIN(ICHR,IRT)
      IF(IRT.EQ.1.AND.ICHR.EQ.13)GOTO 650
      IF(IRT.EQ.1.AND.ICHR.EQ.25)GOTO 999
      GOTO 640
 650  CONTINUE
      WRITE(*,1000)
      WRITE(*,1000)
      WRITE(*,1000)
      WRITE(*,1023)
      WRITE(*,1014)
      WRITE(*,1000)
      WRITE(*,1000)
      WRITE(*,1000)
C      write(*,*)icharr(1),icharr(2),icharr(3)
C      write(*,*)isccnt
 1022 FORMAT(' PRESS <ENTER> TO START')
```

```
 1023 FORMAT(' CONTROL PROGRAM RUNNING')
C
C      MAIN PROGRAM LOOP
C
 700   CONTINUE
C      CHECK FOR KEYBOARD INPUT
       CALL KEYIN(ICHR,IRT)
         IF(IRT.NE.0) THEN
           IF(ICHR.EQ.25) THEN
               goto 800
           endif
         endif
       ierr=mb_chan(icharr,isccnt,isccnt,inbuf)
       if(ierr.ne.0) then
         write(*,*) ' MB_CHAN Error: IERR=',ierr
         goto 700
       endif
       DO 710 I=1,ISCCNT
         RVAL(I)=(INBUF(I)*CONV1)+CONV2-DCOFF
 710   CONTINUE
C
C      SET VOLTAGE LIMIT
C
       RMVOLT=VOMAXF
       RRVOLT=-VOMAXF
C
C      COMPUTE VOLTAGE OUT
C
       VALO=-RVAL(1)*CGAIN
       IF(VALO.GT.RMVOLT)THEN
         VALO=RMVOLT
       ELSEIF(VALO.LT.RRVOLT)THEN
         VALO=RRVOLT
       ENDIF
       IF(VALO.GT.(-VOMIN).AND.VALO.LT.0)THEN
         VALO=0
       ELSEIF(VALO.LT.VOMIN.AND.VALO.GT.0)THEN
         VALO=0
       ENDIF
 730   CONTINUE
C
C      CONVERT VOLTAGE TO BINARY
C
       IVALO=INT(DCON1-(DCON2*VALO))
         IF(IVALO.LT.0)THEN
           IVALO=0
       ELSEIF(IVALO.GT.4095)THEN
```

```
          IVALO=4095
        ENDIF
        ierr=da_out(idac(1),ivalo)
        GOTO 700
 800    CONTINUE
C
C       END OF MAIN PROGRAM LOOP
C
        WRITE(*,*) ' PROGRAM STOPPED---'
        WRITE(*,1000)
        write(*,*) ' OUTPUT VOLTAGE ZEROED'
        write(*,1000)
        ierr=da_out(0,2048)
 999    CONTINUE
        STOP
        END
```

VITA

Linda Morley Hanagan was born in Langhorne, Pennsylvania on May 9, 1962. She graduated from Council Rock High School in Newtown, Pennsylvania. After receiving her Bachelor of Architectural Engineering degree from the Pennsylvania State University in 1985, she worked as a structural consulting engineer for four years. Ms. Hanagan is a registered Professional Engineer in the State of Pennsylvania. Returning to the Pennsylvania State University for graduate study, she received her Master of Science Degree in Architectural Engineering in May 1992. She is currently enrolled as a doctoral student in the Structures Division of the Virginia Polytechnic Institute and State University. Ms. Hanagan has accepted a position as an assistant professor in Civil and Architectural Engineering at the University of Miami, Florida beginning January 1, 1995.

Linda M. Hanagan

Linda M. Hanagan